

DEVELOPMENT AND CHARACTERIZATION OF COMPOSITE PROTON
EXCHANGE MEMBRANES FOR FUEL CELL APPLICATIONS

A THESIS SUBMITTED TO
THE GRADUATE SCHOOL OF NATURAL AND APPLIED SCIENCES
OF
MIDDLE EAST TECHNICAL UNIVERSITY

BY

R. GÜLTEKİN AKAY

IN PARTIAL FULFILLMENT OF THE REQUIREMENTS
FOR
THE DEGREE OF DOCTOR OF PHILOSOPHY
IN
CHEMICAL ENGINEERING

FEBRUARY 2008

Approval of the thesis:

DEVELOPMENT AND CHARACTERIZATION OF COMPOSITE PROTON
EXCHANGE MEMBRANES FOR FUEL CELL APPLICATIONS

submitted by **R. GÜLTEKİN AKAY** in partial fulfillment of the requirements for
the degree of **Doctor of Philosophy in Chemical Engineering Department, Middle
East Technical University** by,

Prof. Dr. Canan Özgen
Dean, Graduate School of **Natural and Applied Sciences**

Prof. Dr. Gürkan Karakaş
Head of Department, **Chemical Engineering**

Prof. Dr. Nurcan Baç
Supervisor, **Chemical Engineering Dept., METU**

Examining Committee Members:

Prof. Dr. Hayrettin Yücel
Chemical Engineering Dept., METU

Prof. Dr. İnci Erođlu
Chemical Engineering Dept., METU

Prof. Dr. Nurcan Baç
Chemical Engineering Dept., METU

Prof. Dr. Ayşe Nilgün Akın
Chemical Engineering Dept., KOU

Assoc. Prof. Ahmet Eraslan
Engineering Science Dept., METU

Date: 05.02.2008

I hereby declare that all information in this document has been obtained and presented in accordance with academic rules and ethical conduct. I also declare that, as required by these rules and conduct, I have fully cited and referenced all material and results that are not original to this work.

Name, Last name : R. Gültekin Akay

Signature :

ABSTRACT

DEVELOPMENT AND CHARACTERIZATION OF COMPOSITE PROTON EXCHANGE MEMBRANES FOR FUEL CELL APPLICATIONS

Akay, R. Gültekin

Ph.D., Department of Chemical Engineering

Supervisor: Prof. Dr. Nurcan Baç

February 2008, 190 pages

Intensive research on development of alternative low cost, high temperature membranes for proton exchange membrane (PEM) fuel cells is going on because of the well-known limitations of industry standard perfluoro-sulfonic acid (PFSA) membranes. To overcome these limitations such as the decrease in performance at high temperatures (>80 °C) and high cost, non-fluorinated aromatic hydrocarbon based polymers are attractive. The objective of this study is to develop alternative membranes that possess comparable properties with PFSA membranes at a lower cost. For this purpose post-sulfonation studies of commercially available engineering thermoplastics, polyether-ether ketone (PEEK) and polyether-sulfone (PES), were performed by using suitable sulfonating agents and conditions. Post sulfonated polymers were characterized with proton nuclear magnetic resonance spectroscopy (H^+ -NMR), sulfur elemental analysis and titration to calculate the degree of sulfonation (DS) values and with TGA and DSC for thermal stability and glass transition temperature (T_g). Chemical stabilities were evaluated by hydrogen

peroxide tests. Proton conductivities of sulfonated PEEK (SPEEK) measured by electrochemical impedance spectroscopy (EIS) were observed to increase linearly with degree of sulfonation (DS). However, above a certain DS SPEEK loses its mechanical stability significantly with excessive swelling which leads to deteriorations in mechanical stability. Therefore, DS of 50-70% were used for the fabrication of composite membranes. To improve mechanical stability, SPEEK polymers were blended with more stable polymers, polyether-sulfone (PES) or in its sulfonated form (SPES) or with polybenzimidazole (PBI). In addition, the composite approach, which involves the incorporation of various inorganic fillers such as zeolite beta, TiO₂, montmorillonite (MMT), heteropolyacids (HPA), was used for further improvement of proton conductivity. Among the composite membranes 20% TPA/SPEEK (DS=68) composites conductivity value exceeded that of Nafion's at room temperature. Effects of various parameters during the fabrication process such as the filler type and loading, DS of sulfonated polymer, casting solvents, and thermal and chemical treatment were also investigated and optimized.

Various blend/composite membranes were fabricated with solvent casting method, and characterized for their proton conductivity, chemical/thermal stability and for evaluating their voltage/current performance at various temperatures in a single cell setup. Chemically and thermo-hydrolytically stable composite/blend membranes such as 25% tungstophosphoric acid (TPA)/PBI(5%)/SPEEK (DS=68) with good single cell performances at 80⁰C were developed (~450 mA/cm² at 0.5 V). The performance of the hydrolytically stable composite/blend membrane prepared with SPEEK (DS=59); 5% PBI; and 10% TiO₂ increased appreciably when the temperature was raised from 80 ⁰C to 90 ⁰C while the performance of Nafion decreases sharply after 80 ⁰C.

Methanol permeability studies were also performed for investigating the potential of fabricated blend/composite membranes for direct methanol fuel cell (DMFC) use. Selectivities (conductivity/methanol permeability)

greater than Nafion 112 ($S=7.3 \times 10^7$) for DMFC were observed for composite/blend membranes such as 10% TiO_2 /10% PES blend with SPEEK (DS=68) with a selectivity of 9.3×10^7 .

The factors that affect proton conductivity measurements were investigated and equivalent circuit analysis was performed with results obtained by electrochemical impedance spectroscopy (EIS). The choice of the conductivity cell (electrodes, cell geometry) and the method (2-probe vs 4-probe) were shown to affect the conductivity analysis.

A systematic development and characterization route was established and it was shown that by optimizing proton conductivity and thermal/chemical stability with blending/composite approaches it is possible to produce novel high performance proton exchange membranes for fuel cell applications.

Keywords: Proton exchange membrane (PEM), composite membranes, fuel cell, sulfonated polyetheretherketone (SPEEK), proton conductivity.

ÖZ

YAKIT PİLİ UYGULAMALARI İÇİN KOMPOZİT MEMBRAN GELİŞTİRİLMESİ VE KARAKTERİZASYONU

Akay, R. Gültekin

Doktora, Kimya Mühendisliği Bölümü

Tez Yöneticisi: Prof. Dr. Nurcan Baç

Şubat 2008, 190 sayfa

Bugün endüstri standardı olan perfloro-sulfonik asit (PFSA) bazlı membranlar bilinen limitasyonlarından dolayı yüksek sıcaklıklarda çalışabilen, düşük maliyetli, alternatif proton değişim membranlı (PEM) yakıt pili membranları üzerine tüm dünyada yoğun çalışmalar yürütülmektedir. Yüksek sıcaklıkta (>80 C) verim düşüklüğü, yüksek maliyet gibi limitasyonların üstesinden gelebilmek için florsuz aromatik hidrokarbon tabanlı polimerler ilgi çekmektedir. Bu çalışmanın amacı PFSA membranlara alternatif, onların özelliklerine yakın daha düşük maliyetli malzemeleri geliştirmek ve karakterize etmektir. Bu amaçla öncelikle ticari olarak bulunabilen ve mühendislik polimerleri olarak bilinen polieter-eter ketone (PEEK) ve polieter-etersülfon (PES) temel yapı olarak seçilerek optimum özellikler için post-sülfonasyon çalışmaları yapılmıştır. Sülfonlanmış polimerler sülfonlama derecelerinin (SD) tayini için H-NMR, kükürt elementel analizi ve titrasyon gibi yöntemlerle, termal dayanım ve cam geçiş sıcaklığı (T_g) tespiti için TGA ve DSC ile karakterize edilmiştir. Kimyasal dayanıklılık yakıt pilinde katotta oluşan oksidatif ortamı simule eden hidrojen peroksit testleriyle incelenmiştir. Proton iletkenlikleri electrokimyasal empedans spektroskopisi (EIS) yöntemiyle incelendiğinde SPEEK membranların iletkenliğinin SD ile lineer olarak arttığı görülmüştür.

Fakat, belirli bir SD üstünde SPEEK'in aşırı şişme sonucu mekanik dayanımının kaybolduğu da tespit edilmiştir. Bu yüzden SD % 50-70 arasında optimize edilmiş daha sonra hazırlanan karışım ve kompozit membranlar için bu aralık kullanılmıştır. Mekanik dayanımı artırmak için daha uyumlu ve dayanıklı PES veya düşük derecede sülfonlanmış PES (SPES) veya polibenzimidazol (PBI) gibi hidrofobik ve bazik polimerlerle karışım yaklaşımı da kullanılmıştır. Buna karşın gözlenen proton iletkenlik düşüşünü karşılamak ve artırmak için zeolit beta, TiO₂, MMT, heteropoliasitler (HPA) gibi inorganik doldurucularla kompozit malzeme hazırlanması yaklaşımı da kullanılmıştır. Kompozit membranlar içinde 20% TPA/SPEEK (DS=68) proton iletkenliği oda sıcaklığında Nafion iletkenliğinden yüksek sonuç vermiştir. Membranların hazırlanma sürecindeki inorganik katkı çeşidi/yüklemesi, sülfonlanmış polimerin SD'si, döküm için kullanılan çözücü, ve termal/kimyasal muamele gibi parametrelerin performans üzerine etkisi incelenmiştir.

Çözücü uçurma yöntemiyle hazırlanan çeşitli kompozit membran karışımları proton iletkenlik, kimyasal/termal dayanım özellikleri için karakterize edildikten sonra içlerinden en iyi sonuç verenler tek hücre yakıt pili test istasyonunda test edilmişlerdir. Geliştirilen kimyasal ve termohidrolitik olarak dayanıklı kompozit/karışım membranlardan 25% tungstophosphoric asit (TPA)/PBI(5%)/SPEEK (DS=68), 80 °C'de yüksek tek hücre yakıt pili performansı vermiştir (~450 mA/cm² at 0.5 V). SPEEK (DS=59)/5% PBI/ 10% TiO₂ kompozit/karışım membran ise 80 °C den 90 °C'ye çıkıldığında daha yüksek performans vermiştir. Nafion'un performansı 80 °C'den sonra belirgin biçimde düştüğünden bu sonuç önemlidir.

Metanol geçirgenlik testleri geliştirilen malzemelerin doğrudan metanol yakıt pili (DMFC) kullanımı için potansiyelinin tespiti için gerçekleştirilmiştir. Proton iletkenliğinin metanol geçirgenliğe oranı olarak tanımlanan seçicilik parametresi (9.3×10^7) 10% TiO₂/10% PES/SPEEK (DS=68) gibi bazı kompozit/karışımlarda Nafion'dan ($S=7.3 \times 10^7$) yüksek çıkmıştır.

Sistematik geliştirme ve karakterizasyon yöntemleri oluşturulduktan ve kullanıldıktan sonra, uygun koşullarla ve malzemelerle geliştirilen karışım/kompozit membranların proton iletkenlik ve termal/kimyasal dayanım özellikleri optimize edildiğinde yeni ve yüksek performanslı proton değişim membranları olarak potansiyeli tespit edilmiştir.

Anahtar Kelimeler: Proton değişim membranı (PEM), kompozit membranlar, yakıt pili, sülfonlanmış polietereketon (SPEEK), proton iletkenliği

To My Mother...

ACKNOWLEDGEMENTS

I would like to express my gratitude to my supervisor Prof. Dr. Nurcan Ba for his continuous encouragement and support with patience without which this thesis would not be possible.

I would like to thank Prof. Dr. İnci Erođlu for her support both morally and technically during my whole education and working period in the department.

The useful comments of my thesis examining committee members, Prof. Dr. Hayrettin Yücel and Assoc. Prof Dr Ahmet Eraslan are gratefully acknowledged.

I am grateful for every possible kind of support, guidance, criticism, encouragement and friendship provided by Serdar Erkan, Ayşe Bayrakeken and Berker Fııcılar at all stages of this work. I would also want to thank our M.S graduates Hülya Erdener and Nadiye Gür for their studies and help.

I am also thankful to the staff of Central Laboratory and Chemical Engineering Department for their help during characterization analyses.

I would like to thank to Sinan Kınıkođlu for his support and help in 3-D drawings used in this dissertation.

Project grant of METU-BAP and TUBITAK (104M364) are gratefully acknowledged.

Last but not the least; I would like to thank my friends for their support and existence.

TABLE OF CONTENTS

ABSTRACT	iv
ÖZ	vii
ACKNOWLEDGEMENTS.....	xi
TABLE OF CONTENTS	xii
LIST OF TABLES.....	xvi
LIST OF FIGURES.....	xviii
LIST OF SCHEMES	xxii
LIST OF ABBREVIATIONS.....	xxiii
LIST OF SYMBOLS	xxiv
CHAPTER 1	1
INTRODUCTION.....	1
CHAPTER 2	8
LITERATURE SURVEY	8
2.1 Fuel Cells.....	8
2.1.1 History.....	8
2.1.2 Types of Fuel Cells	10
2.1.3 Components of Fuel Cells.....	12
2.1.4 Why High Temperatures?	14
2.1.5 Thermodynamics & Efficiency.....	15
2.1.6 Kinetics & Losses.....	19
2.2 Alternative Membranes	25
2.2.1 Properties of a Good Membrane.....	26
2.2.2 Non-Fluorinated Aromatic Hydrocarbon Polymers.....	27
2.2.2.1 Poly(Arylene Ether Ketones) Family	27
2.2.2.2 Poly(Arylene Ether Sulfones) Family	28
2.2.2.3 Polybenzimidazoles (PBI)	29
2.2.3 Composite Membranes.....	30
2.3 Sulfonation.....	34
2.3.1 Sulfonation of Polyetheretherketone (PEEK)	37
2.3.2 Sulfonation of Polyethersulfone (PES).....	43

2.4 Conductivity Data Discrepancy	44
2.5 Proton Transport.....	45
2.6 Proton Conductivity Measurements	57
2.6.1 Electrochemical Impedance Spectroscopy (EIS): Theory	57
2.6.2 2-Probe (2P) vs 4-Probe (4P)	68
CHAPTER 3	73
MATERIALS & METHODS.....	73
3.1 Polymers.....	73
3.1.1 Polyetheretherketones (PEEK)	73
3.1.2 Polyetherethersulfone (PES)	74
3.1.3 Polybenzimidazoles (PBI)	75
3.2 Inorganic Fillers & Modifiers.....	76
3.2.1 Zeolite Beta.....	76
3.2.2 Heteropolyacids (HPAs).....	78
3.3 Solvents	78
3.4 Sulfonation.....	78
3.4.1 Sulfonation of PEEK	78
3.4.2 Sulfonation of PES.....	79
3.5 Zeolite Beta Synthesis	81
3.6 Fabrication of Composite Membranes	81
3.7 Membrane Electrode Assembly (MEA) Preperation.....	82
3.8 Characterization Methods	82
3.8.1 X-Ray Diffraction (XRD).....	82
3.8.2 Scanning Electron Microscopy (SEM) Analysis	83
3.8.3 Thermal Methods (TGA & DSC)	83
3.8.4 Proton Nuclear Magnetic Resonance Spectroscopy (H-NMR)	
.....	83
3.8.5 Titration.....	85
3.8.6 Gas Chromatography (GC).....	85
3.8.7 Elemental Analysis.....	85
3.8.8 Water Uptake	86
3.8.9 Viscosity Measurement.....	86
3.8.10 Stability Tests (Chemical & Hydrothermal)	86
3.8.11 Proton Conductivity Measurements (EIS)	87
3.8.12 Dynamic Mechanical Analysis (DMA)	90

3.8.13 Methanol Permeability Measurement.....	90
3.8.14 Single Cell Tests (Polarization Curves).....	92
CHAPTER 4	95
RESULTS & DISCUSSION	95
4.1 Sulfonation.....	95
4.1.1 Sulfonation of PEEK	95
4.1.1.1 Setting Optimum Reaction Parameters.....	95
4.1.1.2 Determination of DS (H-NMR & Elemental Analysis).....	99
4.1.1.3 Thermal Characterization (TGA & DSC)	106
4.1.2 Sulfonation of PES.....	111
4.1.2.1 Effect of Actual Composition of PES Used	111
4.1.2.2 Comparison of Sulfonation Methods	118
4.1.2.3 Thermal Characterization (TGA & DSC)	124
4.2 Proton Conductivity Measurements and Equivalent Circuit Modelling	127
4.3 Pristine Membranes (SPEEK & SPES).....	138
4.3.1 Effect of Degree of Sulfonation (DS).....	138
4.3.2 Effect of Pre-treatment of the Membrane.....	140
4.3.3 Effect of Casting Solvent.....	140
4.4 Zeolite Beta Composites.....	141
4.4.1 Synthesis of Zeolite.....	141
4.4.2 Loading Effect.....	145
4.4.3 Effect of Si/Al Ratio	145
4.5 SPEEK Based Blends.....	147
4.6 Comparison of Inorganic Fillers	149
4.6.1 Metal Oxides-Clays-Aluminosilicate (zeolite)	149
4.6.2 Heteropolyacid (HPA) Composites	151
4.7 Blend/Composites.....	155
4.8 Temperature Dependence of Proton Conductivity (Activation Energies)	157
4.9 Mechanical Stabilities	160
4.10 Methanol Permeability	161
4.11 Single Cell Tests.....	165
CHAPTER 5	172

CONCLUSIONS.....	172
CHAPTER 6	175
RECOMMENDATIONS.....	175
REFERENCES.....	177
APPENDICES	184
APPENDIX A	184
APPENDIX B	186
APPENDIX C	187
CURRICULUM VITAE.....	188

LIST OF TABLES

Table 2.1. An Overview of Types of Fuel Cells (Thomas, 2001)	11
Table 2.2. Thermodynamic Values of the PEM Fuel Cell Reaction at Various Temperatures (Yang, 2004)	17
Table 2.3. Summary of some Inorganic-Organic Composite Membranes investigated	32
Table 2.4. Conductivity values of Nafion 1100 EW membranes from various studies (Slade et al., 2002)	45
Table 2.5. Common Electrical Elements	63
Table 2.6. Equivalent Circuit Parameters used for Nafion and Chitosan Membranes (Ramirez-Salgado, 2007)	68
Table 3.1. Experimental Conditions of GC for Methanol Permeability Test	91
Table 4.1. Optimum Sulfonation Parameters for PEEK	98
Table 4.2. Summary of DS % values calculated from Elemental Analysis and H-NMR for SPEEK	104
Table 4.3. Summary of characterization results for determination of DS for SPES samples sulfonated at various conditions	114
Table 4.4. Comparison of IEC, DS & inherent viscosity of PES polymers sulfonated at the same conditions	118
Table 4.5. Titration DS results of SPES (acetic anhydride catalyzed)	119
Table 4.6. Titration DS results of SPES samples sulfonated with different procedures	120
Table 4.7. DS of SPES & SPES(Si)	123
Table 4.8. Circuit Elements Used in the Models.....	134
Table 4.9. Equivalent Circuits Fitted for a Composite/Blend Membrane	135
Table 4.10. Parameter Values for Equivalent Circuits Fitted for a Composite/Blend Membrane	136
Table 4.11. Parameter Values for Equivalent Circuit (2) of Composite/Blend Membrane with Equivalent Circuit Fittings for 75 %SPES/SPEEK Blend	138
Table 4.12. Effect of Casting Temp. and Acid Treatment on SPEEK-72	140
Table 4.13. Casting solvent effect on proton conductivity	141
Table 4.14. Conductivity Results of SPEEK-57 based Blends	148
Table 4.15. Conductivity & Water Uptakes of SPEEK-72 Based Membranes (Casting Temp= 80 C)	149
Table 4.16. Comparison of proton conductivities of composite membranes	150
Table 4.17. Loading Effect of TiO ₂ on Proton Conductivity.....	151
Table 4.18. Proton Conductivity and Water Uptakes of HPA Composites	152
Table 4.19. Proton Conductivity of HPA Composites (Loading)	153
Table 4.20. DS and Weight Losses of HPA-Composite Membranes Calculated from TGA Curves.....	155

Table 4.21. Proton Conductivities of PBI/SPEEK blends and their TPA Composites	156
Table 4.22. Mechanical Analysis Results of Composite & Blend membranes	160
Table 4.23. Conductivity, Methanol Permeability & Selectivity (S) of N112 and Zeolite Beta Composites	163
Table 4.24. Conductivity, Methanol Permeability & Selectivity (S) of N112 and Selected Composite/Blends	164
Table 4.25. Summary of Membranes Tested in a Single Cell.....	170

LIST OF FIGURES

Figure 1.1. PEM Fuel Cell	2
Figure 1.2. Chemical structure of Nafion (Savadogo, 1998).....	5
Figure 2.1. First Fuel Cell Demonstration by William Groove in 1839 (Thomas, 2001)	8
Figure 2.2. Direct Methanol Fuel Cell (DMFC)	12
Figure 2.3. Main Components of PEM Fuel Cell	13
Figure 2.4. PEM Fuel Cell Stack	13
Figure 2.5. Efficiency Definitions of any Energy Conversion Device & a Fuel Cell	18
Figure 2.6. A Typical fuel cell polarization curve (Fuel Cell Handbook, 2000)	20
Figure 2.7. (a) Conductivity (S/cm) of SPES-40 composite membranes as a function of temperature (K). (b) Conductivity (S/cm) of Nafion based composite membranes at room temperature (Rogers, 2004)	31
Figure 2.8. Sulfonation level of PEEK as a function of reaction time at room temperature (Kobayashi et al,1998)	38
Figure 2.9. Degree of Sulfonation (DS) vs Sulfonation Reaction Time (Huang et al., 2001).....	39
Figure 2.10. Influence of reaction time on the DS and IEC values of PEEK sulfonated at room temperature (Li et al., 2003).....	40
Figure 2.11. Water uptake as a function of Degree of sulfonation (DS) for SPEEK polymer at room temperature (Li et al., 2003)	40
Figure 2.12. Schematic diagram of a pore within an ion-exchange membrane with fixed anions ($-SO^-$) and cations, some of which are attached (Stern layer), while others form a diffuse layer. In addition, ions of any free-supported acid through self-ionization are shown (Malhotra et al., 1997)	46
Figure 2.13 A “dusty-fluid model” depiction of a PEM. The polymer matrix along with an acid groups is viewed as “dust” particles comprising the PEM (Thampan et al., 2000)	51
Figure 2.14. Conductivity vs relative humidity for sulfonated polyethersulfone (S-PES) (Rogers et al., 2004)	55
Figure 2.15. A dusty-fluid model depiction of a PEM describing proton conductivity through the Nafion polymer matrix and the superacidic dopant (Thampan et al., 2005)	56
Figure 2.16. Room temperature conductivity of samples cast with different solvents (Kaliaguine et al., 2003)	57
Figure 2.17. Flow diagram for the measurement and characterization of a material–electrode system (Barsoukov et al., 2005).....	58
Figure 2.18. (a) Sinusoidal Current Response in a Linear System (b) Current versus Voltage Curve Showing Pseudo-linearity	60
Figure 2.19. (a) Nyquist Plot with Impedance Vector (b) Bode Plot.....	62
Figure 2.20. Effect of frequency on capacitive and inductive reactance...	63

Figure 2.21. Equivalent circuit for the membrane/electrode interface studied: Serial and Parallel Combinations of Circuit Elements	63
Figure 2.22. Equivalent circuit used very often for SOFC and PEMFC (Nicoloso, 1990)	64
Figure 2.23. A simple electrified interface, in which the vertical dotted lines in (a) are represented by the electronic components in (b) (Park et al. 2003)	64
Figure 2.24. Nyquist Plot of an electrified interface (Park et al. 2003)	65
Figure 2.25. Bode Plot of an electrified interface (Park et al. 2003)	65
Figure 2.26. (a) Typical complex impedance responses of humidified PEM (PEEK, DS = 0.42) at different temperatures. Cell area=1 cm ² , membrane thickness=0.9 mm. (b) Experimental and simulated curves. R ₁ = 640Ω, C ₁ = 7.5 × 10 ⁻¹¹ F, R _w = 600 Ω, S _w = 6 × 10 ⁻⁴ s, α = 0.32. (Ciureanu et al., 2003)	67
Figure 2.27. Equivalent Circuits a) chitosan b) Nafion and Nyquist Plot of Chitosan Membranes (Ramirez-Salgado, 2007)	67
Figure 2.28. Bode and Nyquist Plots of Nafion 117; 4-P AC Impedance Method (Sone et al., 1996)	70
Figure 2.29. Sample arrangements for (a) the 2-probe method, (b) the 4-probe method in the direction of thickness, and (c) the 4-probe method in the surface direction (Ma et al., 2006)	71
Figure 2.30. Equivalent circuit for the membrane/electrode interface studied (Ma et al., 2006)	72
Figure 3.1. Zeolite beta structure	77
Figure 3.2. Conductivity Cell (1 st : for water contact)	88
Figure 3.3. Conductivity cell (2 nd : for vapor contact)	88
Figure 3.4. Proton Conductivity Measurement Setup	89
Figure 3.5. Methanol Permeability Cell	91
Figure 3.6. Flowchart of Fuel Cell Test Station	93
Figure 3.7. Fuel Cell Test Station	93
Figure 4.1. H-NMR spectrum of SPEEK-2	102
Figure 4.2. H-NMR spectrum of SPEEK-4	102
Figure 4.3. Degree of Sulfonation (DS) calculated from H-NMR vs S% from elemental analysis	104
Figure 4.4. Comparison of DS values calculated from elemental analysis and H-NMR	105
Figure 4.5. DS vs time of reaction for SPEEK at 50 °C	105
Figure 4.6. TGA of PEEK	106
Figure 4.7. TGA of SPEEK (DS=79)	107
Figure 4.8. TGA of SPEEK (DS=62)	108
Figure 4.9. TGA of SPEEK (DS=68)	109
Figure 4.10. DSC of PEEK	110
Figure 4.11. DSC graph of SPEEK (DS 68%) membrane	111
Figure 4.12. H-NMR a) PES b) SPES (Kim et al., 1999)	112
Figure 4.13. H-NMR spectra of a) PES(1) b) SPES(1)	113
Figure 4.14. H-NMR a) PEES b) SPEES (5) c) SPEES (10) d) SPEES (20) (Benavente, 2000)	116

Figure 4.15. H-NMR spectra of SPES (up) & SPES(Si) (down)	122
Figure 4.16. TGA of PES.....	125
Figure 4.17. TGA of SPES	125
Figure 4.18. DSC of PES	126
Figure 4.19. DSC of SPES	126
Figure 4.20. Proton Conductivities measured with 2-Probe vs 4-probe measurements for various samples.....	128
Figure 4.21. Nyquist (left) and Bode (right) plots of Nafion 115 (first cell; in water)	130
Figure 4.22. Nyquist (left) and Bode (right) plots of 25% SPEEK/PES blend (first cell; in water)	131
Figure 4.23. Bode (let) & Nyquist (right) Plots of SPEEK (DS=68) (4-P; in vapor; RT)	133
Figure 4.24. Bode (left) & Nyquist (right) Plots of SPEEK (DS=68) (2-P; in vapor; RT)	133
Figure 4.25. Bode (left) & Nyquist (right) Plots of a Composite/blend Membrane with Equivalent Circuit Fittings	135
Figure 4.26. Bode (left) & Nyquist (right) Plots with Equivalent Circuit Fittings for 75 %SPES/SPEEK Blend.....	137
Figure 4.27. Equivalent Circuit Fittings used for SPES/SPEEK Blend: (1) Randles Type with Bounded Warburg Element (2) Randles Type with Bounded Warburg Element and CPE.....	137
Figure 4.28. Proton Conductivity vs Degree of Sulfonation (DS) for SPEEK & SPES	139
Figure 4.29. XRD pattern of as synthesized zeolite beta ($\text{SiO}_2/\text{Al}_2\text{O}_3=20$)	142
Figure 4.30. XRD pattern of zeolite beta treated with 95-98 wt% H_2SO_4	143
Figure 4.31. TGA graph of zeolite beta crystals	144
Figure 4.32. SEM micrographs of synthesized zeolite beta crystals.....	144
Figure 4.33. Effect of zeolite loading wt % on proton conductivity of SPEEK/Zeolite beta composites.....	145
Figure 4.34. Effect of zeolite loading wt % on proton conductivity of SPEEK/Zeolite beta composites (Erdener, 2007).....	146
Figure 4.35. Proton Conductivities of PES/SPEEK ratios (25, 50, 75 wt%)	147
Figure 4.36. TGA curves of HPA composites	154
Figure 4.37. Arrhenius behavior of Nafion 112.....	158
Figure 4.38. Arrhenius behavior of SPEEK	159
Figure 4.39. Activation energies for proton conduction of various pristine, blend and composite membranes	159
Figure 4.40. Methanol Concentration Change in Compartment B with respect to Time for N112.....	162
Figure 4.41. Methanol Permeabilities of N112 and Zeolite Beta Composites	163
Figure 4.42. Concentration vs Time for Methanol Permeabilities of N112 and Selected Composite/Blends	164

Figure 4.43. Polarization (V-I) curves of SPEEK (DS=56) at various temperatures	166
Figure 4.44. Polarization (V-I) curves of SPEEK (DS=65)/5% TiO ₂ composite at various temperatures	166
Figure 4.45. Polarization (V-I) curves of 5%PBI/10%TiO ₂ /40%TPA/SPEEK (DS=59)at various temperatures	168
Figure 4.46. Polarization (V-I) curves of 5%PBI/10%TiO ₂ /SPEEK(DS=59) at various temperatures.....	168
Figure 4.47. Polarization (V-I) curve of 25%SPES()/TPA(20%)/SPEEK (DS=74) at various temperatures	169
Figure 4.48. Comparison of fabricated composite and composite/blend membranes with Nafion 112 performance.....	170

LIST OF SCHEMES

Scheme 2.1. Structures of (a) PEEK (b) SPEEK.....	28
Scheme 2.2. Structures of (a) PES (b) SPES.....	29
Scheme 2.3. General mechanism of the sulfonation reactorx Step 1.: Formation of the π -complex, Step 2.: Formation of the arenium ions (σ - complex), Step 3: Termination of the sulfonation by the release of X^+ (Kucera, 1998).....	36
Scheme 2.4. Possible Side Reactions During Sulfonation	36
Scheme 3.1. Structure of Polyetherethersulfone (PEES)	75
Scheme 3.2. Structure of Radel A Polyethersulfone	75
Scheme 3.3. Structure of Benzimidazole group	76
Scheme 3.4. Structure Chemical Structure of Mphi.....	76
Scheme 4.1. Aromatic protons of PEEK and SPEEK.....	101
Scheme 4.2. Repeating unit and proton designations of PEES and SPEES (Benavente et al. 2000)	115
Scheme 4.3. a)Structure of Polyethersulfone (PES) (Aldrich product) & b) Polyethersulfone (PES) (Solvay product)	117

LIST OF ABBREVIATIONS

AFC: Alkaline Fuel Cell
CPE: Constant Phase Element
CSA: Chlorosulfonic Acid
DMAc: Dimethyl Acetamide
DMF: Dimethyl Formamide
DMSO: Dimethyl Sulfoxide
DS: Degree of Sulfonation
DSC: Differential Scanning Calorimetry
EIS: Electrochemical Impedance Spectroscopy
FT-IR: Fourier Transform Infrared
FRA: Frequency Response Analyser
GDL: Gas Diffusion Layer
HPA: Heteropololyacid
HHV: Higher-heating value
H-NMR: Proton Nuclear Magnetic Resonance
HPA: Heteropolyacid
IEC: Ion Exchange Capacity
IUPAC: International Union of Pure and Applied Chemistry
LHV: Lower-heating value
MCFC: Molten Carbonate Fuel Cell
MEA: Membrane Electrode Assembly
MMT: Montmorillonite
NMP: N-Methyl Pyrrolidone
Na-TPA: Disodium Salt of Tungstophosphoric Acid
OCV: Open Circuit Voltage
PAFC: Phosphoric Acid Fuel Cell
PBI: Polybenzimidazole
PEEK: Polyetheretherketone
PEMFC: Proton Exchange Membrane (or Polymer Electrolyte Membrane)
Fuel Cell
PES: Polyethersulfone
PFCA: Perfluoro carboxylic acid
PFSA: Perfluorosulfonic acid
RH.: Relative Humidity
RT: Room Temperature
SEM: Scanning Electron Microscopy
SOFC: Solid Oxide Fuel Cell
SPEEK: Sulfonated Polyether Ether Ketone
SPES: Sulfonated Polyether Sulfone
SPS: Sulfonated Polysulfone
TGA: Thermogravimetric Analysis
TPA: Tungstophosphoric Acid

LIST OF SYMBOLS

D: Diffusion coefficient [cm^2/s]
 E_r : Reversible potential
F: Faradays constant [96500 C/eq]
i: Current density [A/cm^2]
n: # of electrons involved in reaction
 T_d : Thermal Decomposition Temperature
 T_g : Glass Transition Temperature
P: Methanol Permeability [cm^2/s]
R: Solution Resistance
S: Selectivity (σ/P)
Z: Impedance
W: Warburg Resistance
 η : Efficiency
 η_A : Anodic Overpotential
 η_C : Cathodic Overpotential
 η_{ohm} : Ohmic Overpotential
 σ : Proton Conductivity
 ΔH : Enthalpy Change
 ΔG : Gibbs Free Energy Change
 ΔS : Entropy Change

CHAPTER 1

INTRODUCTION

Every living organism consumes energy in nature to survive but human being consumes more for living better. The desire for living in better conditions may be considered natural for human being, however, consuming more energy and in an inefficient way means generating more entropy which is the “degree of disorder” in its simplest definition. With the invention of the internal combustion engine in the past century, and increased growth rate of the population, this process has not only changed the dynamics of the planet rapidly as everybody feels nowadays, but also affected societies all over the world, moreover caused wars and deaths for controlling the limited fossil fuel sources. Today, with this experience gained in the recent decades, everybody agrees that we need to produce and consume energy in increasingly more efficient and nature friendly ways. One of the most promising technologies for this objective is the fuel cell with hydrogen as the fuel for future.

A fuel cell is an energy conversion device that reacts electrochemically, a fuel (hydrogen or hydrogen carrier) and oxygen to produce electricity. Fuel cell technology is the most promising technology today to replace technologies dependent on fossil fuels such as internal combustion engines. They convert chemical energy directly to electrical energy. This is what makes them very different from the conventional combustion based power plants, which convert chemical energy to thermal energy, then thermal energy to kinetic energy, and only then kinetic energy to electrical energy. The thermal to kinetic and kinetic to electrical conversion stages

have efficiency losses. Major loss is in the combustion process that is in the conversion step of chemical to thermal energy. Thermodynamically speaking, there is an ultimate efficiency, which cannot be exceeded by any combustion engine called “The Carnot Limit” which does not limit fuel cells.

The main components and operation of a single fuel cell can be followed from Figure 1.1, showing a schematic of a typical Proton Exchange Membrane Fuel Cell (PEMFC). The half and overall reactions are:

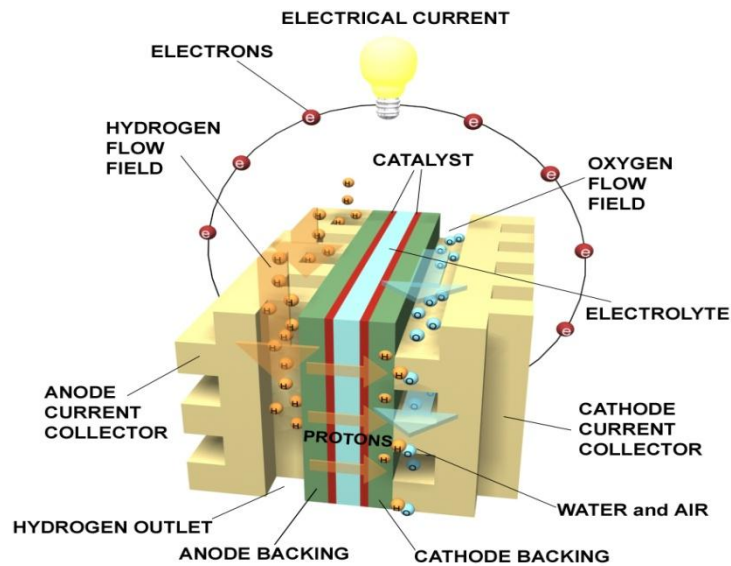
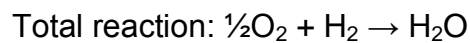
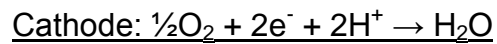
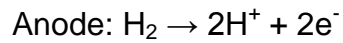


Figure 1.1. PEM Fuel Cell

It is composed of an anode (a negative electrode that repels electrons), a cathode (a positive electrode that attracts electrons) and a polymer

electrolyte membrane that separates these two electrodes. As hydrogen flows into the fuel cell anode, its platinum or other noble metal catalyst helps to separate the hydrogen into protons (H^+) and electrons (e^-). The membrane only allows the protons, but not the electrons to pass through to the cathode side, so the electrons must flow through an external circuit in the form of an electric current. Protons migrate from anode to cathode through membrane and combine with oxygen to form water.

The major challenges to fuel cell commercialization at the point we stand are the cost and durability. The importance of these two challenges varies of course from application to application. For example for a space mission cost may not be as important as durability and reliability whereas for transportation applications, cost is very important.

Today most of the research projects are focused on high temperature PEM operation since this is the shortcut way to reduce the cost by decreasing the need for precious catalyst and the need for cooling systems. Current PEMFC systems at a maximum of $80^\circ C$ limited by the properties of the current state-of-the-art membrane. The cost of fuel cell power systems must be reduced before they can be competitive with conventional technologies. For transportation applications for instance, a fuel cell system should cost about $\$30/kW$ for the technology to be competitive. For stationary systems, the acceptable price seems to be in the range of $\$400-\$750/kW$ (Gasteiger et al.,2003).

The durability of fuel cell systems is questionable since there are not wide experiences on long-term operation. They must achieve the level of durability and reliability of current automotive engines which is around 5,000 hour of operating life which corresponds to about 150,000 miles of distance.

Size and weight should be reduced for transportation applications. This means the management systems must be designed very well. These sub-systems are particularly systems for managing the air, heat and water. For air management new compressor technologies and designs are needed, but thermal and water management problem can be simplified by improving the fuel cell itself. The small difference between the operating and ambient temperatures causes the need for large heat exchangers. The low operating temperature of PEM fuel cells limits the amount of heat that can be effectively utilized in combined heat and power applications.

As can be noticed from the above information the critical problem today in front of the commercialization of fuel cells is the high-temperature operation, which can reduce the cost from number of points such as decrease in catalyst use, simpler system design and effective heat utilization. For this purpose the most important and critical component to be improved is the membrane since it is one of the expensive components and limits the temperature to 80 °C today.

The membrane only allows the protons, not the electrons (also other reactants) to pass through to the cathode side, so the electrons flow through an external circuit in the form of an electric current. Protons migrate from anode to cathode through membrane and electrochemically combine with oxygen to form water. Therefore, the proton conductivity property of the membrane is its most important characteristic.

The polymer electrolyte membrane is a solid, organic polymer, usually poly[perfluorosulfonic] acid (PFSA). In the 1960s when the development of fuel cells was driven by space programs in the US, the PEM materials were crosslinked, sulfonated polystyrenes. Sulfonated fluorocarbon membranes such as Nafion, which was introduced by DuPont in the early 1970s, then started to be used widely instead. Today, Nafion remains the

industry standard, but such materials have the disadvantage of being costly to produce and require heat, high pressure and a high level of hydration to work effectively. Nafion consists of three regions: As it can be seen in Figure 1.2, first region is a teflon-like, fluorocarbon backbone, hundreds of repeating $-CF_2 - CF - CF_2 -$ units in length. Second region is the side chains, $-O - CF_2 - CF - O - CF_2 - CF_2 -$, which connect the molecular backbone to the third region, the ion clusters consisting of sulfonic acid ions, SO_3H^+ .

The negative ions, SO_3^- , are permanently attached to the side chain and cannot move. However, when the membrane becomes hydrated by absorbing water, the hydrogen ions become mobile. Ion movement occurs by protons, bonded to water molecules, hopping from SO_3^- site to SO_3^- site within the membrane. Because of this mechanism, the solid hydrated electrolyte is an excellent conductor of hydrogen ions.

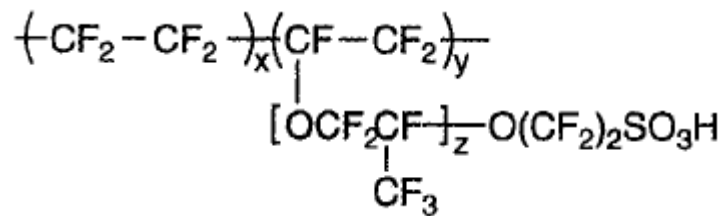


Figure 1.2. Chemical structure of Nafion (Savadogo, 1998)

Despite of these good properties, Nafion and other perfluorinated sulfonic acid (PFSA) membranes have the drawbacks of being costly, being temperature limited because of hydration dependence, and having high methanol crossover properties. Nafion costs more than $\$600/m^2$, which is too high for fuel cell applications in electric vehicles (Appleby, 1999).

The main objective of this study was to develop and characterize novel, cost effective proton exchange membranes for fuel cell applications particularly for PEMFC and DMFC types. The new membranes must satisfy two major criteria which are the cost and the performance under the scope of the introductory information given above.

For the cost criterion, non-fluorinated aromatic hydrocarbon based engineering polymers such as polyethersulfone (PES) and polyetheretherketone (PEEK) which are commercially available were selected as the starting materials but they must be modified by sulfonation for proton conductance and hydrophilicity. Post-sulfonation is a relatively cost-effective and practical method compared to monomer sulfonation. Therefore, the aim of this part of the study was to achieve high sulfonation degrees (DS) and to optimize the sulfonation conditions. During the development of an advanced material, characterization methods, which are crucial for R&D, also adds to the final cost. Therefore, preferring cheaper and practical methods in a logical sequence can also decrease the cost as will be explained later.

For the performance part, both composite and blending approaches were used. Since the most important parameter that affects the final performance of the PEM is the proton conductivity, sulfonation level should to be kept as high as possible. But high DS has a negative effect on the chemical, mechanical and hydrolytic stability so various inorganics can be incorporated in the polymer matrix to help retaining water and increasing the proton conductivity at low DS values. This made the objective of this part clear which was to investigate the effect of inorganic fillers on the proton conductivity of the membranes. Besides, blending with unsulfonated polymers were also investigated since they were shown to have a positive affect particularly on the hydrolytic stability.

Fabrication and characterization of proton exchange membranes includes many steps from the beginning to the end, and each step has critical importance on the final performance of the product and for the evaluation and understanding of the critical parameters. Therefore, each step during modification or characterization has to be performed carefully and also the parameters that may affect these steps should be examined carefully. This brings out the need for a systematic development and characterization methodology, which was also aimed to be established during the study period. Final performance is the power output obtained in a single fuel cell. However, a single cell test is expensive since noble metal catalysts, gases and other materials are consumed and since it is time consuming. Therefore, proton conductivity and stability tests should be performed before the final step. Special attention to proton conductivity measurements was given in the study since the values reported in the literature varies for the similar materials. For this purpose, all factors that may affect the proton conductivity measurements were tried to be investigated and a standard conductivity measurement procedure was used.

CHAPTER 2

LITERATURE SURVEY

2.1 Fuel Cells

2.1.1 History

In 1839, Sir William Grove (1811-1896) who was a British amateur physicist demonstrated the fuel cell principle in his experiment. In his demonstration four cells containing both hydrogen and oxygen in contact with platinum strips using dilute sulfuric acid as the diaphragm were used to produce electricity which is then used to split the water in the upper cell into hydrogen and oxygen (Figure 2.1) (Thomas, 2001). Christian Friedrich Schönbein was also studying on fuel cell independently in the same years (Barbir, 2005).

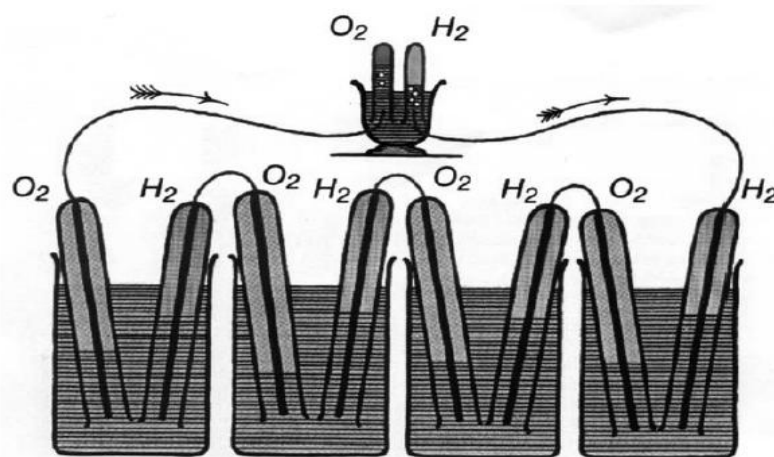


Figure 2.1. First Fuel Cell Demonstration by William Grove in 1839 (Thomas, 2001)

After the first demonstration, with the invention of internal combustion engine scientists focused on this technology and for about 100 years no progress on fuel cells was reported. In 1937, Francis T. Bacon has started working on fuel cells and in 1950's he developed a 5kW fuel cell (Barbir, 2005). In the early 1960's, first application of polymer electrolyte membrane (PEM) fuel cells developed by General Electrics was performed in the Gemini space program. This was followed by the Apollo Program which used fuel cells to supply electricity and drinking water (Barbir, 2005). For a long time fuel cells were considered mainly in space programs since the technology was expensive. However, after 1990's, fuel cells have found other application areas. In 1989, the first polymer electrolyte fuel cell (PEMFC) powered submarine was demonstrated by Ballard, Perry Energy systems and an emerging Canadian company, then in 1993, Ballard established fuel cell powered busses and in the same year the first passenger car running on fuel cell power was produced by Perry energy systems (Barbir, 2005). This took the attention of other car companies on fuel cells and almost every major car company started to develop prototypes powered with fuel cells. Fuel cell applications were also broadened to portable devices such as cellular phones, laptops and military equipments in the recent years. Since establishing hydrogen infrastructure and developing large scale systems are difficult and expensive long term projects it is expected that this technology will be a part of everyday life with portable applications first.

Parallel to the historical development of the technology, there has been an increasing interest on fuel cell research in the recent years in both academic and commercial communities. Below are some of the important dates on the timeline of fuel cell development particularly from the point of electrolyte membrane.

- 1839; William Grove: *Foundations of Fuel Cell Technology*
- 1960's; *Gemini Space Programme (NASA): First polymer electrolyte membrane fuel cell (PEM-FC) applications and usage (1 kW system), polystyrene based short-life membranes with sulfonic acid groups*
- *End of 1960's; Perflourinated sulfonic acid membranes developed for chlor-alkali industry; Nafion (DuPont)*
- 1988; *Dow Chemical produced Nafion like high performance membrane.*
- 1990's; *Dupont took the production rights of Nafion, Asahi Chemical and Asahi glass produced Aciplex-S and Flemion respectively.*
- *Today: DuPont's Nafion is still the industry standard, but new high temperature membranes are on the way.*

2.1.2 Types of Fuel Cells

The main fuel cell technologies available today are (Table 2.1): PEM (polymer electrolyte membrane fuel cell), AFC (alkaline fuel cell), PAFC (phosphoric acid fuel cell), MCFC (molten carbonate fuel cell), SOFC (solid oxide fuel cell). Alkaline fuel cells, used in the space programmes, incorporate an electrolyte of concentrated potassium hydroxide (KOH) and operate at temperatures around 100 °C. Phosphoric Acid fuel cells, which have an electrolyte consisting of concentrated phosphoric acid (H₃PO₄) and operates between 175-200 °C. Molten Carbonate fuel cells use a molten electrolyte of Li₂CO₃/Na₂CO₃ (operating at about 650 °C). Solid Oxide fuel cells, which typically incorporate a hard, porous metal oxide instead of a liquid electrolyte operate between 600-1000 °C.

Table 2.1. An Overview of Types of Fuel Cells (Thomas, 2001)

Fuel Cell	Electrolyte	Operating Temperature (°C)	Electrochemical Reactions
Polymer Electrolyte Membrane (PEMFC)	Solid organic polymer	30-80	Anode: $H_2 \rightarrow 2H^+ + 2e^-$ Cathode: $\frac{1}{2}O_2 + 2H^+ + 2e^- \rightarrow H_2O$ Cell: $H_2 + \frac{1}{2}O_2 \rightarrow H_2O$
Alkaline (AFC)	Aqueous solution of potassium hydroxide soaked in a matrix	90-100	Anode: $H_2 + 2(OH^-) \rightarrow 2H_2O + 2e^-$ Cathode: $\frac{1}{2}O_2 + H_2O + 2e^- \rightarrow 2(OH^-)$ Cell: $H_2 + \frac{1}{2}O_2 \rightarrow H_2O$
Phosphoric Acid (PAFC)	Phosphoric acid soaked in a matrix	175-200	Anode: $H_2 \rightarrow 2H^+ + 2e^-$ Cathode: $\frac{1}{2}O_2 + 2H^+ + 2e^- \rightarrow H_2O$ Cell: $H_2 + \frac{1}{2}O_2 \rightarrow H_2O$
Molten Carbonate (MCFC)	Solution of lithium, sodium, and/or potassium carbonates soaked in a matrix	600-1000	Anode: $H_2 + CO_3^{2-} \rightarrow H_2O + CO_2 + 2e^-$ Cathode: $\frac{1}{2}O_2 + CO_2 + 2e^- \rightarrow CO_3^{2-}$ Cell: $H_2 + \frac{1}{2}O_2 + CO_2 \rightarrow H_2O + CO_2$ (CO ₂ is consumed at anode and produced at cathode, thus it is included in each side of the equation)
Solid Oxide (SOFC)	Solid zirconium oxide with a small amount of yttria	600-1000	Anode: $H_2 + O^{2-} \rightarrow H_2O + 2e^-$ Cathode: $\frac{1}{2}O_2 + 2e^- \rightarrow O^{2-}$ Cell: $H_2 + \frac{1}{2}O_2 \rightarrow H_2O$

Among the different types of fuel cells the one that has the widest application areas is the Polymer Electrolyte (or Proton-Exchange) Membrane Fuel Cell (PEMFC) because of its moderate operation temperature range and its solid proton-exchange membrane. The PEMFC that use methanol instead of hydrogen as the fuel is called Direct Methanol Fuel Cell (DMFC) and was not included as a separate type in the classification. The schematic and the reactions of DMFC were given below:

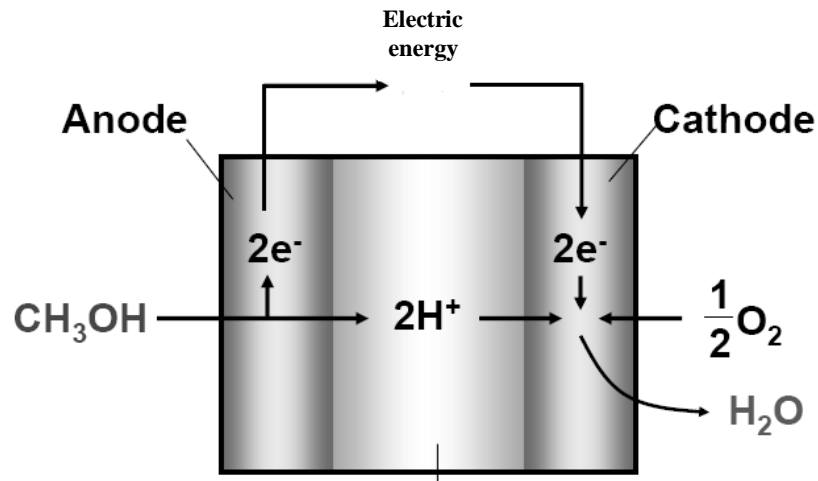
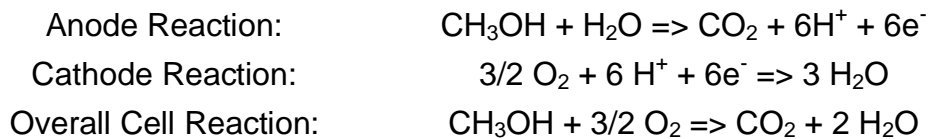


Figure 2.2. Direct Methanol Fuel Cell (DMFC)



2.1.3 Components of Fuel Cells

A single fuel cell mainly consists of, from one end to the other, end plate (gas flow channel), anode (catalyst layer), solid electrolyte (membrane), cathode (catalyst) and end plate again as seen in Figure 2.3. These main components can be slightly different from cell to cell according to the design. For example the catalyst may be coated on the membrane directly or coated on carbon clothes or papers and then pressed to the membrane. In any case, this component which is the heart of the cell is called the membrane-electrode assembly (MEA). MEA is the most important and critical component of the cell. Both the performances of the components alone and the performance of it as a whole depending on the methods of fabrication are critical to the performance of the cell.

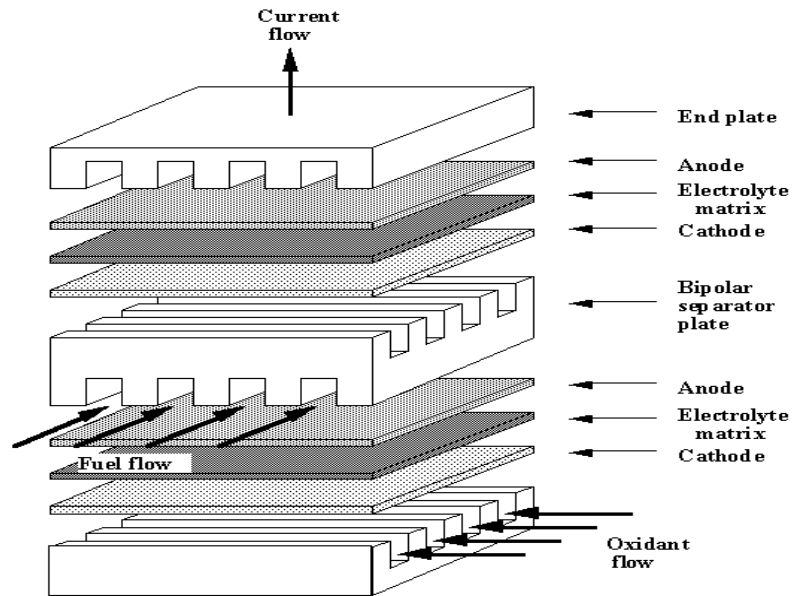


Figure 2.3. Main Components of PEM Fuel Cell

The design of the gas flow channels is also important. Serpentine type is the most accepted design for flow channels. When the single cells are connected in series for obtaining more power it is called a fuel cell stack (Figure 2.4)

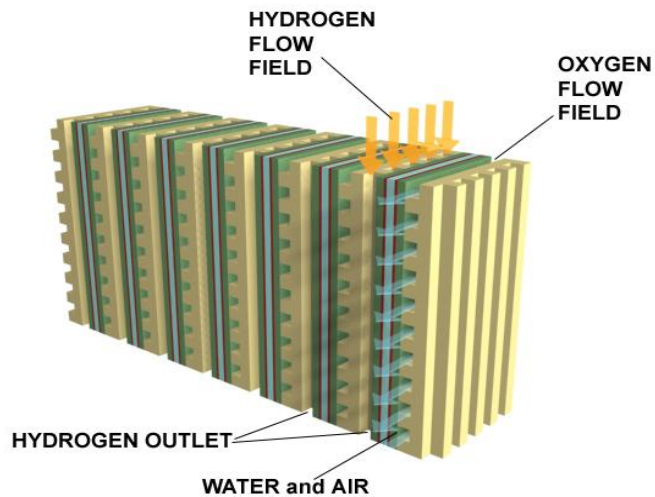


Figure 2.4. PEM Fuel Cell Stack

2.1.4 Why High Temperatures?

In the recent years, massive research studies were conducted to develop membranes that can be used at higher temperatures than the operating temperature of a typical PEM fuel cell with a perfluorosulfonic acid based membrane. As mentioned earlier, one of the limitations for these materials is the temperature range over which water is a liquid. High temperatures are desired for improved electrode kinetics and reduced catalyst poisoning of electrode catalysts by CO that may be found in trace amounts in H₂ produced by reforming. The membrane must contain water that (i.e. must be hydrated) so that the hydrogen ions can carry the charge within the membrane. Operating polymer electrolyte membrane fuel cells at temperatures exceeding 100°C is possible under pressurized conditions, required to keep the water in a liquid state, but this shortens the life of the cell, complicates the system and increases the cost. Perfluorosulfonic acid type Nafion membranes are also not suitable for their high methanol crossover as well as the temperature limitation for direct methanol fuel cells (DMFC). DMFCs look very promising for applications in very small systems, such as cellular phones, laptop computers and other portable electronic devices.

General Motors (GM) automotive system analysis suggested a target that can be achieved for high-temperature membrane operation which is between 110-120°C for H₂-fueled fuel cell vehicles. At this temperature range CO tolerance improves to approximately 50 ppmv CO without air bleed at low anode catalyst loading (0.1-0.2 mg noble metal/cm²) which reduces the purity requirement for on-board stored hydrogen (Springer, 1997). Today a high temperature membrane with a conductivity of 0.1 S/cm at 25% RH (80-120°C) seems to be the most important target for practical applications (Gasteiger, 2003).

2.1.5 Thermodynamics & Efficiency

The reaction between hydrogen and oxygen in a fuel cell is actually an electrochemical reaction consisting of two half-cell reactions. Thermodynamics tells us the maximum electric work that can be obtained is related to the Gibbs-free energy. The overall reaction between hydrogen and oxygen is spontaneous (favorable in forward direction) since the free energy of the products is less than the reactants. The standard free energy change can be calculated from:

$$\Delta G = -nFE_r$$

Where: ΔG is the the free energy change for the reaction and;

n : # of electrons involved in reaction (2)

F : Faradays constant (96500 C/eq)

E_r =Reversible potential

For the standard state (25 °C, 1 atm) ΔG is -229 kJ/mol, so we can calculate that the reversible potential as 1.23 V. This is the value calculated from the maximum useful work associated with the reaction. Another defined potential based on the maximum enthalpy (ΔH) associated with the chemical reaction is called thermoneutral potential, E_t , and is 1.48 V (Srinivasan, 2006).

$$\Delta H = -nFE_t$$

The product, water, of the reaction may be liquid or vapor. The released heat changes according to the state of the product and called higher-heating value (HHV) if it is liquid, lower-heating value (LHV) if vapor. Potential values calculated above are for HHV.

The changes in the potential with respect to temperature and pressure changes can be calculated starting from the basic equation relating Gibbs free energy, enthalpy and entropy change (Srinivasan, 2006):

$$\Delta G = \Delta H - T\Delta S$$

At constant pressure (since variation of ΔH is negligible with temperature), variation of free energy change is:

$$\frac{\partial \Delta G}{\partial T} = -\Delta S$$

Combining this equation with $\Delta G = -nFE_r$:

$$\frac{\partial E_r}{\partial T} = \frac{\Delta S}{nF}$$

The reversible change at any temperature can be calculated using the entropy change of the fuel cell reaction from the equation above. Similarly, Reversible cell potential can also be expressed as a function of pressure by using the basic thermodynamic relationship between Gibbs free energy change and volume change; $dG=VdP$:

$$E_P = E_{P_0} - \frac{1}{nF} \int_{P_0}^P \Delta V dP$$

Where; E_P and E_{P_0} are the cell potentials at pressure P and P_0 respectively. For gaseous reactants and products, the effect of pressure on cell potential is important. But generally, temperature is the more important parameter and pressure is fixed at atmospheric pressure since high pressure operations increases the system complexity and cost. Below

a set of thermodynamic values of the PEM Fuel Cell Reaction calculated at various temperatures were given in Table 2.2 (Yang, 2004).

Table 2.2. Thermodynamic Values of the PEM Fuel Cell Reaction at Various Temperatures (Yang, 2004)

H₂ + 1/2O₂ → H₂O						
1 bar reactant pressure (standard conditions)						
Temp	product H₂O phase	Δ H_{rxn} (kJ/mol)	Δ G_{rxn} (kJ/mol)	η theoretical	E_{tn} (V)	E_{rev} (V)
25°C	LHV (vapor)	-241.8	-228.6	94.5%	1.253	1.185
	HHV (liquid)	-286	-237.3	83%	1.482	1.229
80°C	LHV	-242.3	-226.2	93.3%	1.256	1.172
	HHV	-283.8	-233.7	82.3%	1.471	1.212
130°C	LHV	-242.8	-223.9	92.2%	1.258	1.160
	HHV	-282.1	-230.4	81.7%	1.462	1.195
200°C	LHV	-243.8	-219.1	89.8%	1.259	1.131
600°C	LHV	-247.2	-198.1	80.1%	1.277	1.023
1000°C	LHV	-249.4	-175.8	70.5%	1.288	0.908

As it was stated before, fuel cells are more efficient than the conventional internal combustion engines (about two-fold) since chemical energy is directly converted to electric energy. The definition of the efficiency for an energy conversion device is simply the ratio of useful work obtained from the system to the energy input as shown in Figure 2.5 below.

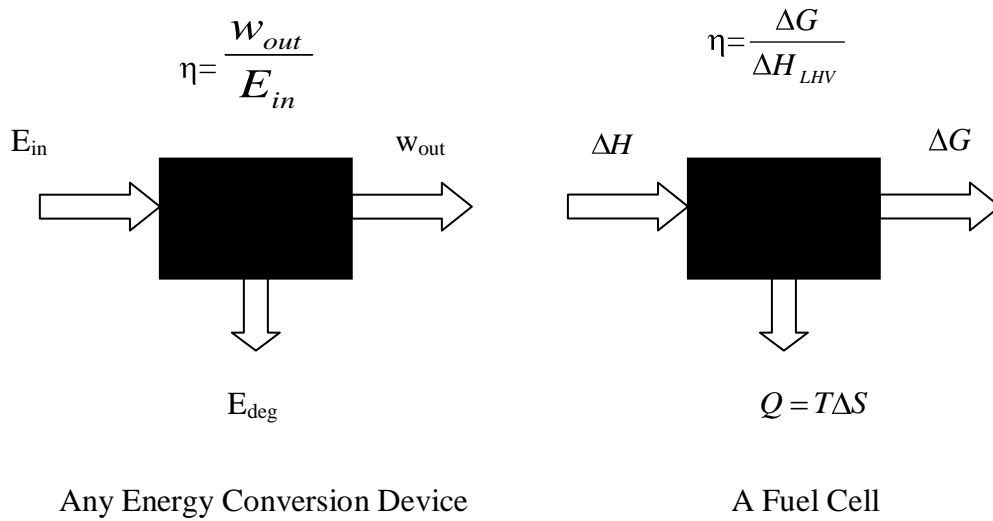


Figure 2.5. Efficiency Definitions of any Energy Conversion Device & a Fuel Cell

By using the $\Delta G = -237.3$ kJ/mol $\Delta H = -286$ kJ/mol values from Table 2.2, the maximum possible (theoretical) efficiency of a PEMFC can be calculated to be 83%. This efficiency is also called the reversible efficiency (η_r) and there are two other definitions of efficiency used which are the voltage efficiency (η_v), the ratio of voltage at a given current density, $E(i)$ to the reversible potential (E_r), and current efficiency (η_i), the ratio of measured current density (i_f) to the theoretical current (i_t) if all the fuel is oxidized at the anode. The product of these three efficiencies is sometimes used for expressing the total efficiency.

$$\eta_r = \frac{\Delta G}{\Delta H} \quad ; \quad \eta_v = \frac{E(i)}{E_r} \quad ; \quad \eta_i = \frac{i_f}{i_t}$$

$$\eta = \eta_r \eta_v \eta_i$$

2.1.6 Kinetics & Losses

Actual voltage that can be obtained from a single fuel cell is always lower than the theoretical maximum voltage calculated in the preceding section because of number of losses, which can be categorized under three main headings: Activation-related losses; ohmic losses and mass-transport-related losses.

Activation-related losses: These losses are caused by the activation energy needed for the electrochemical reactions at the electrodes. These losses depend on the reactions, the performance of the catalysts; electrocatalyst material and microstructure, reactant activities, and on current density.

Ohmic losses: These losses are caused by ionic resistance in the electrolyte and electrodes; electronic resistance in the electrodes, current collectors and contact resistances. Ohmic losses are proportional to the current density, so can be calculated with current interrupt method. They depend on materials used, stack geometry, and on temperature.

Mass-transport-related losses: These losses are related to the mass transport limitations i.e. relative rates of the reactants to the oxidation or reduction rates and depend strongly on the current density, reactant activity, and electrode structure.

All three types of losses can be followed from the Figure 2.6 showing a typical activation-polarization curve (also called V-I curve).

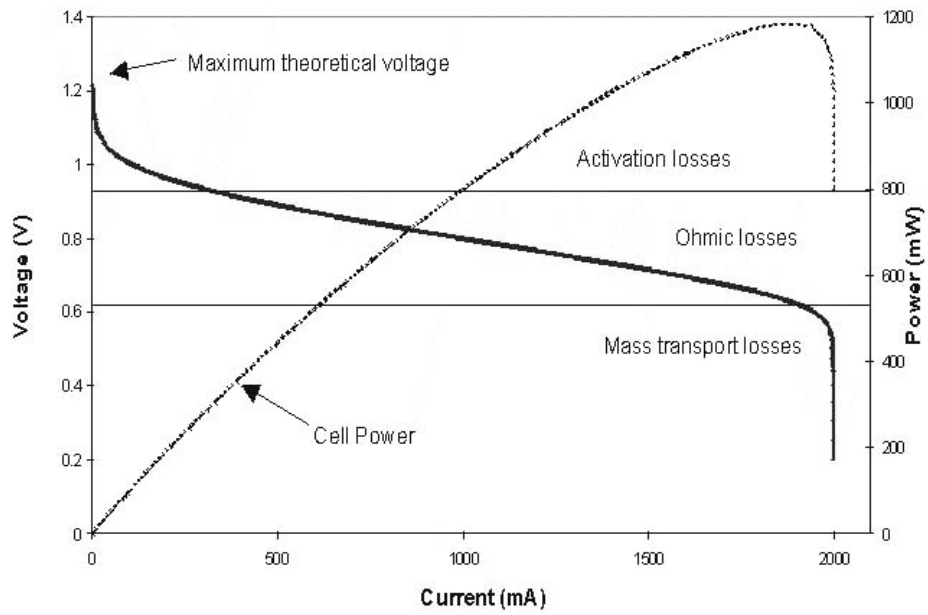


Figure 2.6. A Typical fuel cell polarization curve (Fuel Cell Handbook, 2000)

Below these losses will be explained in more detail:

Charge-transfer Losses:

When current is drawn from the cell voltage deviates from the rest voltage similar to that in batteries. The reason for this is the occurrence of so called overpotentials (polarizations) at the electrode relative to the rest potential of the respective electrode: $\eta_D = U_0 - U$. For the the activation-related charge transfer overvoltage, the reason is the finite velocity of the electron transfer through the phase boundary electrode/electrolyte. Current density and charge transfer overvoltage are related in an exponential fashion, which is known as the Butler-Volmer equation:

$$i = i_+ - |i_-| = i_0 \left(\exp \left[\frac{\alpha z F}{RT} \eta_D \right] - \exp \left[- \frac{(1 - \alpha) z F}{RT} \eta_D \right] \right)$$

Where:

i : current density [A/cm^2]

i_0 : exchange current density [A/cm^2]

i_+ : anodic partial current density of the electrode [A/cm^2]

i_- : cathodic partial current density of the electrode [A/cm^2]

α : a symmetry factor related to the anodic and the cathodic reaction

z : number of electrons which are transferred during the electrode reaction

F : Faraday constant [$F = 96487 \text{ C/mol}$]

η_D : charge transfer overvoltage [V]

At the interface of electrode/electrolyte a dynamic equilibrium is established, at the equilibrium potential ($\eta_D=0$), charge carriers are still crossing the phase boundary although no external current passes through the electrode. The current at $\eta_D=0$ which are equal in both directions is called the exchange current density i_0 and represents a measure for the velocity with which the equilibrium is established. Generally, compared with the oxygen reduction the exchange current densities of the hydrogen oxidation reaction are 3 to 4 orders of magnitude larger.

The importance of the Butler-Volmer equation becomes clear when its limiting forms are investigated. For very small overvoltages (smaller than 0.01 V):

$$\frac{\eta_D F}{RT} \ll 1 \quad \Longrightarrow \quad \eta_D = \frac{RT}{zF} \frac{i}{i_0}$$

For a large overvoltage (larger than 0.1 V) which is positive, the second expression in the Butler-Volmer equation becomes negligibly small. Then:

$$i = i_0 \exp\left[\frac{(1-\alpha)\eta_D z F}{RT}\right]$$

If we put this in a semi-logarithmic form then the resulting equation is called Tafel equation:

$$\eta_D = -\frac{RT}{\alpha z F} \ln i_0 + \frac{RT}{\alpha z F} \ln i$$

In electrochemistry of batteries conventionally, anodic currents are assigned positive (oxidation) and cathodic currents negative (reduction). The Tafel Slope, $RT/(\alpha z F)$ for oxidation and $RT/((1-\alpha)zF)$ for reduction is an important quantity to characterize an electrochemical reaction since it helps commenting on the reaction mechanism.

The Ohmic Losses:

The ohmic loss in the cell consists of the resistance to ionic transport in the electrolyte and the electrode, and the resistance to electron transport through the electrode material, the current distributing structure and the wires. The ohmic overvoltage is linearly related to the resistance:

$$\eta_{Ohm} = i_{eff} R_{Ohm}$$

Where: i_{eff} is the current density and R_{Ohm} is the total resistance of the cell which is composed of the electronic, the ionic and the contact resistance.

Mass-Transport (Concentration Overpotential) Losses:

Mass transport processes close to the electrode are due to diffusion which can be described by the Fick's Law:

$$n_i = -D_i \nabla c_i$$

In one dimension and with the assumption of linear concentration profile it can be integrated to give:

$$n_i = D \frac{(c_0 - c_s)}{\delta}$$

Where: n_i : flux of the species I [mol/s]

c_0 : bulk concentration [mol/dm³]

c_s : surface concentration [mol dm⁻³]

δ : thickness of the Nernstian diffusion layer [cm]

D: diffusion coefficient [cm²/s]

When current flows, according to Faraday's Law, equal amounts of charge are transported by mass transport in the electrolyte and electron transport in the electrical conductors:

$$n = \frac{i}{zF}$$

Combining these two equations:

$$i = zFD \frac{(c_0 - c_s)}{\delta}$$

The maximum current density with which a fuel cell can be operated is reached when the reaction on the electrode surface is so fast with respect to the mass transport so that the concentration at the electrode surface, c_s , is zero. This current density is called the limiting current:

$$i_L = zFD \frac{c_0}{\delta}$$

Then, the concentration overvoltage caused by the mass transfer can be calculated from the difference between the concentration dependent electrochemical potential in the electrolyte and at the electrode given below respectively:

$$E = E^0 - \frac{RT}{zF} \ln c_0 \qquad E_s = E^0 - \frac{RT}{zF} \ln c_s$$

So, finally concentration overvoltage loss can be formulated as:

$$\eta_{Conc} = E - E_s = \frac{RT}{zF} \ln \frac{c_s}{c_0}$$

Combining with Fick's Law:

$$\eta_{Conc} = \frac{RT}{zF} \ln \left(1 - \frac{i\delta}{zFDc_0} \right)$$

Finally, the potential after overpotential losses can be formulated as follows if the overpotentials of charge-transfer and concentration are combined for anode and cathode separately:

$$\eta_A = \eta_{D,A} + \eta_{Conc,A}$$

$$\eta_C = \eta_{D,C} + \eta_{Conc,C}$$

$$U = U_{rev} - \eta_A - \eta_C - \eta_{Ohm}$$

2.2 Alternative Membranes

As discussed before PFSA membranes have some drawbacks such as high production cost, fluorinated production process and low glass transition temperature around 110-130°C which limits the fuel cell operating temperature to below 100°C. Therefore, a number of alternatives have been investigated in the last decades. Membrane materials alternative to Nafion can be classified in four groups: 1) Modifications of perfluorinated polymers, 2) sulfonated thermostable polymers based on hydrocarbon backbones containing an aromatic ring, 3) blends of polymers with acids, and 4) composites including filled polymers, polymer blends, and organic/inorganic membranes (Libby, 2001). Modifications of PFSA membranes still have the problem of high cost and fluorinated production but can be thought for a shortcut solution for the need of increase of operation temperature. However, best solution seems to concentrate on cheap and commercially available aromatic hydrocarbon based membranes and their composites and/or blends. In the following sections research on some of the aromatic hydrocarbon polymers, their composites

filled with various inorganic fillers and their blends investigated in the literature will be summarized.

2.2.1 Properties of a Good Membrane

According to the fundamentals given in the preceding sections, properties of a good membrane may be summarized as follows:

- *High proton conductivity ($> 1 \times 10^{-2} \text{ S/cm}$)*
- *Good conductivity above $100 \text{ }^\circ\text{C}$*
- *Low methanol crossover ($< 1 \times 10^{-7} \text{ cm}^2/\text{s}$ diffusion coefficient)*
- *High ion exchange capacity ($> 1.0 \text{ meq/g}$)*
- *Low water swelling ($< 30\%$ per dry weight)*
- *Good mechanical, chemical, and thermo-oxidative stability*
- *That can operate at high temperatures ($>80 \text{ }^\circ\text{C}$)*

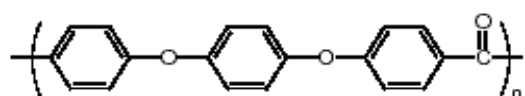
In this list, some values, especially proton conductivity and methanol crossover values can vary from method to method. Therefore, for a healthier comparison Nafion should be used as a reference material in the same experimental conditions and method used.

2.2.2 Non-Fluorinated Aromatic Hydrocarbon Polymers

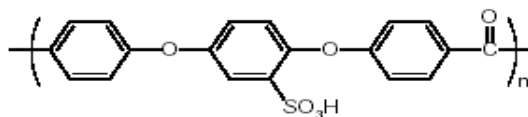
There are large number of non-fluorinated aromatic hydrocarbon polymers that can be alternative to PFSA membranes, however number of them are commercially available and investigated for some of their properties in the literature. Among them, highest number of researches were performed on polyetherketones (PEK) since they can be relatively easily sulfonated. Polysulfones were also investigated but very less compared to PEK family. These two are thermally and chemically very stable high performance engineering plastics, which have a wide range of applications from plastic components industry, electronics industry, and membrane industry such as desalination, pervaporation, gas separation, reverse osmosis etc., they are primarily candidates for medium temperature (80-120 °C) operations, but have the possibility to be modified and used at higher temperatures by incorporation of inorganic fillers or blending with other compatible polymers. Third group is particularly candidate for high temperature (>150 °C) applications since their proton conduction mechanism is based on a liquid electrolyte, phosphoric acid, doped on them. This group which has excellent stability at high temperatures is the polybenzimidazole (PBI).

2.2.2.1 Poly(Arylene Ether Ketones) Family

Polyetheretherketone (PEEK) which is the mostly studied member of the poly(arylene ether ketone) family consists of sequences of ether (-O-) and carbonyl (-CO-) linkages and phenyl rings. Scheme 2.1 below shows the chemical structure of PEEK and sulfonated PEEK (SPEEK).



(a)



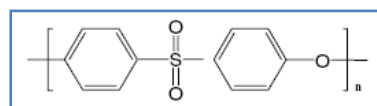
(b)

Scheme 2.1. Structures of (a) PEEK (b) SPEEK

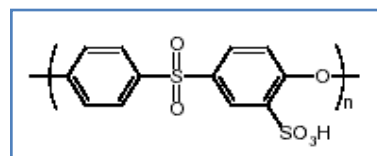
They have potential for fuel cell applications for their high thermal and chemical stability, mechanical strength and improvable proton conductivity via sulfonation (Zaidi, 2000). Their sulfonated form was first used for water electrolysis and first tested for fuel cell application in 1997 (Rikukawa, 2000; Savadogo, 1998).

2.2.2.2 Poly(Arylene Ether Sulfones) Family

Polyethersulfone which is the most common member of this family has a sulfonyl ($-SO_2-$), a carbonyl ($-CO$) and two phenyl groups in its repeating unit as shown in the scheme below. Scheme 2.12 below shows the chemical structure of PES and sulfonated PES (SPES).



(a)



(b)

Scheme 2.2. Structures of (a) PES (b) SPES

2.2.2.3 Polybenzimidazoles (PBI)

Another membrane material being studied is polybenzimidazole (PBI), which is much cheaper and has a much lower permeability for hydrogen than Nafion. There are a lot of research going on to develop this material for use in fuel cells, in particular for use as a polymer electrolyte. PBI, which is a basic polymer, fall into two categories according to the temperature range in which they exhibit their proton conductivity. Phosphoric-acid doped polybenzimidazole (PBI) is a high-temperature membrane that can operate at temperatures up to approximately 200°C (Wainright, 2003). At 200°C, its conductivity is 0.06-0.08 S/cm with a RH of 5-10%. Yurdakul et al. (2007) also synthesized high molecular weight PBI and showed that conductivity close to Nafion can be achieved at high doping levels and at high temperatures (~150 °C). At high temperatures the conductivity of this membrane is very good, however, it decreases rapidly as temperature decreases, to 0.01-0.02 S/cm at 15-30% RH and 80°C. The problem for PBI seems to be the stability in the presence of liquid water (leaching of the acid).

2.2.3 Composite Membranes

The composite membrane approach offers to overcome most of the drawbacks of conventional membranes used today but there is limited published data on these membranes particularly their single cell test data. Generally speaking, in this approach, an inorganic proton conductor is incorporated into a polymer matrix. This approach combines the mechanical stability of the polymer matrix with the high conductivity of solid inorganic proton conductors such as heteropolyacids, zeolites, and layered phosphates (Libby, 2001). In the study of Zaidi et al. (2000) various heteropolyacids were dispersed in sulfonated PEEK to produce membranes giving conductivities of about 10^{-1} S/cm above 100 °C.

Researchers first used composite approach on Nafion. Watanabe et al. (1998) found that the incorporation of platinum, or oxides such as SiO₂ and TiO₂, improves the fuel cell performance due to self humidification. Liu et al. (2003) also studied self-humidifying composite membranes including a multi-layer of nafion-PTFE-and Pt with promising results for dry conditions. There are large number of studies on modified perfluorinated sulfonic acid membranes but it should be emphasized at this point that this material is costly to produce and at high temperatures (above nearly 130 °C) the polymer begins to soften particularly in the presence of methanol.

An example of composite membrane material studied particularly for DMFC is the one prepared with 10% perfluorosulfonic acid (PFSA) solution and boron phosphate (BPO₄) (Mikhailenko et al., 1998). The contents of solid BPO₄ in the composite membrane varied from 10 wt% to 50 % thus decreasing the PSFA ionomer, which would result a decrease in the cost of the membranes. The conductivity of the composite membranes measured both at room temperature and at higher temperatures, was found to increase with the incorporation of boron phosphate particles into PSFA. In the study the conductivity was observed to increase 2-3 times

and in some cases to very high values at higher temperatures without sacrificing its flexibility. The characterization techniques for the membrane used in those studies were x-ray diffraction, differential scanning calorimetry and scanning electron microscopy. The glass transition temperature was also found to increase with increasing of BPO_4 content.

Another group incorporated zeolites (4A and Beta) and fumed silica in Nafion and SPES-40 membranes (Bac et al., 2004). They synthesized Nafion membranes using an evaporation and recasting technique and SPES-40 membranes by dissolution of the polymer in the solvent DMAc. The inorganic additives were incorporated into the Nafion and SPES-40 solutions using ultrasonication and the solutions cast on glass surface in this study. With a loading of 15% silica, conductivity of the composite membrane was found to be higher than recast Nafion 117 at low relative humidity (Rogers, 2004).

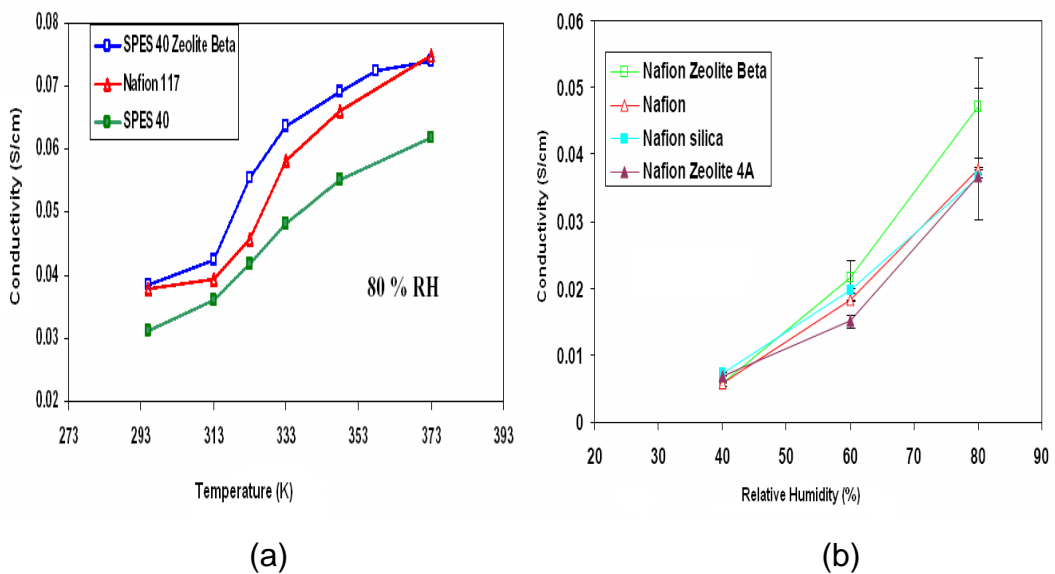


Figure 2.7. (a) Conductivity (S/cm) of SPES-40 composite membranes as a function of temperature (K). (b) Conductivity (S/cm) of Nafion based composite membranes at room temperature (Rogers, 2004)

A summary of some of the inorganic-organic composite membranes under development was given in Table 2.3.

Table 2.3. Summary of some Inorganic-Organic Composite Membranes investigated

Polymer Matrix	Inorganic Filler	Results	Reference
SPEK-SPEEK	ZrP + (SiO ₂ , TiO ₂ , ZrO ₂)	Reduced methanol crossover	Nunes et al., 2002
SPEEK	SiO ₂ , ZrP, Zr-SPP	0.09 S/cm at 100°C, 100% RH	Bonnet et al., 2000
SPEEK	HPA	10 ⁻¹ S/cm above 100°C	Zaidi et al., 2000
SPEEK	BPO ₄	5×10 ⁻¹ S/cm, 160°C, fully hydrated	Mikhailenko et al., 2001
SPEEK	SiO ₂	3-4×10 ⁻² S/cm at 100°C, 100%RH	Rozière et al., 2000
SPSF	PWA	0.15 S/cm at 130°C, 100%RH	Hickner et al., 2001
SPSF	PAA	2×10 ⁻² S/cm, 80°C, 98% RH	Genova-Dimitrova, 2001
SPSF	PAA	H ₂ /O ₂ cell, 500 h at 80°C & 4 bars	Baradie et al., 1998
PBI	ZrP + H ₃ PO ₄	9×10 ⁻² S/cm at 200°C, 5% RH	He et al., 2002
PBI	SiWA + SiO ₂	2.2×10 ⁻³ S/cm at 160°C, 100% RH	Staiti et al., 2001
PBI	PWA + SiO ₂ +	Td > 400°C; 1.5×10 ⁻³ S/cm at 150°C,	Staiti et al., 2000
SPES-40	-	0.139 S/cm, 85 °C 100%RH	Ma et al., 2003

The composite membrane approach offers to overcome most of the drawbacks of conventional membranes used today but there are limited published data on these membranes, particularly single cell test data.

Generally speaking, in this approach, an inorganic filler having properties of proton conductance and/or hygroscopicity is incorporated into a polymer matrix. This approach combines the mechanical stability of the polymer matrix with the high conductivity of solid inorganic proton conductors such as heteropolyacids, zeolites, and layered phosphates (Libby et al., 2001). In the study of Zaidi et al (2000) various heteropolyacids were dispersed in sulfonated PEEK to produce membranes giving conductivities of about 10^{-1} S/cm above 100 °C.

To summarize, the reported benefits of organic/inorganic composite membranes include increased conductivity at low relative humidity and high temperatures, increased mechanical strength, and lower water swelling. Several sulfonated polymer/inorganic composite systems have been investigated in the literature, but there has been little information of single cell test data, the transport properties of these organic/inorganic composites and also there has been little data on how the inorganic additives function in the composites. Because of the very high proton conductivity values of heteropolyacids (HPAs) as solid proton conductors, they have been utilized in heterogeneous catalysis and also in fuel cell researches in the recent years.

Zaidi et al. (2000) investigated the effects of HPAs in sulfonated PEEK. They reported that an increase in degree of sulfonation as well as introduction of these fillers resulted in increased T_g and enhanced membrane hydrophilicity, resulting a gain in proton conductivity. The conductivity of the composite membranes they prepared exceeded 10^{-2} S/cm at room temperature and reached values of about 10^{-1} S/cm above 100 °C.

Immobilization method of HPAs can be covalent binding, adsorption, ion-pair formation or the entrapment of the molecule so called “ship-in-a-bottle” process. Applicability of these methods are restricted except covalent bonding which has a broad application area. In the “ship-in-a-bottle” process which has gained interest in the recent years particularly for zeolites as the ship, the problem may be the size of the molecule to be “entrapped” and the possibility of diffusion outside.

2.3 Sulfonation

Sulfonation reaction is a typical electrophilic substitution reaction in which an $-\text{SO}_3\text{H}$ group is “attached” to the molecule. It is necessary for the proton transfer through the membrane. The reaction conditions, sulfonating agent and the polymer to be sulfonated are important factors for the sulfonation degree to be achieved.

Sulfonation reaction is used widely for changing the character of the polymers for different applications. Hydrophobic materials can be made hydrophilic by introducing the cationic $-\text{SO}_3\text{H}$ group, this is important for applications such as reverse osmosis, electrolysis, membrane separations, pervaporation, purification with ion exchange etc..

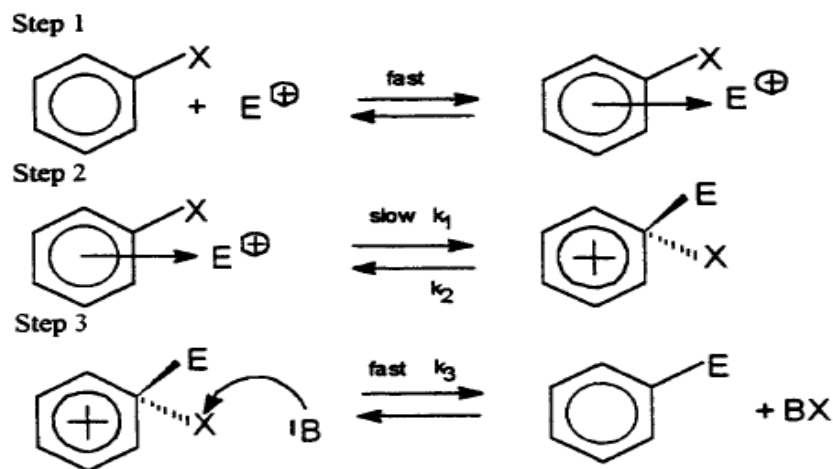
For sulfonation two routes can be followed. The first is the relatively cheap and easy method of post sulfonation in which the polymer is sulfonated by common suitable sulfonating agents such as H_2SO_4 , SO_3 , and its complexes, such as acyl and alkyl sulfates and chlorosulfonic acid. Temperature, acid to polymer ratio, and reaction time are the important parameters affecting the degree of sulfonation in this method. Second route is to sulfonate the monomer first and then polymerization of this

sulfonated monomer. This method is more tedious but the advantage is more control on the sulfonation particularly for the positions of the attached $-\text{SO}_3\text{H}$ group.

In the important review for sulfonation of polymers, Kucera et al (1998) states that sulfonation proceeds easily for the aromatics, even though the dissociation energy of the C-H bond is higher in aromatic (428 kJ/mol) than in aliphatic (374-384 kJ/mol) compounds and the reason for this was explained by the two-step reaction mechanism where the rate of SO_3 insertion to hydrocarbons alone cannot control the reaction rate. Besides, they also stated that one, two, or three $-\text{SO}_3\text{H}$ groups may be attached to one carbon atom of the aliphatic chain, whereas only one $-\text{SO}_3\text{H}$ group may be attached to the carbon atom of an aromatic ring.

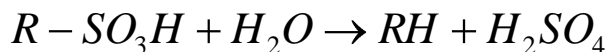
Sulfonating agents can be categorized by the type of the reaction they participate. These are: 1) Sulfonating agents derived from sulfur trioxide including sulfuric acid, chlorosulfonic acid, fluorosulfonic acid, free sulfur trioxide and its complexes, halogen derivatives of sulfuric acid etc. 2) Nucleophilic agents such as sulfites and hydrogen sulfites, and sulfur trioxide 3) Radically reacting agents: sulfurylchloride (SOCl_2), blends of gases: sulfur dioxide and chlorine etc. The first group reagents are frequently used for sulfonation of aromatics since they exhibit most effective sulfonation capability (Kucera, 1998). The sulfonation can be carried on under heterogeneous or homogeneous conditions.

General mechanism of the sulfonation reaction is as follows:

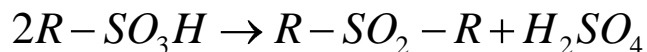


Scheme 2.3. General mechanism of the sulfonation reaction Step 1.: Formation of the π -complex, Step 2.: Formation of the arenium ions (σ -complex), Step 3: Termination of the sulfonation by the release of X^+ (Kucera, 1998)

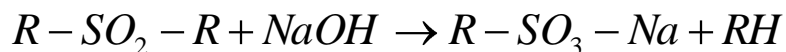
Two other possible side reactions that can occur during sulfonation are desulfonation and crosslinking reactions as can be followed from the schemes following.



Desulfonation by a reaction with water (hydrolysis)



Crosslinking reaction



Decomposition of sulfones

Scheme 2.4. Possible Side Reactions During Sulfonation

As stated before, sulfonation of polymers can be carried out under either homogeneous or heterogeneous mediums. In homogeneous sulfonation the polymer first dissolved in a suitable solvent that would not interact with the sulfonating agent. This method is advantageous from the point of homogeneity of the sulfonation, however, the possible solvent interactions and the possible difficulties for separating the sulfonated product from the mixture are the potential problems. In heterogeneous sulfonation, the sulfonating agent also serves as a solvent, in the typical examples solid polymer is dissolved in the sulfonating agent quickly and then the sulfonation reaction is carried on under the desired reaction conditions. The disadvantage of this method is the possibility of heterogeneous sulfonation especially at the dissolution period of the polymer. To decrease the heterogeneous sulfonation, the dissolution period must be kept as short as possible.

The reaction parameters, suitable sulfonating agents and the kinetics of the reaction widely differ with the characteristics of the polymer to be sulfonated. Therefore, in the following two section studies on the sulfonation of the PEEK and PES will be reviewed separately.

2.3.1 Sulfonation of Polyetheretherketone (PEEK)

Most of the sulfonating agents can be used for the sulfonation of PEEK since its sulfonation is relatively easy. Chlorosulfonic acid (CSA) and complexes of SO_3 can be used for a fast sulfonation but they may cause polymer degradation by breaking the main polymer chains or may cause crosslinking side reactions. Also the control of the degree of sulfonation would be difficult. Therefore, mild sulfonating agents such as sulfuric acid with a concentration of 95-98% were used commonly. The sulfonation rate of PEEK in sulfuric acid can be controlled by changing the reaction time

and the acid concentration and so can provide a sulfonation range of 30 to 100% without degradation and crosslinking reactions (Bishop, 1985).

Kobayashi et al (1998) sulfonated Poly(oxy-1,4-phenylene-oxy-1,4-phenylene-carbonyl-1,4-phenylene) (PEEK) and poly(4-phenoxybenzoyl-1,4-phenylene, Poly-X 2000) (PPBP), by using 95% sulfuric acid at room temperature and 10g/100 mL polymer to acid ratio in order to convert these polymers to proton-conducting polymers. They determined the DS by elemental analysis and back titration. They reported that above 30% sulfonation, the S-PEEK polymers were soluble in DMF, dimethylsulfoxide (DMSO), or N-methylpyrrolidone (NMP); above 70%, they were soluble in methanol and at 100%, in water. The reported DS change for PEEK with time of reaction is given in Figure 2.8.

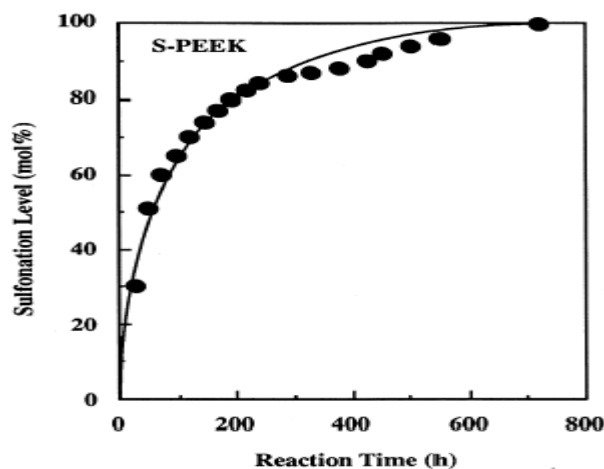


Figure 2.8. Sulfonation level of PEEK as a function of reaction time at room temperature (Kobayashi et al,1998)

At room temperature, the sulfonation of PEEK proceeds slowly and takes several days to achieve moderate sulfonation levels (DS over 50%). Time of reaction required to achieve the same DS drop to several hours at

elevated temperatures around 50 °C (Huang, 2001). However, at this temperature controlling the DS and achieving reproducible DS values is difficult as can be seen from the figure below.

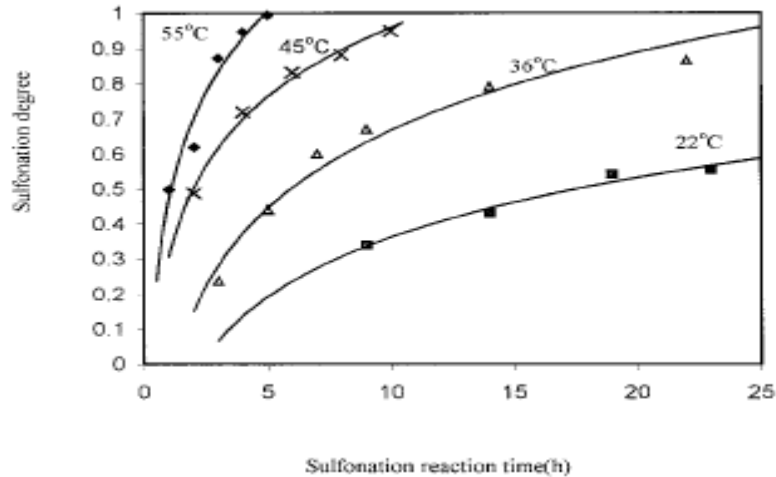


Figure 2.9. Degree of Sulfonation (DS) vs Sulfonation Reaction Time (Huang et al., 2001)

According to the study the sulfonated polymers containing 65 mol% sulfonic acid showed high through-plane proton-conductivities of 10^{-2} – 10^{-4} S/cm at room temperature and PPBP showed more stable conductivities at high temperatures compared to PEEK. 80% sulfonated PEEK's decomposition temperatures were slightly above 300 °C whereas that of PPBP's were above 200 °C.

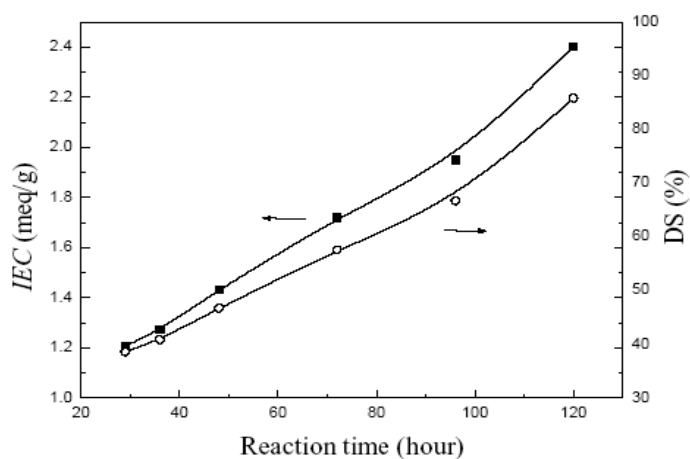


Figure 2.10. Influence of reaction time on the DS and IEC values of PEEK sulfonated at room temperature (Li et al., 2003)

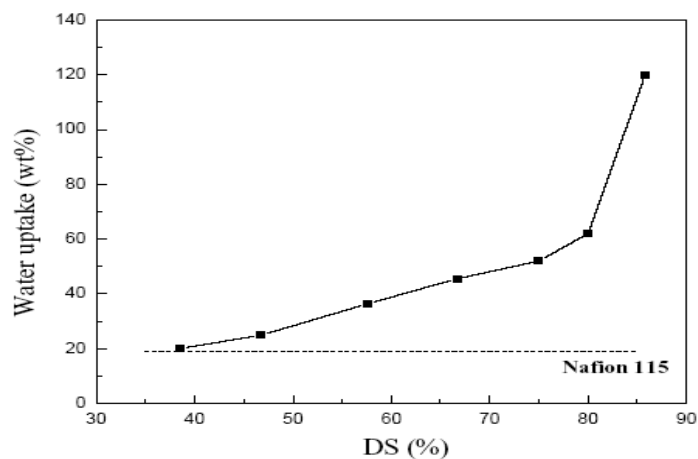


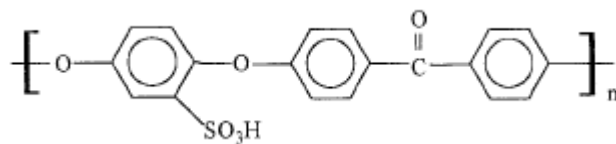
Figure 2.11. Water uptake as a function of Degree of sulfonation (DS) for SPEEK polymer at room temperature (Li et al., 2003)

Mikhailenko et al (2001) sulfonated PEEK heterogeneously with H_2SO_4 at room temperature in a reaction time varying between 24 to 112 hr in order to increase the sulfonation degree before incorporating BPO_4 to fabricate composite membranes. For achieving the degree of sulfonation (DS)

values of 50, 72 and 80 calculated by titration or elemental analysis, water uptakes (wt.%) of 28, 52 and 54; conductivities (S/cm) of 2×10^{-3} , 14×10^{-3} and 27×10^{-3} were obtained in this study. They also reported that below 45% DS poor conductivity about 10^{-5} was observed.

Chang et al (2003) again sulfonated PEEK with H_2SO_4 but this time they reported that DS values between 30-100% was controlled with varying the time between 4 h and 20 h but also by varying the reaction temperature. 3×10^{-3} S/cm of conductivity and 0.6 V-80 Ma/cm² of performance on the polarization curve were achieved for the SPEEK in this study.

Sulfonation is not only used for fuel cell membranes but also for other membrane applications such as pervaporation and ultrafiltration. It improves membrane properties such as better wettability, higher water flux, higher antifouling capacity, better permselectivity, and increased solubility in solvents for processing in these applications (Huang, 2001). Huang et al (2001) investigated the kinetics of this reaction for PEEK by using H_2SO_4 as the sulfonating agent. They reported that it is a second order reaction and occurs at only the ring shown in the scheme 2.1 at any four positions since the electron density of the other two aromatic rings in the repeat unit is relatively low due to the electrophilic nature of the neighboring carboxyl group. Also the SPEEKs prepared were characterized in terms of ion-exchange capacity (IEC), ¹H-NMR, contact angle, and solubility.



Scheme 2.1. (b) Repeat unit of sulfonated poly(ether ether ketone)

Kaliaguine et al. (2003) sulfonated PEEK with H_2SO_4 with time varying between 14-140 hr and temperatures between room temperature and 80°C . When temperature was increased to $50-80^\circ\text{C}$ the reaction time decreased to several hrs.

Selecting the appropriate sulfonating agent and the reaction conditions for the polymer are two important considerations. In the literature, there is a trend to use sulfuric acid (H_2SO_4) for PEEK and chlorosulfonic acid (ClSO_3H) for polyethersulfone (PES), which are the polymers planned to be studied. PES is difficult to sulfonate because of the electron withdrawing sulfone linkages which deactivate the adjacent aromatic rings for electrophilic substitution. For H_2SO_4 the reaction temperature may be increased but than this may cause polymer degradation and loss of mechanical stability of the polymer. Therefore ClSO_3H which is a stronger sulfonating agent is suggested and used in some recent studies (Kim, 1999; Guan, 2005). Guan et al. used H_2SO_4 as solvent and ClSO_3H as sulfonating agent.

Dissolution time of PEEK in sulfuric acid should be as short as possible to prevent heterogeneous sulfonation. According to Daoust et al (2001) dissolution time of PEEK decreases if polymer is dried.

It is believed that the presence of water decomposes the pyrosulfonate intermediate to inter or intra molecular sulfone crosslinks (Nagarale, 2006). SPEEK should be kept in wet condition to prevent crosslinking (Nagarale, 2006). It has been observed that part of the membranes left in dry conditions (open atmosphere) for a long time become brittle.

2.3.2 Sulfonation of Polyethersulfone (PES)

Polyethersulfone has been investigated for its potential use in pervaporation studies. For pervaporation, similar to the fuel cell application the membrane should be hydrophilic and sulfonation is required. But because of the electrophilic sulfone group in the structure this is not easy.

Byun et al. (2000) used $\text{SO}_3\text{-TEP}$ (triethyl phosphate) (2:1) complex as sulfonating agent and dichloromethane (DCM) as the solvent for PES and carried on the reaction for 4 hours at room temperature and achieved an IEC of 1.08. Researchers confirmed sulfonic acid attachment with FTIR and H-NMR. In the H-NMR spectrum, the proton attached to the aromatic group of 7.28 ppm was shifted downfield to 8.30 ppm. From DSC results they concluded that glass transition temperature was increased for the sulfonated polymer to around 260 °C.

Kerres et al (1996) reported that the poly(aryl ether) sulfone materials they have studied only became water soluble when the sulfonation level was greater than 65%. It was necessary to sulfonate PES by up to 90 mol% to obtain membrane materials with conductivities comparable to Nafion (Nolte, 1993). But water uptake also significantly increases and the mechanical stability decreases.

Kerres et al. (1996) reported that the poly(aryl ether)sulfone materials they have studied only became water soluble when the sulfonation level was greater than 65%. It was necessary to sulfonate PES by up to 90 mol% to obtain membrane materials with conductivities comparable to Nafion (Nolte et al., 1993). But water uptake also significantly increases and the mechanical stability become a problem.

Guan et al. (2005) sulfonated PES with chlorosulfonic acid with varying acid/polymer ratio and the time of reaction. They concluded from atomic force microscopy (AFM) images that there is a threshold value for DS around 40 % over which water channels interconnect, water uptake and proton conductivity jumps to higher values.

2.4 Conductivity Data Discrepancy

The discrepancies in the reported conductivity data in the literature are summarized in

Table 2.4. (Slade et al., 2002). The reasons of these discrepancies are generally as follows: The method of measurement, the differences in conductivity cells for EIS measurements, in-plane vs thru-plane measurements, differences in pre-treatment of membranes, solvents used during casting (for alternative membranes except Nafion) etc..

Since there are a number of reasons affecting proton conductivity results, which are the most important parameter for the development of these materials, the details of the measurement conditions must be given. Therefore, a special attention was given to the proton conductivity measurements in this study.

Table 2.4. Conductivity values of Nafion 1100 EW membranes from various studies (Slade et al., 2002)

Table I. Conductivity measurements on Nafion 1100 EW membranes.							
Nafion membrane	Electrolyte	Technique	Membrane thickness (μm)	Area resistance ($\Omega \text{ cm}^2$)	Conductivity (S cm^{-1})	Resistivity ($\Omega \text{ cm}$)	Ref.
117	Water vapor RH 100% (25°C)	AC impedance	175	0.25	0.070	14.3	13
117	Immersed in 1 M H_2SO_4 (20°C)	DC current pulse	231	0.26	0.088	11.4	14, 15
	Immersed in 1 M H_2SO_4 (80°C)			0.10	0.231	4.33	
117	Immersed in water (30°C)	AC impedance	175	0.18	0.100	10.0	16-19
	Immersed in water (90°C)			0.09	0.19	5.3	
	Water vapor RH 100% (30°C)			0.29	0.06	16.6	
117	Immersed in 2 M HCl (25°C)	DC method	200	0.30	0.066	15.2	20
117	Immersed in 1 M H_2SO_4 (25°C)	“Kelvin” four-point probe	200	0.14	0.140	7.1	21
117	Immersed in water (25°C)	AC impedance	200	0.20	0.100	10.0	
112	Immersed in water (25°C)	AC impedance	60	0.06	0.100	10.0	
117	Immersed in water (20°C)	AC impedance	175	0.19	0.090	11.1	22
117	Water vapor	AC	210	0.15	0.140	7.1	23
112	RH 100% (65°C)	impedance	52	0.06	0.144	6.9	
117	Immersed in 1 M H_2SO_4 (25°C)	AC impedance	175	0.23	0.076	13.2	24, 25
117	Water vapor RH 100% (30°C)	AC impedance	200	0.29	0.068	14.7	26
117	Water vapor RH 100% (20°C)	AC impedance	200	0.25	0.078	12.8	27
117	Water vapor RH 100% (20°C)	AC impedance	175	0.35	0.050	20.0	28
117	Immersed in water (20°C)	AC impedance	170	0.21	0.080	12.5	29
115	<i>In situ</i> , humidified gases (95°C)	AC impedance	125	0.17	0.074	14.1	30
117	<i>In situ</i> , humidified gases (60°C)	Current-pulse	203	0.19	0.105	9.5	31

2.5 Proton Transport

Proton transport in polymer ion-exchange membranes have been discussed in the literature and some models both structural and

mechanistic were proposed. One of them is the structural three-zone pore model proposed by Yeager and Gierke and Hsu (Malhotra et al., 1997). In this model: (i) a low dielectric constant region consisting of the hydrophobic fluorocarbon polymer matrix, (ii) a high dielectric constant inverted micellar region containing ion clusters including the sulfonate exchange sites, counterions, and sorbed water, and (iii) the interfacial region consisting mostly of the pendant side chains of the sulfonate groups and a small amount of water exist (Figure 2.12).

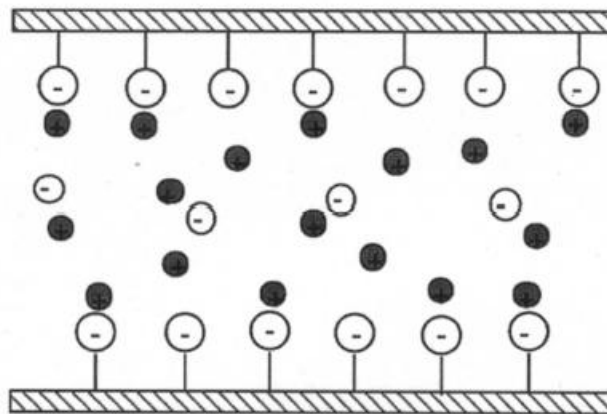


Figure 2.12. Schematic diagram of a pore within an ion-exchange membrane with fixed anions (-SO^-) and cations, some of which are attached (Stern layer), while others form a diffuse layer. In addition, ions of any free-supported acid through self-ionization are shown (Malhotra et al., 1997)

When the membrane is dry, protons are attached firmly to each anionic group on the surface so for the electroneutrality to be maintained. In the presence of water, however, the protons become solvated and form hydronium ions, $\text{H.XH}_2\text{O}$, e.g., H_3O , H_5O , H_7O , H_9O_4 , within the hydrophilic core (Malhotra, 1997). In the presence of an electric field each proton drags some water from anode to cathode and this is called electro-osmotic

drag, which is important for the dehydration of the anode side limiting the current (Eikerling et al., 1998).

Eikerling et al. (2001) and co-workers attempted to develop a semi-phenomenological model for proton transport in polymer membranes particularly Nafion and discussed the available experimental data on membrane conductance and make some conclusions about the optimal membrane architecture. High rate of proton exchange in the hydrogen-bonded system causes the excess proton to be accommodated equally among the other water protons. There is therefore no free excess proton in water. According to the literature, there are three main options. First, the excess proton can be a part of an H_3O^+ ion, in which all three protons are equivalent. Second, it can reside in a Zundel H_5O_2^+ cation complex with a proton between two water molecules, binding them in a cluster. Third, it can be present as an Eigen H_9O_4^+ cluster, which consists of H_3O^+ and three strongly bound H_2O molecules, each attached to one of the H_3O^+ protons (Eikerling, 2001). Their model started from a single pore including the series model and random network model and extended to overall. In a single pore, they have distinguished surface and bulk mechanisms of proton transport. This complex semi-phenomenological modeling approach seemed to be promising however, experimental validation seem to be lacking.

Thampan et al. (2000) and co-workers developed a model for the conduction of protons in hydrated Nafion or like membranes based on the dusty-fluid model founded on the generalized Stefan-Maxwell equations and including diffusion and convection, for transport and the percolation model for structural aspects. The derivation and fundamental equations of this model are as follows:

Generalized Stefan-Maxwell Equation:

$$-\frac{c_i}{RT} \nabla_T \mu_i^e = \sum_{\substack{j=1 \\ j \neq i}}^n \frac{c_i c_j}{c D_{ij}} (v_i^D - v_j^D) \quad (i = 1, 2, \dots, n) \quad \text{[1]}$$

The generalized Stefan-Maxwell equation describes the diffusional velocity of species i , v_i^D , in a continuum fluid taking electrochemical potential gradient as the driving force.

If we consider diffusional transport in an ion-exchange membrane with large molecular weight “dust” species ($j=M$), within the framework of the dusty-fluid model (DFM) ($v_M^D=0$), Eq. 1 results in:

$$-\frac{c_i}{RT} \nabla_T \mu_i^e = \sum_{\substack{j=1 \\ j \neq i}}^n \frac{c_i c_j}{c D_{ij}^e} (v_i^D - v_j^D) + \frac{c_i}{D_{im}^e} v_i^D \quad (i = 1, 2, \dots, n) \quad \text{[2]}$$

where the continuum diffusion coefficients D_{ij} have been replaced by their “effective” counterparts D_{ij}^e , to account for the space-filling aspect and tortuosity of the membrane, the latter reducing the effective driving force gradient. D_{im}^e accounts for frictional interaction between species i and the matrix or dust particles. Each sulfonic acid group along with its associated PTFE backbone is treated as the dust species M , with an $EW \cong 1100$ for Nafion for example. The effective and continuum diffusion coefficients are interrelated through:

$$D_{ij}^e = K_1 D_{ij}$$

where K_1 is the DFM structural constant for thermomolecular diffusion coefficient. Frequently $K_1 = \epsilon^q$ suffices, where ϵ is the volume fraction of the phase through which the diffusion is occurring. A common value for this so called Bruggeman exponent is $q=1.5$. Alternatively if percolation model is adopted which includes a percolation threshold ϵ_0 below which the diffusion is not possible owing to the lack of connectivity of the phase through which the diffusion occurs, then:

$$K_1 = (\epsilon - \epsilon_0)^q$$

where the critical exponent q is a universal constant predicted to be 1.5, although it is frequently used as a fitted parameter. The threshold value ϵ_0 can be determined from experiments as a fitted parameter. The effective membrane diffusion coefficient may similarly be written as :

$$D_{lm}^e = K_0 D_{lm}$$

where K_0 is the DFM constant for the matrix diffusion coefficient. Unlike for K_1 , however, no general relationship is available to relate K_0 to the structural properties of the membrane for liquid phase diffusion but for gaseous diffusion, relations are available for the corresponding effective Knudsen diffusion coefficient interms of the porosity, tortuosity factor, and the mean pore radius. It may be treated as a fitted parameter again.

The total species velocity comprises a convective and a diffusive component:

$$v_i = v_i^D + v$$

The convective velocity resulting from a pressure gradient and/or potential gradient may be given by Schögl's equation:

$$v = -\frac{B_0}{\eta} \left[\nabla p + \left(\sum_{j=1}^n c_j z_j \right) F \nabla \Phi \right] \quad \text{[1]}$$

With eq. 3 in eq. 2, DFM takes the following form in terms of the total species fluxes $\mathbf{N}_i = c_i v_i$:

$$-\frac{c_i}{RT} \nabla_T \mu_i^e = \sum_{\substack{j=1 \\ j \neq i}}^n \frac{1}{c D_{ij}^e} (c_j N_i - c_i N_j) + \frac{N_i}{D_{im}^e} + \frac{c_i B_0}{\eta D_{im}^e} \left[\nabla p + \left(\sum_{j=1}^n c_j z_j \right) F \nabla \Phi \right] \quad \text{[2]}$$

When summed over all species, the Stefan-Maxwell terms cancel resulting in:

$$\left[\nabla p + \left(\sum_{j=1}^n c_j z_j \right) F \nabla \Phi \right] = -\frac{RT}{W} \sum_{j=1}^n \frac{N_j}{D_{jm}^e} \quad \text{[3]}$$

$$\text{where } W = 1 + \frac{B_0 c RT}{\eta} \sum_{h=1}^n \frac{x_h}{D_{hm}^e} \quad \text{[4]}$$

An alternative form using previous equations is:

$$-\frac{c_i}{RT} \nabla_T \mu_i^e = \sum_{\substack{j=1 \\ j \neq i}}^n \frac{1}{c D_{ij}^e} (c_j N_i - c_i N_j) + \frac{N_i}{D_{im}^e} + \frac{c_i B_0 RT}{\eta D_{im}^e W} \sum_{j=1}^n \frac{N_j}{D_{jm}^e} \quad \text{[5]}$$

which may be written in a more compact form:

$$-\frac{c_i}{RT} \nabla_T \mu_i^e = \sum_{j=1}^n H_{ij}^e N_j \quad \text{[6]}$$

with effective frictional coefficients incorporating the convective terms being:

$$H_{ij}^e = (\delta_{ij} - 1) \left(\frac{x_i}{D_{ij}^e} + \frac{c RT B_0 x_i}{\eta W D_{im}^e D_{jm}^e} \right) + \delta_{ij} \left(\frac{1}{D_{im}^e} + \sum_{\substack{h=1 \\ h \neq i}}^n \frac{x_h}{D_{ih}^e} - \frac{c RT B_0 x_i}{\eta W (D_{im}^e)^2} \right) \quad \text{[7]}$$

Kronecker delta function defined as:

$$\delta_{ij} = \begin{cases} 0 & (j \neq i) \\ 1 & (j = i) \end{cases}$$

Eq. 8 may be inverted to a form that is explicit in species flux:

$$N_i = -\frac{1}{RT} \sum_{j=1}^n \kappa_{ij}^e c_j \nabla_T \mu_j^e \quad [0]$$

where κ_{ij} are the elements of the matrix $[H^e]^{-1}$, with elements of the effective frictional coefficient matrix $[H^e]$ given in eq. 9. The current density then can be obtained from:

$$i = F \sum_{i=1}^n z_i N_i \quad [1]$$

They also included the thermodynamics of dissociation of the acid groups in the presence of polar solvents such as water. Their results provided excellent correlation with a variety of experimental data (Figure 2.14).

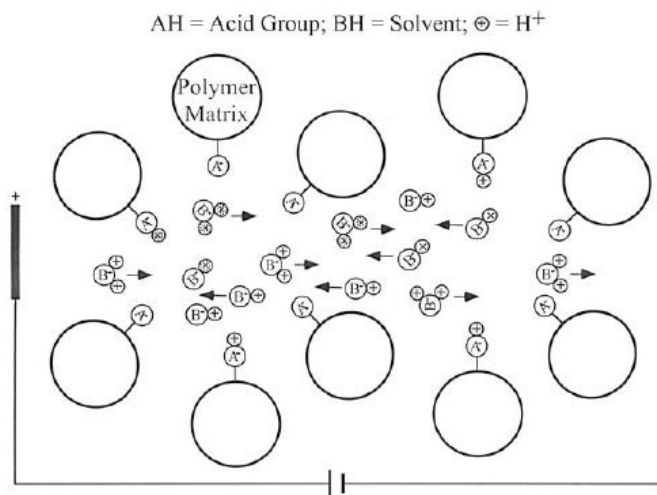


Figure 2.13 A “dusty-fluid model” depiction of a PEM. The polymer matrix along with an acid groups is viewed as “dust” particles comprising the PEM (Thampan et al., 2000)

The membrane imbibes a polar solvent BH (e.g., HOH, CH₃OH), that solvates the protons from the pendant acid HA forming BH²⁺ that serves as the charge carrier.

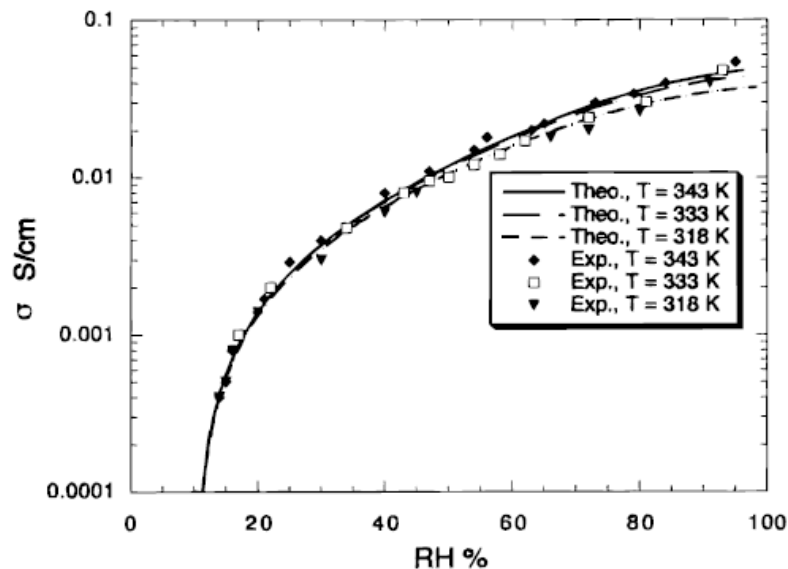
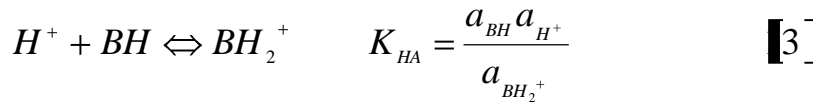
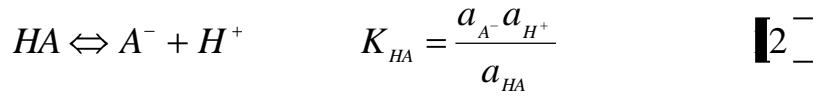


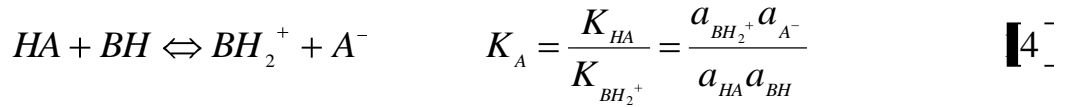
Figure 2.14. The experimental results for conductivity of Nafion 117 with theoretical predictions (Thampan et al., 2000)

Proton Transport in ionomeric membranes:

As depicted in the Figure 2.13. above that depicts “dusty fluid model”, PEM can be visualized as a dusty fluid, in which, an acid group (HA) is tethered to each dust particle (sulfonic acid group in Nafion) and they are supposed to be distributed spatially uniformly. The molecular weight of the dust species is equal to the PEM equivalent weight therefore. For the general model given above transport of proton only for charged species I is considered. In the absence of a polar solvent, the protons are firmly attached to the acid groups A⁻ so they exhibit very low conductivity being in the order of 10⁻⁷ S/cm. In the presence of a proton acceptor solvent BH (examples are: HOH, CH₃OH etc.) however, these acid groups dissociate:



Overall reaction for protonation of the solvent is then:



It is assumed for simplicity that each proton is associated with a single solvent molecule although it is not likely to be true, in fact this number changes with λ , the number of solvent molecules per acid site. In addition, it was assumed that each acid group gives up a single proton which is the case for sulfonic acid groups.

The model was adopted to composite membranes by Thampan et al (2005). According to the study, for the composite membrane final DFM equations can be updated as follows:

Conductivity:

$$\sigma = (\varepsilon - \varepsilon_0)^q \left(\frac{\lambda_{H^+}}{1 + \delta_{AH} + \delta_{ZH}} \right) (c_{AH,0} \alpha_{AH} + c_{ZH,0} \alpha_{ZH})$$

where: $\delta_{AH} = D_{12} / D_{1M}$ and $\delta_{ZH} = D_{12} / D_{1Z}$. Here D_{12} / D_{1M} , and D_{1Z} are the diffusion coefficients for $(H_3O^+)/\text{solvent } (H_2O)$, $H_3O^+/\text{PEM matrix}$ and $H_3O^+/\text{additive particle}$, respectively. E and ε_0 are the volume fraction of

water in the membrane and the percolation threshold, respectively, where ε is a function of the water uptake ($\lambda_{\text{H}_2\text{O}}$).

$$\varepsilon = \frac{\lambda_{\text{H}_2\text{O}}}{\frac{V_{\text{M}}}{V_{\text{H}_2\text{O}}} + \lambda_{\text{H}_2\text{O}}}$$

V_{M} is the effective partial molar volume of the PEM and is calculated as

$$\bar{V}_{\text{M}} = \bar{V}_{\text{PEM}}(1 - \omega_{\text{Z}}) + \bar{V}_{\text{Z}}\omega_{\text{Z}}$$

where the partial molar volume of the additive,

$$\bar{V}_{\text{Z}} = d_{\text{Z}} / (6c_{\text{ZH}_0}^*)$$

where $c_{\text{ZH}_0}^*$ is the surface acid site density of the additive (mol/cm^2) and d_{Z} is the additive particle size. Also ω_{Z} is the mass fraction of the additive in the composite PEM. E_0 is defined in a similar manner, being based on the water uptake at monolayer coverage. The Bruggeman, or critical, exponent $q= 1.5$, and λ_{H^+} is the equivalent conductance of a proton in water.

Dusty-fluid model was also shown to be very successful in the study of Rogers and coworkers (Rogers, 2004). Figure 2.14 shows the comparison of model results with experimental data for sulfonated polyethersulfone (S-PES).

Composite membranes offer improved properties such as high temperature operation, better water management, decreased methanol permeability. For methanol permeability the composite theory simply tells that protons can be transferred on a direct path through polymer and the

inorganic phase whereas methanol only follows the path in the polymer phase.

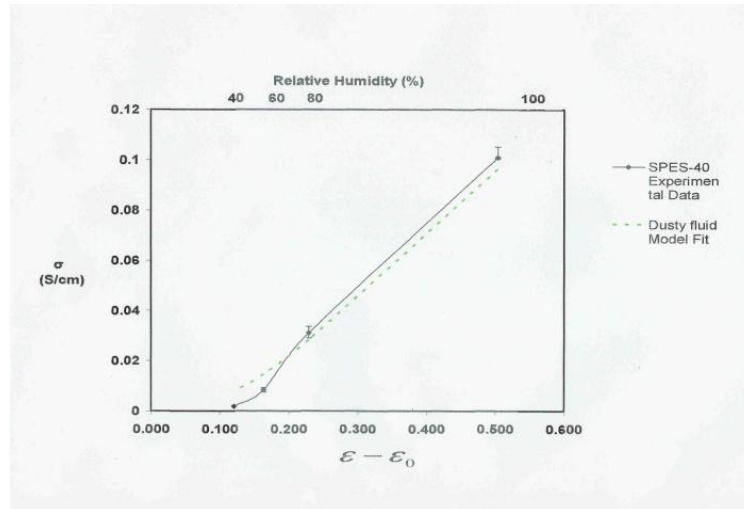


Figure 2.14. Conductivity vs relative humidity for sulfonated polyethersulfone (S-PES) (Rogers et al., 2004)

Composite membranes are promising for operation at high temperatures (>100 °C) as evident from the literature, however, the wide range of investigation have not been systematic. Thampan et al (2005) and co-workers recently developed a systematic approach to design high temperature composite membranes. They discussed higher temperature composite proton-exchange membranes for PEMs with adequate performance under low relative humidity based on experimental and theoretical considerations and reported that the nanostructured ZrO_2 /Nafion PEM exhibiting an increase of 10% in IEC, 40% increase in water sorbed, and 5% enhancement in conductivity vs. unmodified Nafion 112 at 120°C and 40% RH is a promising composite membrane for PEM fuel cell applications. On the modeling side they extended the dusty fluid model (DFM) used in their previous study by adding inorganic additive as

an additional dust species immobilized within the polymer matrix (Figure 2.15).

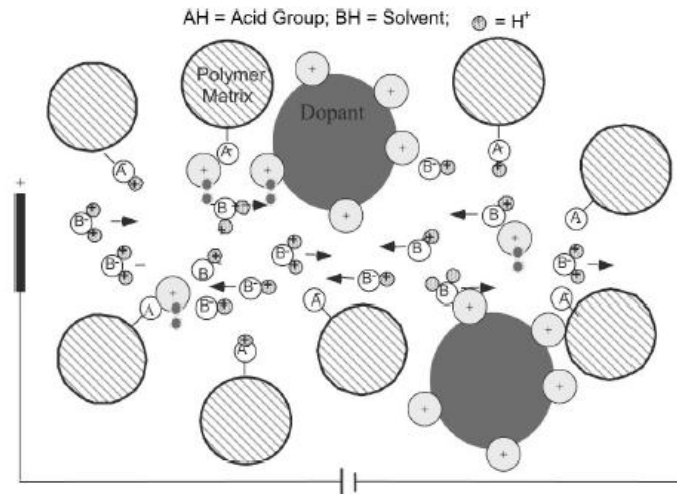


Figure 2.15. A dusty-fluid model depiction of a PEM describing proton conductivity through the Nafion polymer matrix and the superacidic dopant (Thampan et al., 2005)

Kaliaguine et al. (2003) and Slade et. Al. (2002) also reported about the discrepancies in the proton conductivity values for the same materials in the literature. After recognizing this, they investigated the reasons of these discrepancies and found that the solvent used for casting affects the conductivity. They reported that dimethylformamide (DMF) strongly decreased the membrane conductivity by more than one order of magnitude because of the formation of the strong hydrogen bonding of sulfonic acid groups with DMF evidenced by 1H -NMR. In addition, it was stated that some of the discrepancies in the reported conductivities might be caused from the measurement methods. Figure 2.16 shows conductivity versus DS for PEEKs prepared with solvents DMF and DMAc in this study and indicates how solvent affects conductivity clearly.

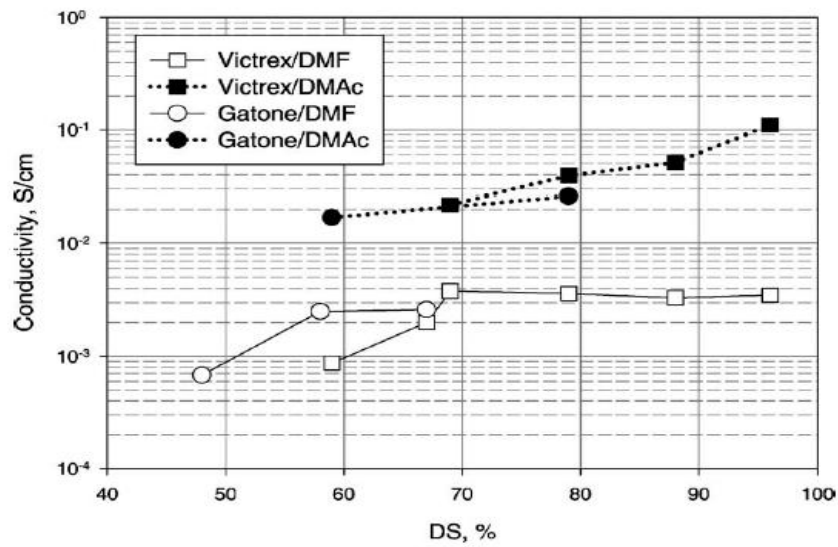


Figure 2.16. Room temperature conductivity of samples cast with different solvents (Kaliaguine et al., 2003)

2.6 Proton Conductivity Measurements

2.6.1 Electrochemical Impedance Spectroscopy (EIS): Theory

EIS is an emerging characterization method in materials science in the recent years since it involves a relatively simple electrical measurement that can readily be automated and whose results may often be correlated with many complex materials variables: from mass transport, rates of chemical reactions, corrosion, and dielectric properties, to defects, microstructure, and compositional influences on the conductance of solids. Because of the ease of use and information that it offers this tool has been used also in chemical sensor and fuel cell researches to predict their aspects of the performance (Barsoukov et al., 2005). A flow diagram describing a general characterization procedure using EIS is presented in Figure 2.17 below:

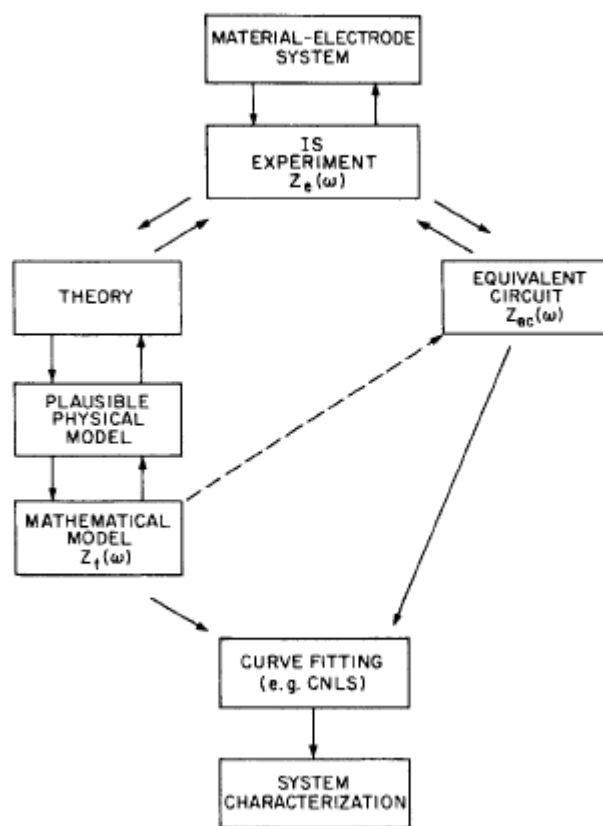


Figure 2.17. Flow diagram for the measurement and characterization of a material–electrode system (Barsoukov et al., 2005)

Note: CNLS stands for complex nonlinear least squares fitting

Impedance (reverse of conductivity) can be thought simply as the AC version of the resistance I in the well known $V=IR$ eqn (Ohm’s Law) used for DC. However, Ohm’s Law is valid for an ideal resistor, real circuit elements are more complex.

Assumptions of an ideal resistor are (Ohm’s Law):

- Obeys Ohm’s Law at all current and voltage levels
- It’s resistance value is independent of frequency
- AC current and voltage signals through a resistor are in phase with each other

Impedance is a more general circuit parameter. Like resistance, impedance is a measure of the ability of a circuit to resist the flow of electrical current. Unlike the resistance, impedance is not limited by the simplifying properties listed above.

Real circuits may include resistors, inductors, capacitors and other component materials. The impedance (Z) is defined as the ratio of the voltage to the current at a given frequency, and it is represented as a complex quantity that consists of a real part (resistance, Z' or R) and an imaginary part (reactance, Z'' or $(X_C - X_L)$) with phase angle θ as described in the equations below:

$$Z' = |Z| \cos \theta$$

$$Z'' = |Z| \sin \theta$$

$$\theta = \tan^{-1} \left(\frac{Z''}{Z'} \right)$$

EIS is a powerful, non-destructive method for analysis of various electrochemical systems. Using various techniques, accurate kinetic and mechanistic information can be obtained for the electrochemical system under investigation. EIS can be used to obtain information on various applications such as batteries and energy sources, corrosion, anodic behavior of metals, electrocrystallisation of metals, photoelectrochemistry, molten salts, semiconductor-electrolyte interface, organic, electrochemistry, biology and bioelectrochemistry, semiconductors etc.

Electrochemical impedance is usually measured by applying a small excitation signal (AC potential (potentiostatic) or AC current (galvanostatic)) to an electrochemical cell and measuring the current through the cell. A very small signal is given so that the cell's response is

pseudo-linear. In a linear (or pseudo-linear) system, the current response to a sinusoidal potential will be a sinusoid at the same frequency but shifted in phase.

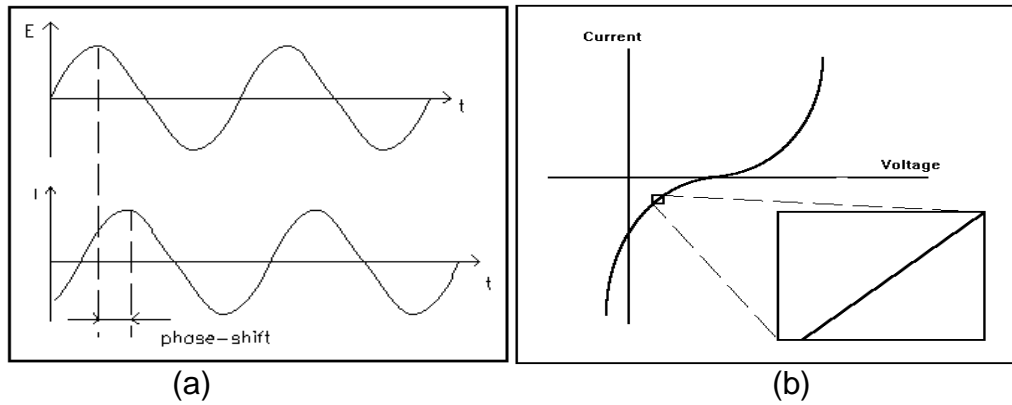


Figure 2.18. (a) Sinusoidal Current Response in a Linear System (b) Current versus Voltage Curve Showing Pseudo-linearity

In a typical EIS experiment, a small (1-10 mV) AC signal is applied to the cell. The small signal makes it sure that the output will be in the pseudo-linear segment of the cell's current versus voltage curve. The excitation signal expressed as a function of time, $E(t)$, is the potential at time t , E_0 is the amplitude of the signal, and ω is the radial frequency.

$$E(t) = E_0 \cos(\omega t)$$

Relationship between radial frequency (ω , radians/s) and linear frequency (f , Hz) is:

$$\omega = 2\pi f$$

In a linear system, the response signal, I_t , is shifted in phase (Φ) and has a different amplitude, I_0 :

$$I(t) = I_0 \cos(\omega t - \Phi)$$

The impedance of the system can be calculated by an expression analogous to Ohm's Law as:

$$Z = \frac{E(t)}{I(t)} = \frac{E_0 \cos(\omega t)}{I_0 \cos(\omega t - \Phi)} = Z_0 \frac{\cos(\omega t)}{\cos(\omega t - \Phi)}$$

The impedance is therefore expressed in terms of a magnitude, Z_0 , and a phase shift, Φ . Using Eulers relationship,

$$\exp(j\Phi) = \cos\Phi + j \sin\Phi$$

Where, j is the imaginary number ($\sqrt{-1}$)

it is possible to express the impedance as a complex function. The potential is described as,

$$E(t) = E_0 \exp(j\omega t)$$

and the current response as,

$$I(t) = I_0 \exp(j\omega t - J\Phi)$$

The impedance is then represented as a complex number,

$$Z = \frac{E}{I} = Z_0 \exp(j\omega t) = Z_0 (\cos \Phi + j \sin \Phi)$$

Impedance has real and imaginary parts. There are two widely used plots for data presentation: “Nyquist” and “Bode” plots (Figure 2.19). If the real part is plotted on the Z axis and the imaginary part on the Y axis of a chart, “Nyquist plot” is obtained. The impedance is plotted with log frequency on the x-axis and both the absolute value of the impedance ($|Z| = Z_0$) and phase-shift on the y-axis. In the Nyquist plot frequency data can not be followed so Bode must be plotted and used for following frequency as well.

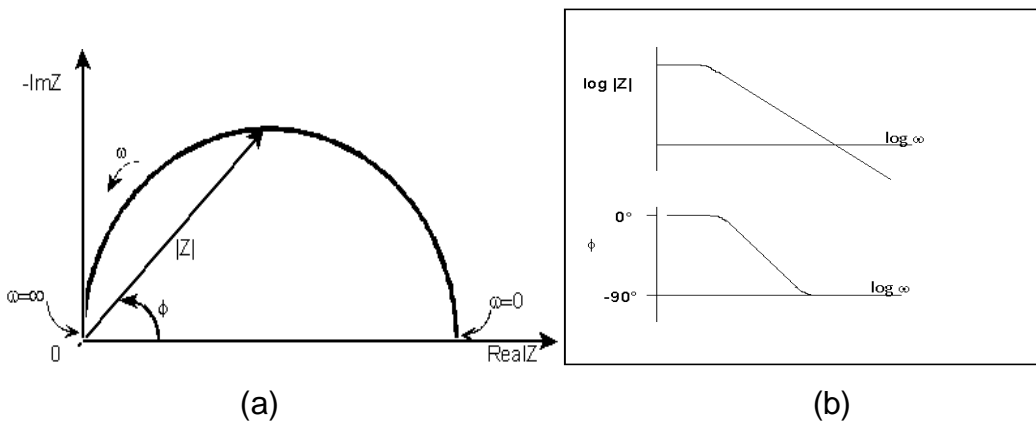


Figure 2.19. (a) Nyquist Plot with Impedance Vector (b) Bode Plot

EIS data are commonly analyzed by fitting it to an equivalent electrical circuit model. Most of the circuit elements in the model are common electrical elements such as resistors, capacitors, and inductors. To be useful, the elements in the model should have a basis in the physical electrochemistry of the system. As an example, most models contain a resistor that models the cell’s solution resistance.

Table 2.5. Common Electrical Elements

<u>Component</u>	<u>Current vs. Voltage</u>	<u>Impedance</u>
resistor	$E = IR$	$Z = R$
inductor	$E = L \, di/dt$	$Z = j\omega L = j2\pi fL$
capacitor	$I = C \, dE/dt$	$Z = 1/j\omega C = 1/j(2\pi fC)$

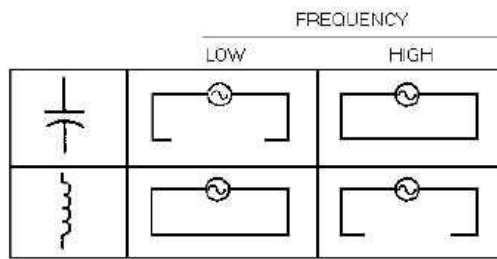


Figure 2.20. Effect of frequency on capacitive and inductive reactance

For any given value of L and C if the applied frequency is increased, X_C decreases and X_L increases. If we increase the frequency enough, the capacitor acts as a short and the inductor acts as an open and vice versa.

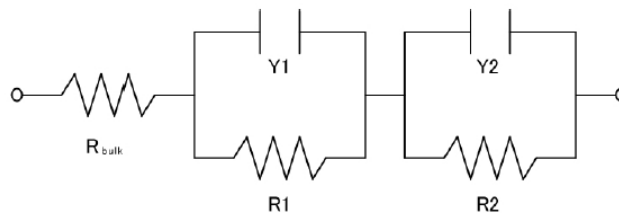


Figure 2.21. Equivalent circuit for the membrane/electrode interface studied: Serial and Parallel Combinations of Circuit Elements

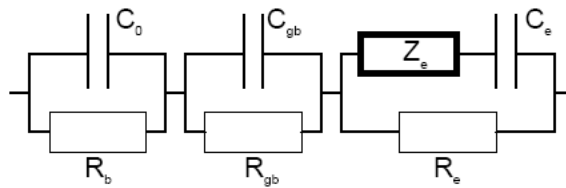


Figure 2.22. Equivalent circuit used very often for SOFC and PEMFC (Nicoloso, 1990)

In the equivalent circuit of SOFC, R_b is the bulk resistance, C_0 the corresponding capacitance, R_{gb} and C_{gb} are the resistance and capacitance of the grain boundary, R_e is the kinetic resistance and C_e the capacitance of the electrode, and Z_e is the mass transfer contribution (Warburg impedance).

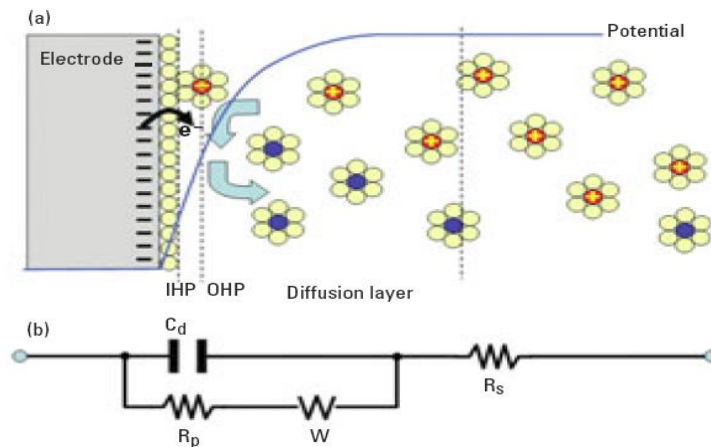


Figure 2.23. A simple electrified interface, in which the vertical dotted lines in (a) are represented by the electronic components in (b) (Park et al. 2003)

(a) Red: oxidants with a positive charge, IHP: The inner Helmholtz plane, OHP: outer Helmholtz planes

(b) An equivalent circuit: C_d : Double layer capacitor, R_p : Polarization resistor; W : Warburg resistor, R_s : Solution resistor.

$$Z(\omega) = R_s + \frac{R_p}{1 + j\omega R_p C_d} =$$

$$R_s + \frac{R_p}{1 + \omega^2 R_p^2 C_d^2} - \frac{j\omega R_p^2 C_d}{1 + \omega^2 R_p^2 C_d^2} = Z' + jZ''$$

Note: Warburg Component neglected

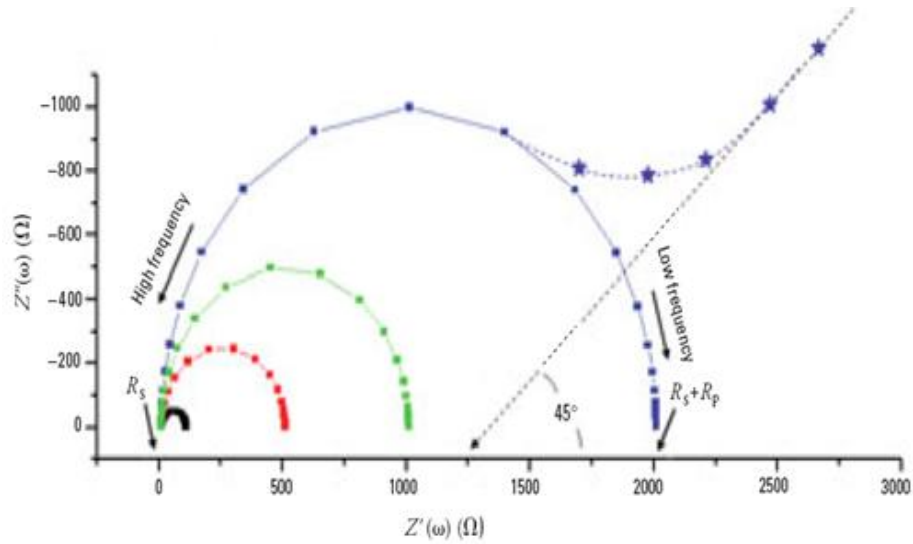


Figure 2.24. Nyquist Plot of an electrified interface (Park et al. 2003)

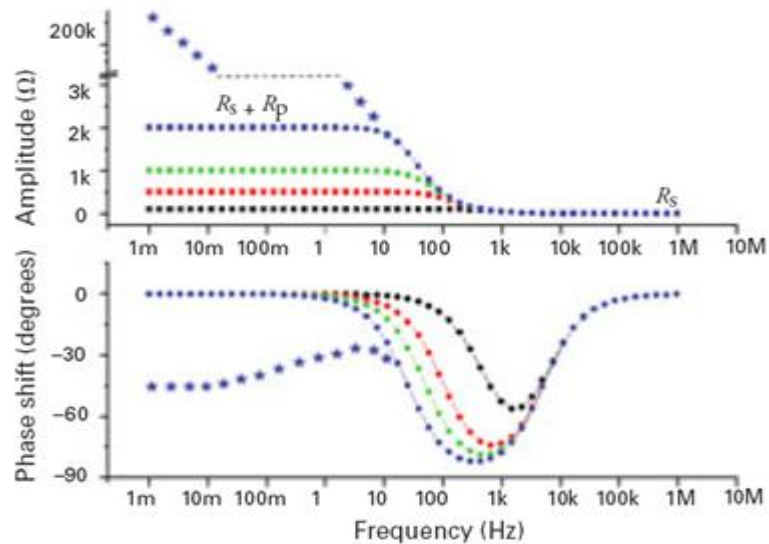


Figure 2.25. Bode Plot of an electrified interface (Park et al. 2003)

Note: Rp black, 100 Ω ; Rp red, 500 Ω ; Rp green, 1 k Ω ; Rp blue, 2 k Ω

EIS may be performed in either potentiostatic (constant voltage) or galvanostatic (constant current) mode depending on the type of analysis. The electrical impedance of an electrochemical cell can be measured either directly with an Impedance Analyzer such as the Solartron model 1260A (or Agilent 4294A as in our first measurements), or with a combination of a Frequency Response Analyser (FRA) and an electrochemical interface (ECI), such as the Solartron 1255A and 1287A units.

EIS can be useful not only for PEM electrical resistance estimation, but also can provide an important additional information on their behavior depending on the temperature, water content and some other parameters (Ciureanu et al., 2003).

Ciureanu et al. (2003) studied hydrated SPEEK sandwiched between blocking stainless steel electrodes by impedance spectroscopy at various temperatures and calculated proton diffusion constants from Warburg impedances according to the equivalent circuit shown in Figure 2.26. which consists of a resistor–capacitor pair with a generalized Warburg finite length element in series with the resistor.

$$(Z = R_w[\coth(l_s w \omega) \alpha] / (l_s w \omega) \alpha)$$

In the circuit and the equation R_1 represents a bulk resistance of the specimen and C corresponds to the capacitance of the measurement cell. The Warburg element reflects diffusion of charge carriers (protons) within the membrane ($S_w = L_2/D$, where L is the effective diffusion thickness and D the effective diffusion coefficient). The slope of the straight line in the purely diffusional case should be 45° corresponding to $\alpha = 1/2$, however

they obtained $\alpha = 0.32$ for $T = 42\text{ }^{\circ}\text{C}$ and commented that the value obtained from this fitting indicates partially capacitive behavior which becomes still more distinctive with temperature.

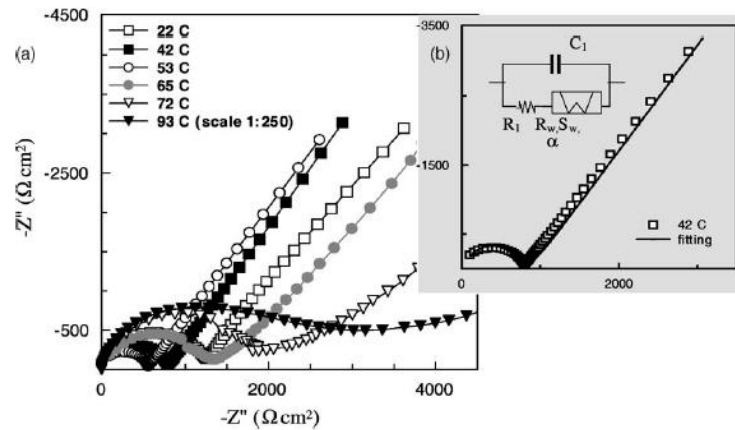


Figure 2.26. (a) Typical complex impedance responses of humidified PEM (PEEK, DS = 0.42) at different temperatures. Cell area=1 cm², membrane thickness=0.9 mm. (b) Experimental and simulated curves. $R_1 = 640\Omega$, $C_1 = 7.5 \times 10^{-11}\text{ F}$, $R_w = 600\ \Omega$, $S_w = 6 \times 10^{-4}\text{ s}$, $\alpha = 0.32$. (Ciureanu et al., 2003)

Ramirez-Salgado (2007) studied chitosan behavior in a similar cell with EIS. The equivalent circuit models and Nyquist plot were given in Figure 2.27.

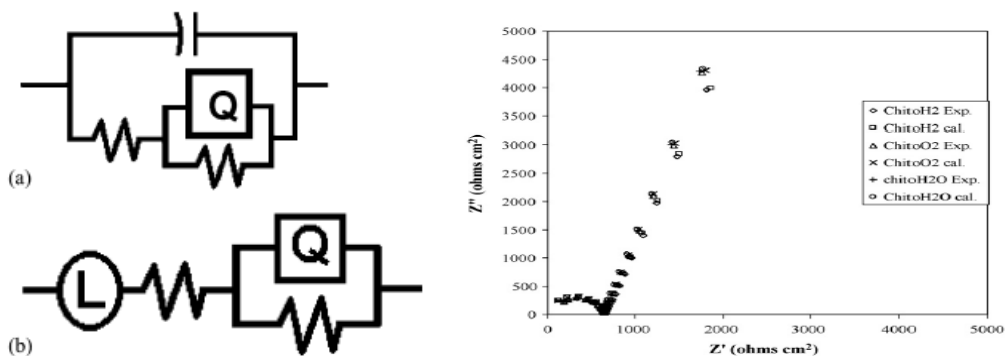


Figure 2.27. Equivalent Circuits a) chitosan b) Nafion and Nyquist Plot of Chitosan Membranes (Ramirez-Salgado, 2007)

The difference of these models from Ciureanu et al.'s study is the lack of Warburg component. For chitosan membranes they used a two time constant model with a constant phase element instead of a capacitor. For Nafion an inductor component in series with a typical Randles circuit with CPE again instead of a capacitor was used. The circuit parameters for chitosan and Nafion calculated in the study were summarized in Table 2.6.

Table 2.6. Equivalent Circuit Parameters used for Nafion and Chitosan Membranes (Ramirez-Salgado, 2007)

Nafion (water hydration)		Chitosan (water hydration)	
L_0 (H)	8.78×10^{-8}	C_1 (F)	3.7×10^{-5}
R_0 (Ω)	0.83	R_1 (Ω)	0.92
Q_1 (Ss^{n1})	1.2×10^{-4}	Q_2 (Ss^{n1})	6.3×10^{-5}
α_1	0.78	α_2	0.83
R_1 (Ω)	1.87×10^{19}	R_2 (Ω)	5.7×10^5

There are only a few studies on EIS modelling of the proton conductive membranes since the method is relatively new.

2.6.2 2-Probe (2P) vs 4-Probe (4P)

The impedance in the two-probe method is obtained from the voltage drop to a constant current flow through the same electrodes. Therefore, the impedance in the two probe method reflects many impedance components, in the pathway that the current flows, such as the lead inductance (I_{lead}), the lead resistance (r_{lead}), and the stray capacitance (C_{stray}) between two leads. In other words, the extra impedance derived

from these impedance components is added to the measurement result including the impedance of sample materials. So 2-probe method is limited to sample materials only with the high impedance above 10 K ω (Lee et al., 2005). Most of other researchers also (eg. Deslouis et al., 1995) mentioned the necessity of using a four-electrode arrangement to measure the very low impedance of membranes.

Zavodzinski et al. (1993) measured conductivity using an ac impedance method with two electrodes. Using this two—electrode method for a material with a low resistance, a high frequency (from 1 to 6 kHz) is needed to separate membrane resistance from interfacial capacitance, while the measurements can be practically affected by the electric fields produced by other instruments, especially in the high-frequency range.

Cahan et al. (1993) reported that they used a four-electrode system for impedance measurements and successfully measured membrane impedance, which is separated from interfacial capacitance over a wide range of frequency from dc to 105 Hz.

Sone et al. (1996) measured the impedance of Nafion 117 with 4-P AC Impedance Method and successfully separated the ionic resistance from the capacitance and charge-transfer resistances (Figure 2.28).

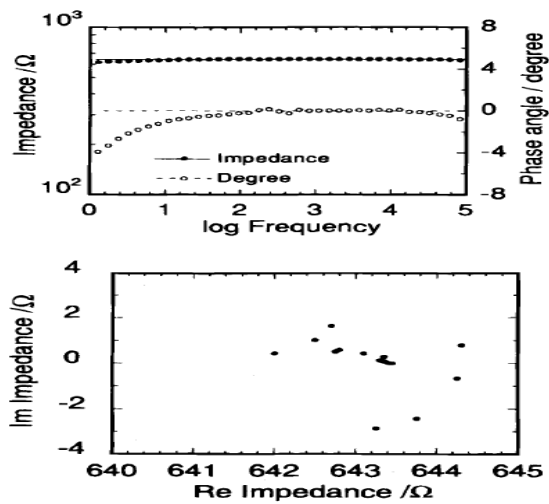


Figure 2.28. Bode and Nyquist Plots of Nafion 117; 4-P AC Impedance Method (Sone et al., 1996)

Lee et al. (2005) investigated a precise proton conductivity measurement system and compared 2-probe vs 4-probe as well as two different humidity conditions: water-vapor state and liquid-water state. They also investigated the effect of contact resistance between the membrane sample and electrodes on proton conductivity by using the two conductivity-cell configurations. They concluded that the values of proton conductivities measured using the four-probe method were always higher (2-5 times) than those measured using the two-probe method at ambient humidity and temperature. In addition, they reported completely different impedance behaviors for the identical Nafion membranes observed from the Nyquist impedance plots: “All Nyquist plots derived from the two-probe method represented the inductive reactance derived from various components, such as Pt electrodes, electric conductive leads, and a potentiometer in the path of current flow rather than the capacitive reactance between Pt electrodes. The effect of the contact resistance on the proton conductivity was more severe in the two-probe measurement, and this factor should be seriously considered in the water vapor state. The four-probe method well reflected the proton conductivity behavior of Nafion membrane in the wide

range of temperature and humidity, as compared with the two-probe method with reasonable proton conductivity in the low humidity”. Some researchers measured conductivity through plane which is assuming that the material is isotropic; however especially for composite materials anisotropy is inevitable. Therefore, some researchers try to develop measurement techniques to obtain conductivity in the direction of the thickness.

Ma et al. (2006) (National Institute of Advanced Industrial Science and Technology, Japan) used 2-probe method for membrane conductivity measurements with an emphasis on the effect of interface complexity between membrane and electrodes and the feasibility of using this method for measurements. Compared to the conductivity in the direction of thickness, the resistance measured in along the plane reaches as high as

1000 Ω , which features a large cell constant (L/A in $\sigma=L/(R \cdot A)$). The four-probe method yields narrower data dispersion and smaller relative errors, thus this method is commonly used to measure the proton conductivity of the PFSA membrane along the plane.

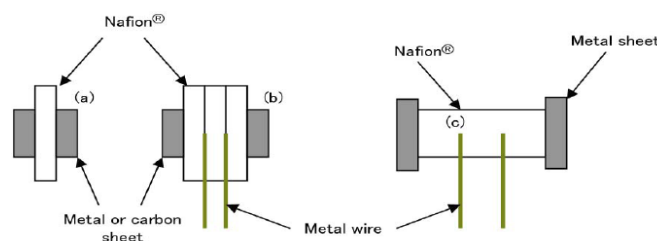


Figure 2.29. Sample arrangements for (a) the 2-probe method, (b) the 4-probe method in the direction of thickness, and (c) the 4-probe method in the surface direction (Ma et al., 2006)

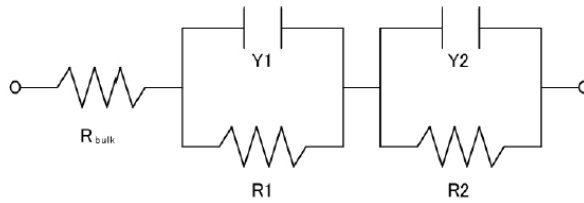


Figure 2.30. Equivalent circuit for the membrane/electrode interface studied (Ma et al., 2006)

Their experiments confirm that equivalent circuit fitting can separate membrane resistance from the interface components and good contact at the interface between the membrane and electrode can be attained by coating the electrode with Nafion solution, and conductivity results are similar to results using 4-probe measurements in the surface direction.

CHAPTER 3

MATERIALS & METHODS

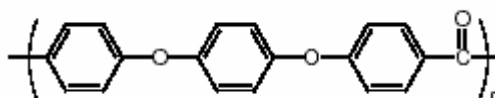
In this chapter, all the materials and methods used in this study will be explained. Some of the methods were used widely in this study, therefore, these methods such as the proton conductivity measurement and proton nuclear magnetic resonance spectroscopy (H-NMR) will be explained in more detail.

3.1 Polymers

3.1.1 Polyetheretherketones (PEEK)

Polyether ether ketone (PEEK), which started to commercialize in the early 1980s, belongs to the polyaryletherketone family consisting of partially crystalline polymers that are suitable for use at high temperatures. Polyetheretherketones [poly(oxa-p-phenylene-oxa-p-phenylene-oxy-p-phenylene) or PEEK] with molecular formula, $(OC_6H_4OC_6H_4COC_6H_4)_n$, are highly crystalline polymers and have very good thermal, chemical, and mechanical stability suitable for a wide range of applications. As it is clear from the name they have repeating monomers, ether (actually two) and ketone groups. They have many application areas such as automotive industry, electrical engineering (insulation, connectors), appliances (handles, cooking equipment), medicine etc. In the recent years researchers also investigated its possible use in fuel cell applications. Its glass transition temperature is around 150 °C while melting point is around 330 °C. As it is obvious that having a melting point means PEEK is a semi-

crystalline polymer. The chemical structure of PEEK is given in scheme 2.1 (a). PEEK used in this study was in the form of small extrudates.



Scheme 2.1. (a) Structure of polyetheretherketone (PEEK)

3.1.2 Polyetherethersulfone (PES)

It's IUPAC name is Poly(1,4-phenylene ether-sulfone) with molecular formula: $(C_{12}H_{10}O_4S)_n$. Polyethersulfone (PES) is an aromatic thermostable polymer having similar uses and properties with PEEK. However, the main difference is that PES is amorphous, its glass transition temperature (T_g) is much above PEEK, around 220 °C. Its chemical stability is not as strong as PEEK but enough for possible fuel cell applications. Chemical structure is given below in Scheme 2.2 (a).

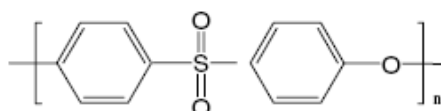
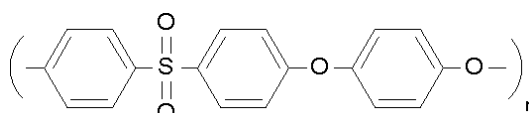


Figure 2.2 (a) Structure of Polyethersulfone (PES)

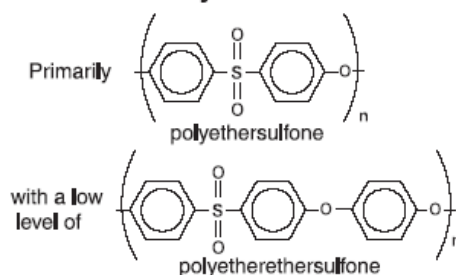
PES used in this study was obtained from Sigma-Aldrich. PES used in part of this study was the product of Solvay Advanced Polymers in the form of clear amber pellets of nearly 3 mm in diameter. Manufacturer reported in their product sheets that this product has some amount of polyetherethersulfone as well.

PEES (Poly(1,4-phenylene ether-ether-sulfone) with molecular formula $(C_6H_4-4-SO_2C_6H_4-4-OC_6H_4-4-O)_n$ has only one more phenylene group with ether linkage compared to PES, but this changes its sulfonation properties therefore, it was also used in the study.



Scheme 3.1. Structure of Polyetherethersulfone (PEES)

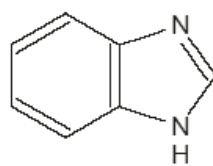
RADEL A Polyethersulfone



Scheme 3.2. Structure of Radel A Polyethersulfone

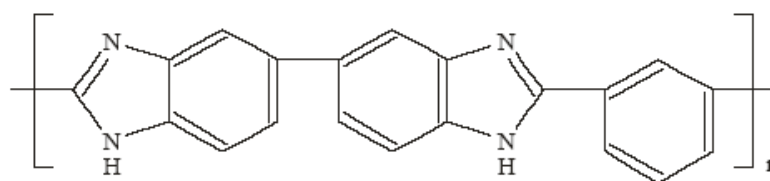
3.1.3 Polybenzimidazoles (PBI)

PBI is a basic, high performance thermoplastic polymer suitable for many engineering applications such as reverse osmosis, semiconductors and electrical circuits etc. It takes its name from the functional group benzimidazole which is shown below:



Scheme 3.3. Structure of Benzimidazole group

Poly [2,2'-(m-phenylene)-5,5'-bibenzimidazole] (MpbI), a fully aromatic type of benzimidazoles, is the widely studied and commercialized one (Hoechst Celanese Corporation under the trade name of celazole) because of its toughness, non-flammability, processability, thermal and chemical stability (Salamone, 1996). Its structure is shown below:



Scheme 3.4. Structure Chemical Structure of mPBI

3.2 Inorganic Fillers & Modifiers

3.2.1 Zeolite Beta

Zeolites are three-dimensional, microporous, crystalline solids with well-defined structures that contain aluminum, silicon, and oxygen in their regular framework; cations and water are located in the pores. The silicon and aluminum atoms are tetrahedrally coordinated with each other through shared oxygen atoms. Zeolites are natural minerals that are mined in many parts of the world but most zeolites used commercially are produced

synthetically. Since they have void space (cavities or channels) that can host cations, water (hygroscopic) they have many application areas such as adsorption, catalysis and ion-exchange, gas separation etc.. Because of their hygroscopic and proton conducting properties, they are selected as inorganic filler candidate for the composite membrane. It is also supposed to give some mechanical stability.

One candidate for the incorporation of inorganic crystals in non-fluorinated organic polymer membranes for a composite membrane that will be fabricated is zeolite beta. Zeolite Beta is a high-silica aluminosilicate with a three-dimensional, 12-membered ring pores with an interconnected channel system (Eapen, 1994). Because of the high Si/Al ratio it has desired acidic properties. Zeolite beta (Figure 3.1) has a tetragonal crystal structure.

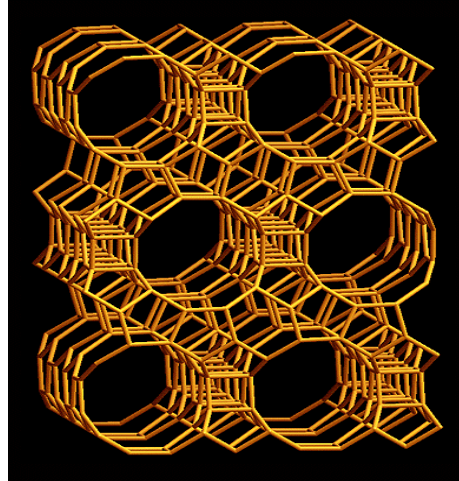


Figure 3.1. Zeolite beta structure

3.2.2 Heteropolyacids (HPAs)

Heteropolyacids (HPA) are known with their exceptionally high proton conductivities especially in their crystalline form with certain number of water molecules in their structure (Staiti et al., 1998). They have been utilized and investigated particularly for heterogeneous catalysis applications. In the recent years researches for fuel cell applications were also observed in the literature, but the main problem is the water solubility and therefore leaching of the heteropolyacids (Giordano et al., 1997).

HPAs used in this study were phosphotungstic acid (or tungstophosphoric acid; TPA) with chemical formula, $H_3PO_4W_{12}.XH_2O$ (MW: 2880.17) produced by Acros and Silicotungstic acid (STA) with chemical formula, $H_4O_{40}SiW_{12}.Xh_2O$ (MW: 2878.29) produced by Sigma-Aldrich. Both acids were in powder form and used without further modification.

3.3 Solvents

Dimethylacetamide(DMAc),N-Methylpyrrolidone(NMP), dimethylformamide (DMF) were used as casting solvents without further treatment.

3.4 Sulfonation

3.4.1 Sulfonation of PEEK

General Sulfonation Procedure for PEEK:

- Dry PEEK at 100 °C for 12 hrs.

- Add x gr dried and ground PEEK in y ml H₂SO₄ (95-97%) gradually under strong stirring at room temperature (Polymer(g)/acid(ml)=x/y; eg: 5/125)
- Filter undissolved parts of the mixture after 2 hrs of dissolution time
- Raise temperature to reaction temperature (T of reaction mixture reaches steady state in ~15 minutes on magnetic stirrers hot plate)
- After a determined reaction time pour reaction mixture slowly into an ice-cold distilled water under strong stirring
- Filter and wash the precipitate several times with distilled water until pH of the washing water is >5
- Dry SPEEK at 60-100 °C gradually, finally at 100 °C for 12 hrs

3.4.2 Sulfonation of PES

General Sulfonation Procedure for PES:

Method 1:

- Dry PES at 100 °C for 12 hrs
- Add x gr PES in y ml DCM gradually under strong stirring at room temperature (Polymer(g)/acid(ml)=x/y; eg: 5/50)
- Mix x ml ClSO₃H with y ml DCM (eg: x/y= 20/100)
- Bring reaction medium temperature to -5 °C by using ice water bath

- Add determined amount of (5-20 ml) ClSO_3H drop by drop into the mixture
- After determined reaction time pour reaction mixture slowly into an ice-cold distilled water under strong stirring
- Filter and wash the precipitate several times with distilled water until pH of the washing water is >5 Dry SPES at $100\text{ }^\circ\text{C}$ for 12 hrs
- Dry SPES at $100\text{ }^\circ\text{C}$ for 12 hrs

Method 2:

- Dry PES at $100\text{ }^\circ\text{C}$ for 12 hrs
- Add x gr PES in y ml H_2SO_4 (95-97%) gradually under strong stirring at room temperature (eg: $x/y=5/100$)
- Wait until complete dissolution or filter undissolved parts of the mixture after 2 hrs of dissolution time
- Bring the reaction medium temperature to $-5\text{ }^\circ\text{C}$ by using ice water bath
- Add a determined amount of (5-20 ml) ClSO_3H drop by drop into the mixture
- After a determined reaction time pour the reaction mixture slowly into an ice-cold distilled water under strong stirring
- Filter and wash the precipitate several times with distilled water until pH of the washing water is >5
- Dry SPES at $100\text{ }^\circ\text{C}$ for 12 hrs

3.5 Zeolite Beta Synthesis

Zeolite Beta synthesis was performed by Hülya Erdener and Nadiye Gür, former fuel Cell Research group members as part of their M.S. studies (Erdener, 2007; Gür, 2005)). Zeolite Beta can be hydrothermally synthesized at different $\text{SiO}_2/\text{Al}_2\text{O}_3$ ratios with a batch composition of 2.2 Na_2O : 1.0 Al_2O_3 : x SiO_2 : 4.6 $(\text{TEA})_2\text{O}$: 440 H_2O (Akata, 2004). In the hydrothermal synthesis, an alkaline precursor solution was prepared by dissolving NaOH (JT Baker) in deionized water in a polyethylene bottle and stirred until being homogenous. Then the organic template, tetraethyl ammonium hydroxide (TEAOH, Aldrich, 35 wt % in water) and the aluminum source (sodium aluminate, Riedel de Haën) were added and the mixture was stirred vigorously at 60°C for five minutes. Then the silica precursor solution (Colloidal Silica, Sigma-Aldrich, AS-40) was introduced into the mixture. The resulting gel was poured into Teflon lined autoclaves and kept at 150°C for a reaction period of 3-10 days. After the synthesis, zeolites were washed, filtered and calcined at 550°C to remove the organic template from the zeolite structure. The synthesized zeolite was in the Na^+ -Beta form and was converted into a more proton conductive (H^+ -Beta) form by acid treatment with H_2SO_4 (Merck, 95-98 wt %).

3.6 Fabrication of Composite Membranes

All the membranes were prepared by using solvent-casting method. Polymer/solvent ratio was around 5% (mg/mL). Both magnetic stirring and ultrasonic stirring were used consecutively for at least 2 hours for each. The solutions were poured onto clean glass petri-dishes and dried generally at 80 ° but sometimes above this temperature when high boiling point solvents were used. Membranes were removed from the glass petri-

dishes by swelling them in de-ionized water. Membranes were kept in 1 M H_2SO_4 at least for 2 hrs for complete protonation before conductivity analysis.

3.7 Membrane Electrode Assembly (MEA) Preparation

MEA preparation methods established by Bayrakceken et al. (2008) and Sengül (2007) were used. Electrodes were prepared by spraying method. Catalyst solution prepared according to the procedure described in Appendix was sprayed by using a spray gun onto the carbon paper. The target loading of Platinum catalyst was 0.4 mg/cm^2 and loading of Nafion ionomer in the electrode layer was 30% by weight (of catalyst + ionomer). The membranes to be tested was hot pressed between two electrodes at $130 \text{ }^\circ\text{C}$ for 3 minutes and then placed in the single cell.

3.8 Characterization Methods

3.8.1 X-Ray Diffraction (XRD)

The synthesized zeolites were characterized by a Philips PW 1729 X-ray diffractometer using $\text{CuK}\alpha$ radiation. The XRD analyses were performed for zeolite beta samples before calcinations and characteristic peaks of zeolites were observed around $2\theta \sim 7.8^\circ$ and $2\theta \sim 22.4^\circ$.

3.8.2 Scanning Electron Microscopy (SEM) Analysis

The morphology of the zeolite and composite membranes were monitored by scanning electron microscopy analyses (NORAN Instrument, JSM 640 Scanning Microscope).

3.8.3 Thermal Methods (TGA & DSC)

Shimadzu, DSC-60 and Shimadzu, DTG-60H instruments were used for thermal characterization. For DSC and TGA analysis, in the first runs, samples were heated to 160 °C from room temperature, cooled down, then in second run heated to 800 °C. Heating rate was 10 °C/min under nitrogen gas.

3.8.4 Proton Nuclear Magnetic Resonance Spectroscopy (H-NMR)

Magnetic resonance spectroscopy (NMR) applications have become one of the most powerful techniques for determining the chemical structures in the past fifty years. They are used particularly for determining the structure of organic compounds. Among the other spectroscopic methods, it is the only one in which a complete analysis and interpretation of the entire spectrum can be done.

It is based on the electromagnetic properties of the matter particularly of the proton. The nuclei of many elemental isotopes have a characteristic spin (I). Some nuclei have integral spins ($I = 1, 2, 3 \dots$), some have fractional spins ($I = \frac{1}{2}, \frac{3}{2}, \frac{5}{2} \dots$), and a few have no spin, $I = 0$ (^{12}C , ^{16}O , ^{32}S , \dots). Isotopes of particular interest for application are ^1H , ^{13}C , ^{19}F and ^{31}P , all of which have $I = \frac{1}{2}$.

A spinning charge generates a magnetic field, and the resulting spin-magnet has a magnetic moment (μ) proportional to the spin. In the presence of an external magnetic field (B_0), two spin states exist, $+1/2$ and $-1/2$. The magnetic moment of the lower energy $+1/2$ state is excited with the external field, but that of the higher energy $-1/2$ spin state is opposed to the external field. The difference in energy between the two spin states is dependent on the external magnetic field strength which is very small. If lower energy state is excited with a radiation in the radio frequency range some of them will go into the upper energy state. Basically from this phenomenon information about the matter under investigation can be obtained. The H NMR spectrum of an organic compound provides information concerning:

- the number of different types of hydrogens present in the molecule
- the relative numbers of the different types of hydrogens
- the electronic environment of the different types of hydrogens
- the number of hydrogen “neighbor” a hydrogen has

The magnetic field range displayed in the output is very small compared with the actual field strength (only about 0.0042%). Therefore, It is common approach to refer to small increments such as units of parts per million (ppm). For example, the difference between 2.3487 T and 2.3488 T is about 42 ppm. Instead of designating a range of NMR signals in terms of magnetic field differences, it is common to use a frequency scale. So for example at 2.34 T the proton signals extend over a 4,200 Hz range (for a 100 MHz RF frequency, 42 ppm is 4,200 Hz). Most organic compounds exhibit proton resonances that fall within a 12 ppm range (Lambert, 2003).

In this study, a high resolution Bruker Biospin Digital 300 MHz NMR Spectrometer located in Central Laboratory of Middle East Technical University was used. Dimethyl sulfoxide (DMSO) was used as the solvent and trimethylsilane (TMS) as the standard. 10-20 mg dried samples were dissolved in 1 ml solvent for the measurement.

3.8.5 Titration

For titration analysis, a pre-determined amount (~0.5 g) sulfonated polymer was placed in 3M NaCl solution and kept for one day. The solution was then titrated with 0.1M NaOH solution. Thus the ion exchange capacity of the polymer can be easily found as mili-equivalents per gram polymer and can be used to find the degree of sulfonation of the PEEK polymer according to:

$$DS = \frac{M_w * IEC}{1000 - 81 * IEC}$$

3.8.6 Gas Chromatography (GC)

GC used for methanol permeability measurements was HP 5890 series 2 model equipment with a Porapack-Q column.

3.8.7 Elemental Analysis

The elemental analyzer used was LECO, CHNS-932 located in the central laboratory of METU. It offers a rapid simultaneous multi-elemental

determination of carbon, hydrogen, nitrogen, and sulfur in homogenous microsamples (2 milligrams).

3.8.8 Water Uptake

Membranes were dried at 100°C to remove the moisture prior to measurements. The dried membranes were weighed and immersed in H₂O and kept for 1 day. Then wetted membranes were blotted with dry absorbent paper prior to weighing. The membrane water uptake was calculated with reference to the dry membrane weight according to the following equation.

$$\text{Water Uptake} = \frac{W_{wet} - W_{dry}}{W_{dry}} \times 100\%$$

3.8.9 Viscosity Measurement

Viscosity was determined by the ratio t/t_0 , where (t) is the efflux time of a given volume of solution and (t_0) is the efflux time of the equivalent volume of pure solvent. Values are commonly determined with a capillary viscometer.

3.8.10 Stability Tests (Chemical & Hydrothermal)

Both chemical and thermo-hydrolytic stability are important for a proton exchange membrane candidate for fuel cells since the operating medium is harsh producing peroxide radicals particularly on the cathode side and since operating at 100 % R.H.

3% H₂O₂ with 4 ppm Fe⁺⁺⁺ ion was used to simulate an oxidative operation for chemical stability tests. Samples were kept in this solution for at least 6 hours at 60 °C. For thermo-hydrolytic stability tests membranes were kept in a vacuum oven at 100% R.H. at 80 °C for at least 6 hours. The determination of the chemical stability was qualitative.

3.8.11 Proton Conductivity Measurements (EIS)

For conductivity measurements conductivity cells made from teflon were designed and constructed. During the course of this study, the design of the conductivity cell was improved. The first the cell (Figure 3.2) was designed to measure conductivity in water and was used in the earlier experiments. Second cell (Figure 3.3) was constructed to perform measurements in water vapor. The first cell has a circular depth with a diameter of 1.5 cm, for filling water to obtain 100% RH condition and 4 platinum wire electrodes (diameter~0.5 mm) utilizing both 2-probe and 4 probe measurements, with separation of 2.5 between inner ones and 1 cm between inner and outer electrodes. In between the two teflon blocks a silicon gasket for good contact was used. Second cell was similar except the openings between 4-electrodes on each side for rapid equilibration with water vapor for 100% R.H., and the length between inner electrodes was 1 cm. The diameter of the platinum wire electrodes was smaller than the ones used in the first cell (~0.3 mm).

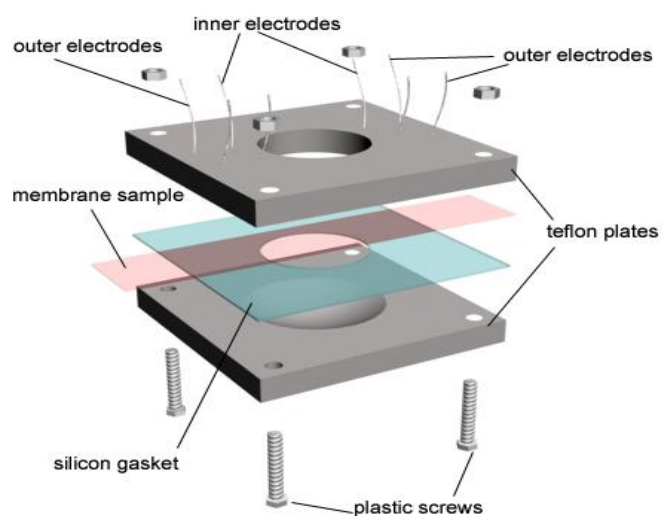


Figure 3.2. Conductivity Cell (1st: for water contact)

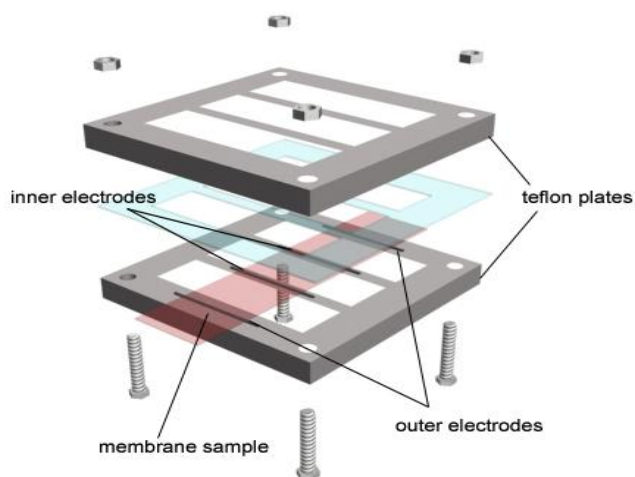


Figure 3.3. Conductivity cell (2nd: for vapor contact)

For part of the conductivity measurements, Agilent 4294 Impedance Analyzer that works in the frequency range of 40 Hz to 110 MHz was used. From the output of this instrument conductivity could only be calculated from the impedance values where the phase angle was close to zero. The output was Bode type. For the rest of the experiments Gamry

750 potentiostat (Frequency range: 10 Hz-300 kHz) coupled with a personal computer was used and the software, Gamry Echem Analyst, enable data analysis through both Bode and Nyquist plots and equivalent circuit fitting possible. Measurements were performed in the potentiostatic mode and the amplitude of the AC signal applied to the cell was set to 10 mV rms (root mean square) for obtaining linear responses as discussed in the literature part. Temperature experiments were performed both in water and vapor environment. Temperature was controlled with a magnetic stirrer with heater (Figure 3.4). The equation below was used to calculate the ionic conductivity from resistance values.

$$\sigma = \frac{l}{R.S}$$

where σ (mS/cm), l (cm), R (k Ω), and S =width*thickness (cm²) denote the ionic conductivity, distance between the reference electrodes, the resistance of the membrane, and the cross-sectional area of the membrane, respectively.

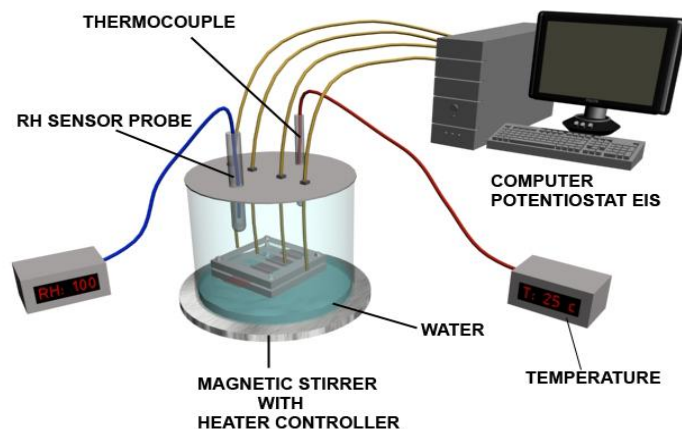


Figure 3.4. Proton Conductivity Measurement Setup

Membrane samples were cut into 1 cm wide strips and more than 4 cm in length to easily stretch them after putting water into the compartment and sample elongates to final length to decrease the error caused by swelling. The wet thicknesses were measured by a micrometer at 3 to 5 points according to check dimensional homogeneity and averaged. Samples were kept in deionized water before the measurements.

3.8.12 Dynamic Mechanical Analysis (DMA)

DMA was used for determining tensile strength (Mpa) and elongation at break. The mechanical strength of the membranes was measured with a vertical film stretching device (Instron 3367 Mechanical Tester). The dimensions of the samples were set to 15 mm in width, 50 mm in length. The experiments were performed with a constant stretching speed of 5 mm/min in ambient air.

3.8.13 Methanol Permeability Measurement

Methanol permeability measurements were performed by using a permeability cell (Figure 3.5) with two compartments and Gas Chromatography (GC) with a flame ionization detector (FID).

The cell's compartments were filled with 80 ml 2M methanol in one side and distilled water in the other. GC used was HP 5890 series 2 model equipment with a Porapack Q column. The conditions of the experiment were given in Table 3.1.

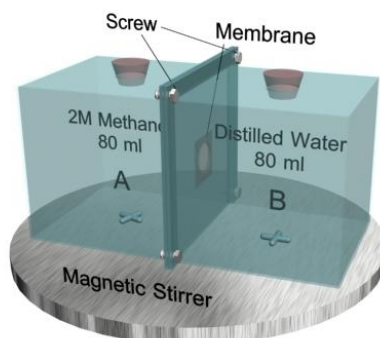


Figure 3.5. Methanol Permeability Cell

Table 3.1. Experimental Conditions of GC for Methanol Permeability Test

Carrier Gas	Nitrogen (N ₂)
Carrier Gas Pressure	21 psi
Injection Temperature	220 °C
Column Temperature	140 °C
Detector Temperature	230 °C
Detector Type	FID
Injection amount	1 mL

The methanol concentration change was recorded at nearly every 10 minutes in a total of 1-1.5 hours. The area under the methanol peak from the GC chromatogram was converted to concentration data using the calibration curve obtained by measuring the known concentrations of methanol (0-2 M) and then methanol permeability was calculated from the slope of $C_B(t)$ vs. time plot sketched by the help of the following formula (Tricoli, 1998).

$$C_B(t) = \frac{A(DK)C_A(t - t_0)}{V_B L}$$

Where; $C_B(t)$: Methanol concentration in compartment B at time t
 A : Effective membrane area
 D : Methanol diffusivity
 K : Partition constant between the membrane and the solution

C_A : Methanol concentration in compartment A
 V_B : Volume of compartment B
 L : Thickness of the membrane
 t : Time

Then; since permeability (P)=DK (cm²/s):

$$P = (DK) = \frac{C_B(t)V_B L}{AC_A(t - t_0)}$$

3.8.14 Single Cell Tests (Polarization Curves)

The fabricated membranes were tested in single cell setup located in Fuel Cell Research Laboratory in the Chemical Engineering Department of Middle East Technical University (METU) (Figure 3.6 and Figure 3.7).

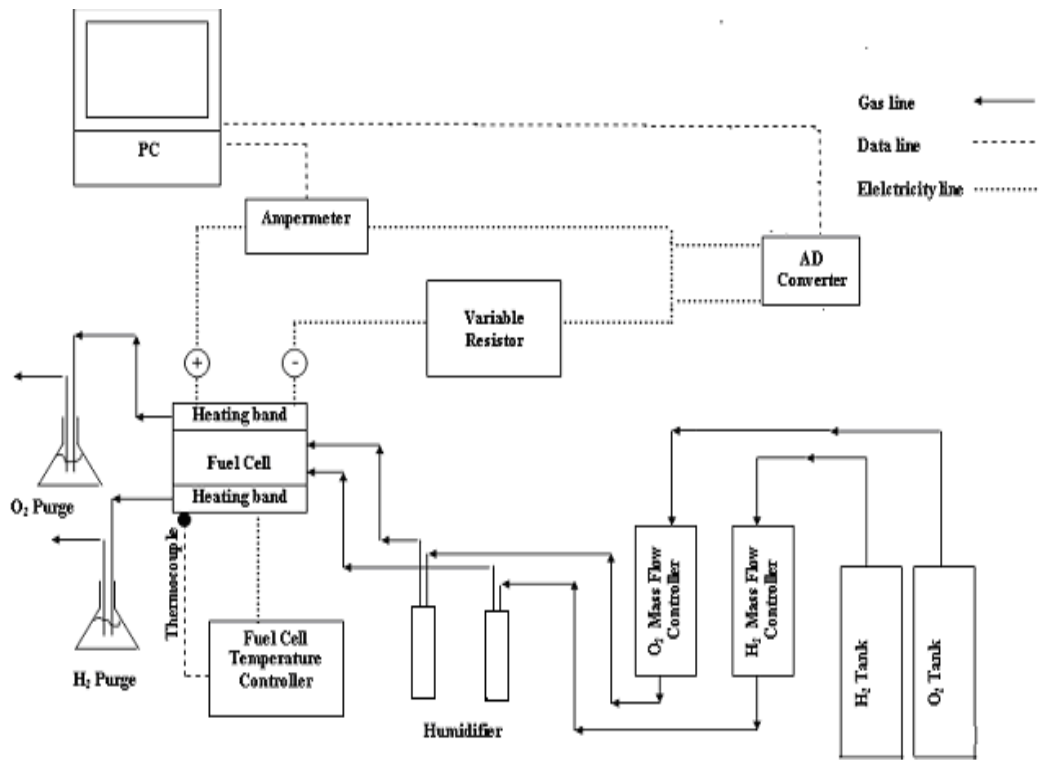


Figure 3.6. Flowchart of Fuel Cell Test Station

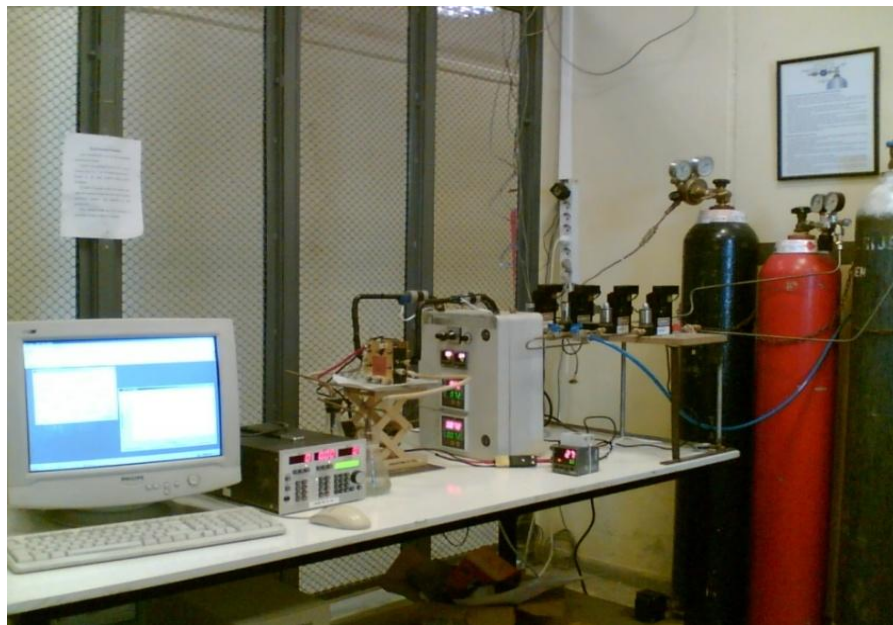


Figure 3.7. Fuel Cell Test Station

In a typical single cell test the parameters were as follows: $T_{\text{cell}}=70\text{ }^{\circ}\text{C}$
 $T_{\text{humid}}= 80\text{ }^{\circ}\text{C}$ for both anode and cathode $T_{\text{cgasline}}=80\text{ }^{\circ}\text{C}$ for both anode
and cathode . $V_{\text{gas}} = 0.1\text{ slm}$ for both H_2 and O_2 .

The electrode preparation with spraying, MEA preparation with hot press,
single cell test protocols explained in more detail in appendices were
developed by Erkan (2005), Bayrakceken et al. (2007) and Sengül (2007).

CHAPTER 4

RESULTS & DISCUSSION

4.1 Sulfonation

4.1.1 Sulfonation of PEEK

4.1.1.1 Setting Optimum Reaction Parameters

As it was stated in the literature survey part, degree of sulfonation (DS) of SPEEK depends on many factors such as temperature, time, acid type and concentration, humidity of the polymer and medium, stirring rate, and ratio of acid to polymer. Among these; temperature, time and ratio of acid to polymer are the most important ones. It is possible to sulfonate PEEK up to high DS values even over 100 % by controlling these parameters. PEEK is not soluble in common solvents before sulfonation, however as DS increases (above ~40%) it becomes soluble since hydrophilic sulfonic acid groups attached to the aromatic ring changes its chemical character. But above a certain DS (~70%) it first becomes soluble in hot water and methanol then around and above 100% DS in water at room temperature. Thermal and mechanical stability also decreases as DS increases. Swelling, which was observed frequently during washing with hot water, is another problem at high DS values. Because of these limitations observed during preliminary experiments, SPEEK with a DS in a narrow range were produced for using it as the polymer matrix for composite membranes.

At room temperature, the sulfonation of PEEK proceeds slowly and takes several days to achieve moderate sulfonation levels (DS over 50%) (Huang et al., 2001). Time of reaction required to achieve the same DS drop to several hours at elevated temperatures around 50 °C. However, difficulty of controlling the degree of sulfonation at these temperatures also increases as experienced from several experiments. This was observed in a set of experiments where 10 g dried PEEK was dissolved in 250 ml H₂SO₄ (95-97%) at room temperature for 2 hours and then undissolved parts were filtered, reacted with sulfuric acid at around 50 °C and 5 samples were taken in certain time intervals. It was observed that while 1st sample did not dissolve completely in DMAc meaning DS is below ~40%, swelling started at 3rd sample and the last sample was completely water soluble meaning DS was above 80%. In this set, times of reactions were 2, 5, 7, 9 and 11 hours. This result showed that ideal time of reaction is between 2 and 5 hours at temperatures around 50 °C. Since it was stated in the literature that sulfonation around 50 °C does not affect the main polymer chain (Li, 2003; Huang, 2001), sulfonation studies of PEEK were carried on at around this temperature changing the time, and sometimes acid-to-polymer ratio to achieve the desired DS.

First sulfonation experiments showed that PEEK obtained and used with no further modification (it was in pellet form) did not dissolve in the time intervals reported and recommended in the literature at room temperature. During these first trials complete dissolution took a long time (several hours-up to 8-10 hrs) as opposed to 1-2 hr dissolution time reported in the literature, since the pellets agglomerated in the acidic medium and stuck to each other and to the walls of the glass reactor. To solve this problem first the temperature was raised after 1 hr from room temperature to 50-60 °C to increase the dissolution rate. However, it is obvious that as the time of dissolution increases, undissolved parts will not be sulfonated while

dissolved parts are being sulfonated which causes a heterogeneous character of the final product.

To overcome this problem PEEK was ground into fine powder with a grinder and dried at 100 C at least for 12 hrs before sulfonation for the rest of the experiments since it was reported that humidity of PEEK decreases the dissolution and sulfonation times (Huang et al., 2001, Daoust et al., 2001). The dissolution temperature was also set to the reaction temperature and dissolution periods were decreased from several hours to 15-20 minutes. However, it should be noted that though the dissolution period was shortened, since the temperature is around 50 °C, sulfonation period for the dissolved part also decreased and the dissolved part would be more sulfonated than the undissolved part. As a result, it can be concluded that it is impossible to prevent heterogeneity of sulfonation completely for the post-sulfonation method.

The ratio of acid to polymer was also increased in part of experiments to decrease the dissolution time, since it was reported in some of the literature that the amount of excess acid does not affect sulfonation. This decreased the dissolution time a little, however, it was observed that increasing acid ratio (50/1 for example; 5 g PEEK in 250 ml H₂SO₄; 50-55 °C) made SPEEK soluble in hot water in very short times, around 3-3.5 hrs. This was either because of the increase of the DS or caused by polymer chain degradation although it was not supposed to occur in sulfuric acid (95-97%) as stated above according to the literature. Therefore, acid to polymer ratio (mL/g) was decreased to 25/1-20/1 gradually at which more controllable sulfonation was observed. Lower ratios were also used for more controllable reaction, however, in this case dissolution period increased. These observations showed that all three

parameters of time, temperature and acid/polymer ratio are very important and to be controlled for the desired degree of sulfonation.

After several experiments these parameters were optimized and fixed for obtaining a DS between 50-70 (Table 4.1).

Table 4.1. Optimum Sulfonation Parameters for PEEK

Temperature (°C)	Time (hrs)	Acid/polymer ratio
~50	~4	~20

Another practical experimental problem was the washing of sulfonated polymer. It was observed that as DS increases removing excess acid, which is important for accurate titration and quantitative detection of sulfonic acid groups as well as preventing possible problems during casting step, from the SPEEK was getting difficult. At high temperatures and longer times, even after several washings with distilled water, pH of the washing water was still below 5 (pH of distilled water ~5-6). This was probably because of the increasing swelling with increasing DS. Removing acid from the swelled polymer is much more difficult. A dialysis tubing system was used in some of the studies for removal of residual acid. In this study, after few times of washing, SPEEK was left in distilled water overnight, and next day washed again several times.

To obtain SPEEK with a DS around 60%, at 50 °C, 15 g PEEK in 300 ml sulfuric acid was dissolved in 10 minutes (at the reaction temperature), then reacted for about 4 hrs and a DS of 59 (H-NMR) was obtained. This DS seemed to be ideal for fuel cell operation since all the samples having DS above 60 were dissolved above 80 °C. However, the membranes prepared from this polymer also showed poor hydrolytic stability after 80

°C, even though there was no problem during hot pressing at 150 °C. There may be two possible reasons for this stability problem: As DS increases swelling increases and after a threshold water uptake value the structure solvates in hot water and a degradation of the main chain causing a decrease in the M_w of the sulfonated polymer occurring during the dissolution of PEEK at high temperatures in sulfuric acid both may have an effect on this mechanism.

To observe the effect of RH of the medium, experiment above was reproduced with the same conditions except passing N_2 gas for removing water vapor, the product dissolved in oven at around 70 °C showing the effect of water vapor in the medium (RH which is typically around 30 %) on the sulfonation. It can be concluded from this experiment that one of the reasons of difficulty in controlling the DS of PEEK particularly at high temperatures is the RH of the medium which can change from day to day. All these experiences showed that the reaction conditions must be controlled strictly for obtaining reproducible DS values for the sulfonation of PEEK.

4.1.1.2 Determination of DS (H-NMR & Elemental Analysis)

The most practical way of calculating IEC or DS is titration. However, titrations performed by different methods always gave lower DS values compared to other methods. The method of titration used in some of the studies in which dissolving SPEEK in solvents (DMF or DMAc) then calculating the released amount of H^+ by titrating with 0.1 M NaOH, which gives the mmoles of sulfonic acid groups directly did not give consistent results. The reasons may be the the residual acid in the structure not washed away or H-bonds formed between the sulfonic acid groups and solvent especially DMF. Ion-exchange with NaCl or NaOH and then titration with NaOH or HCl (back-titration) also resulted generally in low

values and inconsistent results when it was repeated for reproducibility. In titration, the reason of the low DS values compared to other methods such as H-NMR is probably because only surface ions for exchanging can be reached.

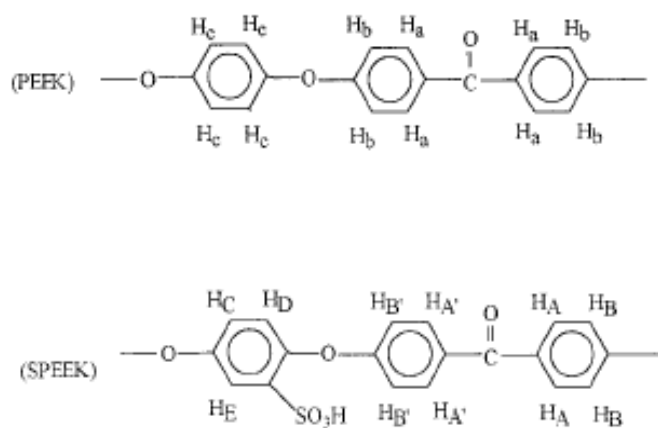
There are three other possible determination methods for sulfonic acid groups attached which are FTIR, H-NMR and S-elemental analysis. Among these FTIR is generally used for qualitative determination. H-NMR is more reliable from titration since it shows chemically bonded sulfonic acid groups. Also quantitative calculation is possible from integral areas of the peaks. Elemental analysis were also used and gave consistent results in increasing behavior as will be shown, but because of the hydrophilicity of SPEEK it must be dried well before the measurement since humidity might affect the weight percentage of sulfur.

In Scheme 4.1, nomenclature of aromatic protons of PEEK and SPEEK repeat units are shown. When a sulfonic acid group is attached to the hydroquinone group the signal expected for C position protons at about 7.25 ppm are differentiated into three different types. A 0.25 ppm downfield shift for the E position proton is observed so the signal at 7.51 that can be seen from Figure 4.1 and Figure 4.2 indicates the attached SO_3H group. As the degree of sulfonation (DS) increases intensity of H_E increases. DS can be calculated from the integration values given in the NMR by using the equation below using relative integrated peak areas.

$$\frac{n}{12-2n} = \frac{A_{H_E}}{\sum A_{H_{AA'BB'CD}}} \quad (0 \leq n \leq 1)$$

$$DS = n \times 100\%$$

Here A_{H_E} is the integration area of proton in the position E and the denominator is the sum of the area of the rest of the aromatic protons.



Scheme 4.1. Aromatic protons of PEEK and SPEEK

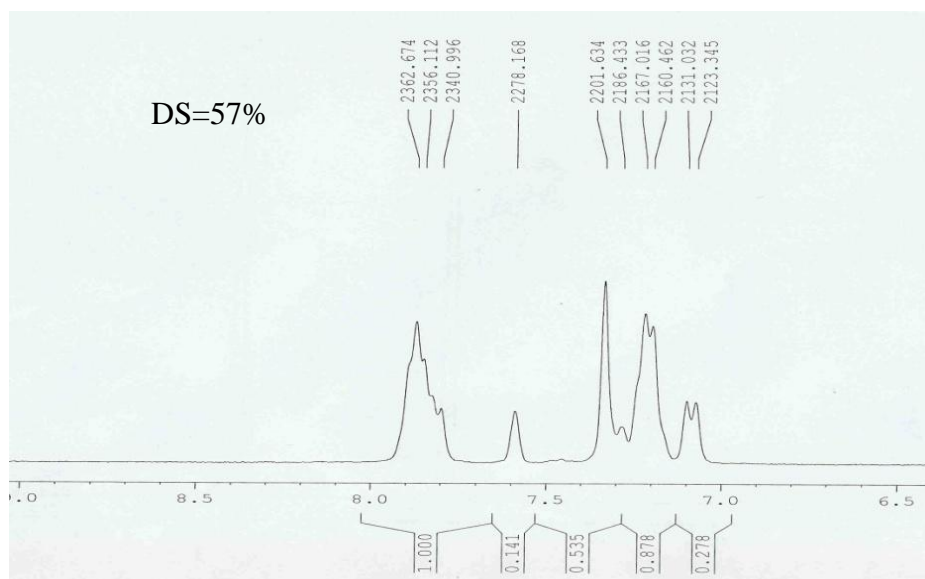


Figure 4.1. H-NMR spectrum of SPEEK-2

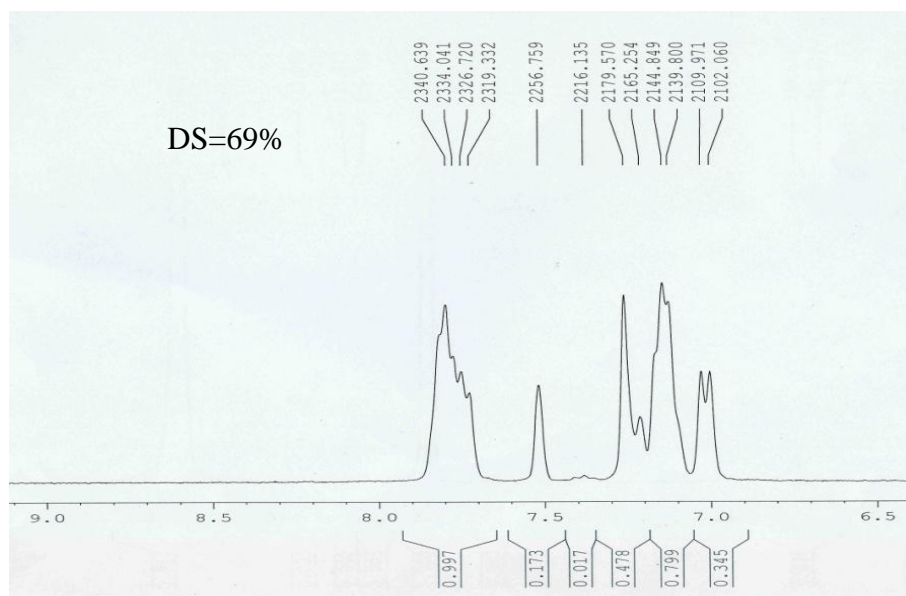


Figure 4.2. H-NMR spectrum of SPEEK-4

The two spectra show only the aromatic proton signals and the intensity of H_E can easily be compared. SPEEK-2 with 57% DS was 2 hr sulfonated

while SPEEK-4 with 69% was 4 hr sulfonated PEEK at same temperature (~55 °C).

DS from sulfur weight percent was calculated according to the following formula assuming that only one sulfone group per monomer unit is attached as assumed in most of the studies up to 100%. Since PEEK unit does not have sulfur in its structure all the sulfur came from sulfonic acid groups and the calculation is straight forward which is not the same for PES as will be seen in the next part.

$$DS = S/32 / ((100 - S/32 * 81) / M_w)$$

Here S/32 is the number of moles of sulfur as well as number of moles of sulfonic acid group since there is one sulfur per sulfonic acid group, and denominator is the number of moles of repeat unit of PEEK excluding sulfonic acid group.

Comparison of calculated DS values from S-elemental analysis results (S wt %) and DS values calculated from H-NMR results were given in Table 4.2, Figure 4.3 and Figure 4.4. DS values calculated from elemental analysis were found to be always below DS values calculated from H-NMR with a little difference. The moisture absorbed by hydrophilic SPEEK before elemental analysis may be the reason of this. Also the increase in difference as DS increases validates this. But in H-NMR results moisture does not affect the results. As can be seen from Table 4.2, sample 1's DS% is 38 from elemental analysis and 44 from H-NMR. It is known that around DS=40% SPEEK dissolves difficultly in solvents, however, it dissolved easily in DMAc and in DMSO for H-NMR analysis. Therefore, it is obvious that elemental analysis results were less than the actual DS

values because of the humidity and heterogeneity problem (elemental analysis equipment used in this study takes 1-2 mg sample only) possibly, and H-NMR results are more reliable for the determination of DS.

Table 4.2. Summary of DS % values calculated from Elemental Analysis and H-NMR for SPEEK

Sample	S% (elemental)	DS% (elemental)	DS% (NMR)
1	3.8	38	44
2	5	52	57
3	5.2	54	59
4	5.4	56	69
5	6	64	72
6	6.26	67	80

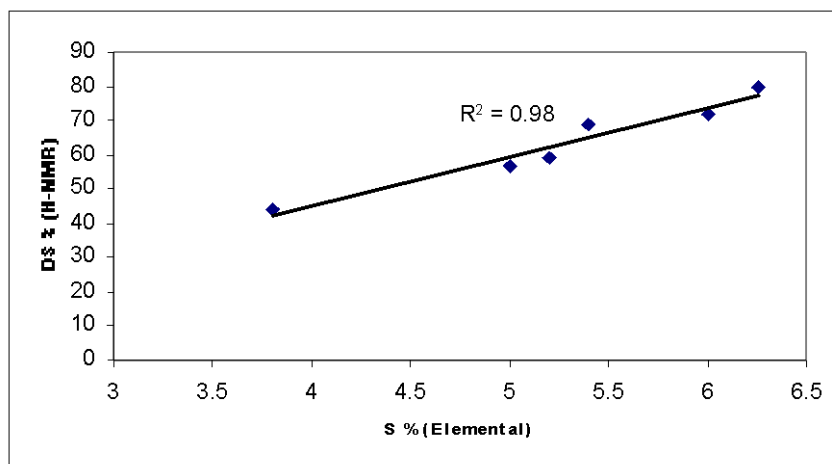


Figure 4.3. Degree of Sulfonation (DS) calculated from H-NMR vs S% from elemental analysis

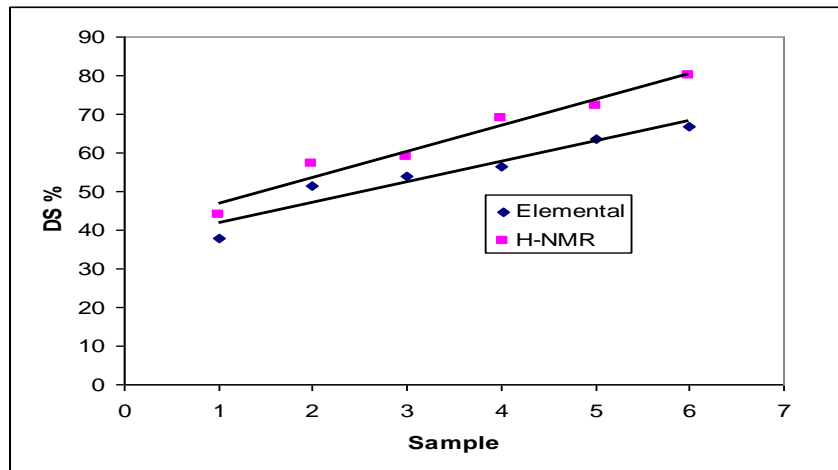


Figure 4.4. Comparison of DS values calculated from elemental analysis and H-NMR

Using optimum post-sulfonation parameters selected as discussed above which are 20:1 acid-to-polymer ratio, 50 °C dissolution and reaction temperature, and 4-5 hr. reaction time, DS was controlled around 60-70% as can be followed from Figure 4.5. For obtaining DS around 60 %, time should be reduced to 3-4 hr.

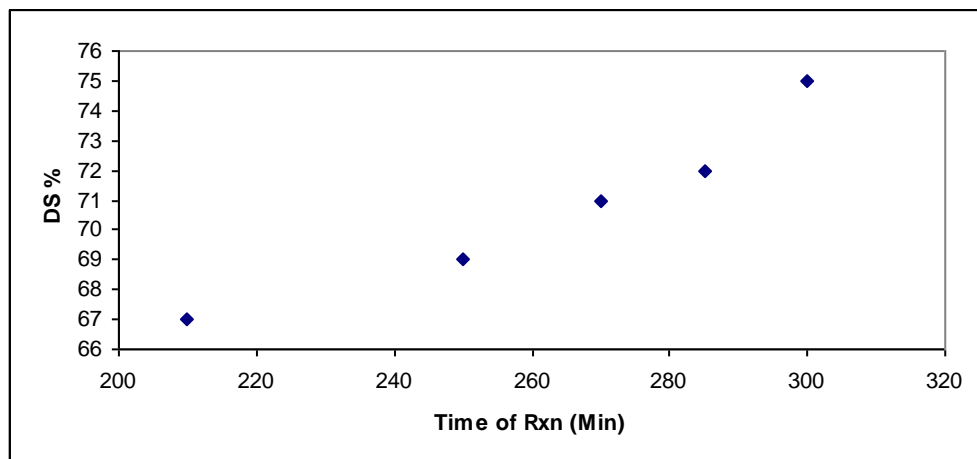


Figure 4.5. DS vs time of reaction for SPEEK at 50 °C

4.1.1.3 Thermal Characterization (TGA & DSC)

TGA and DSC give information on thermal behaviors of the polymers and the change in thermal characteristics as sulfonic acid groups attached to the chain increases. DSC is important particularly for determination of the glass transition temperature (T_g). T_g is an important parameter for membrane operation temperature.

From Figure 4.6, thermal degradation starting temperature can be observed to be above 550 °C for PEEK which is consistent with the manufacturer's reported value.

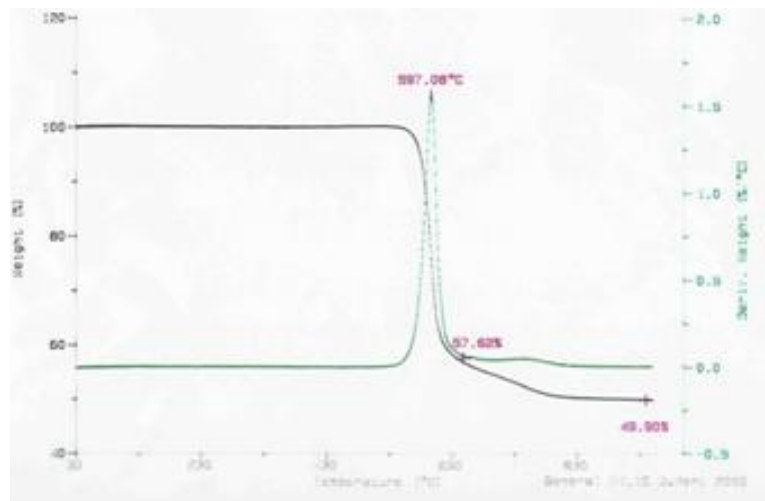


Figure 4.6. TGA of PEEK

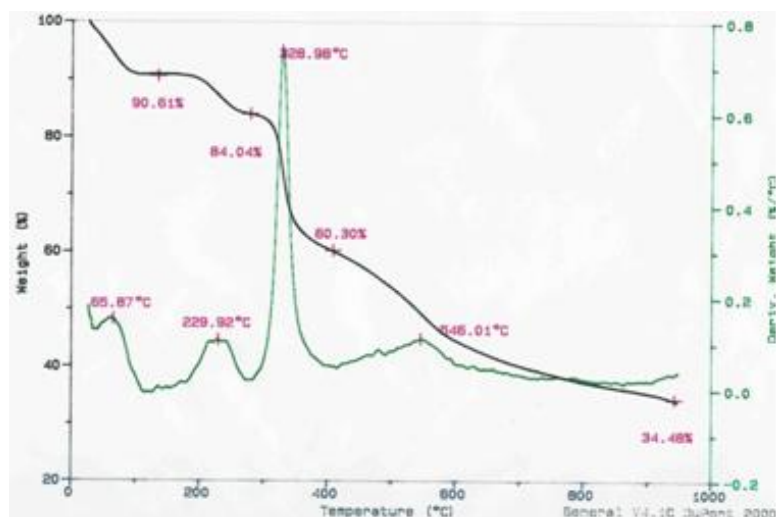


Figure 4.7. TGA of SPEEK (DS=79)

In the literature (Chang et al., 2003; Xing et al., 2003) a two step weight loss in the TGA analysis of SPEEK was reported which are considered to be the loss of sulfonic acid group and the loss of polymer by degradation of chains respectively. The loss of $-\text{SO}_3\text{H}$ group was also reported to be about 20% which is reasonable when it is considered that the theoretical maximum $-\text{SO}_3\text{H}$ weight percentage is 22 % as will be shown below. If sulfonated polymer is not heated before analysis, a certain amount of water will exist and give a third weight loss step at the beginning. Looking at Figure 4.7 it can be seen that there are four step losses, the first one starting at 80°C is definitely the water loss but the second one starting at about 200°C is interesting since it is not expected, the third one is probably sulfonic group loss and then polymer degradation starts after 400°C . The second step loss may also be sulfonic group loss, which means that this is a two step loss for SO_3H . This may be possible because of two reasons. First, DS of this SPEEK sample was found to be high, at high DS, and for high temperature sulfonation there is the possibility for than one sulfonic group attached to one PEEK unit. Then, these second type groups will definitely be lost first. Another possible reason is that this sample was

probably heterogeneously sulfonated as discussed before because of the long dissolution time at room temperature. This means even if DS is below 100% some units could have been sulfonated by more than one sulfonic group again.

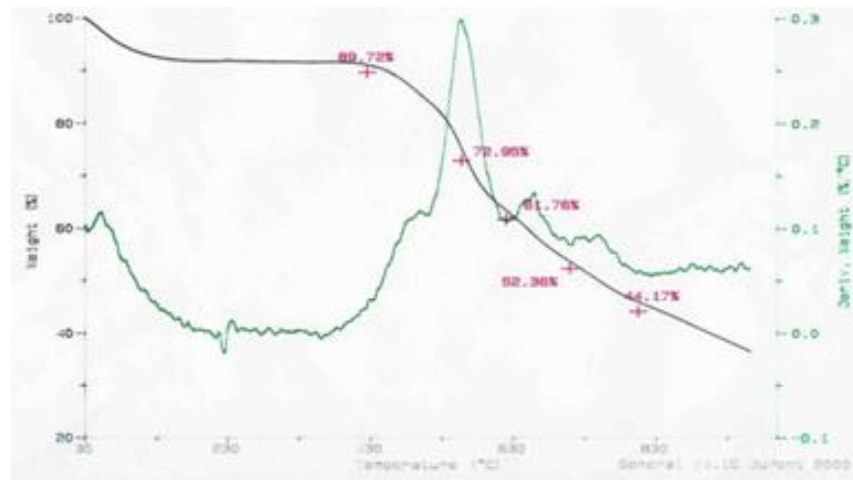


Figure 4.8. TGA of SPEEK (DS=62)

The second TGA (Figure 4.8) of SPEEK shows a smoother curve with 3 step losses. About 10% water is lost until ~100 C, then sulfonic group detaches however this time transition to loss of polymer chain is not clear. Comparing two it is obvious that polymer degradation starts earlier for the more heterogeneously and more sulfonated SPEEK (DS=79) than SPEEK (DS=62).

From TGA it is possible to calculate the percentage loss of $-\text{SO}_3\text{H}$ assuming that the first step loss (after water loss) is accounted to this loss. This percentage may be theoretically calculated as follows:

$$W(-\text{SO}_3\text{H lost}) = \frac{81 \cdot n}{288 + 81 \cdot n}$$

Where; $n=DS$, 288 =molecular weight of one PEEK unit, $81=M_w$ of SO_3H

Then theoretically maximum W% at 100% sulfonation (assuming one SO_3H per unit) is: 22% Then $DS= n$ can be calculated from $n=288W/(81-81W)$.

For SPEEK (DS=68) since transition is not clear it is difficult to calculate the DS exactly but a DS of 60-70%, which is consistent with the H-NMR result, can be estimated. TGA results can be used to calculate approximate DS values for checking and comparison purposes. From the TGA data (Figure 4.9), weight losses were calculated and DS was found to be around 65% which is very close to the DS value calculated from H-NMR proving that the first step loss is caused by $-SO_3H$ loss.

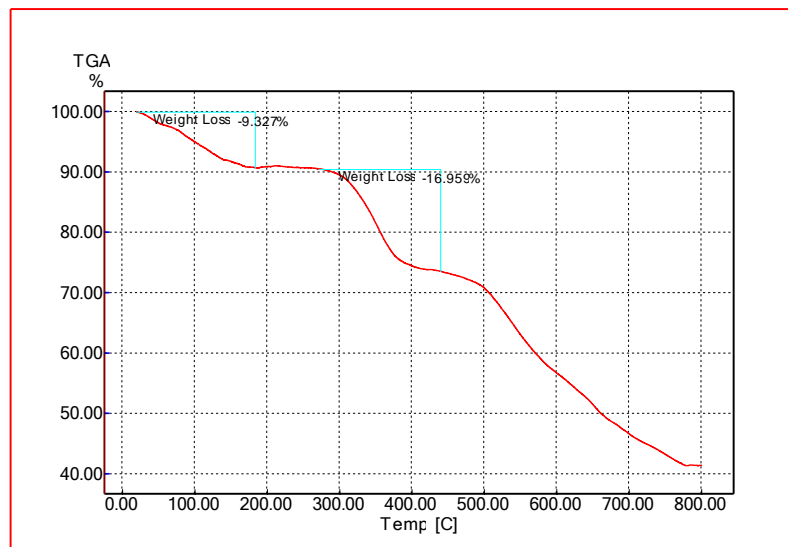


Figure 4.9. TGA of SPEEK (DS=68)

The two step losses which account for sulfonic acid group loss and the main chain decomposition respectively can be clearly seen from the.

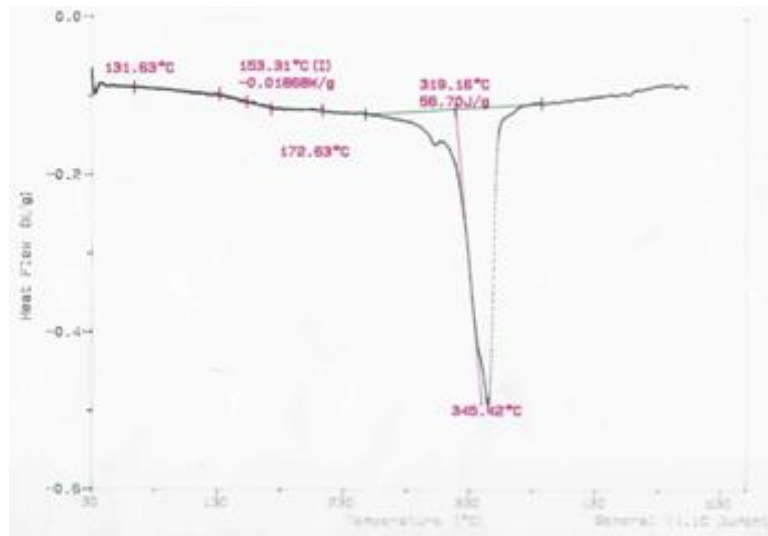


Figure 4.10. DSC of PEEK

From Figure 4.10, two important thermal characteristics, glass transition temperature (T_g) and melting point I can be observed since PEEK is a semi-crystalline polymer. T_g is around 150 °C and T_m is around 330 °C as expected. T_g is increased to about 190 °C for 68% sulfonated SPEEK sample (Figure 4.11). This is expected since the sulfonic acid groups interact, and form ionic groups that decrease the mobility of the chains. In addition, the semi-crystalline structure of the PEEK turn into an amorphous structure as the DS increases which is clear from the disappearance of the melting peak.

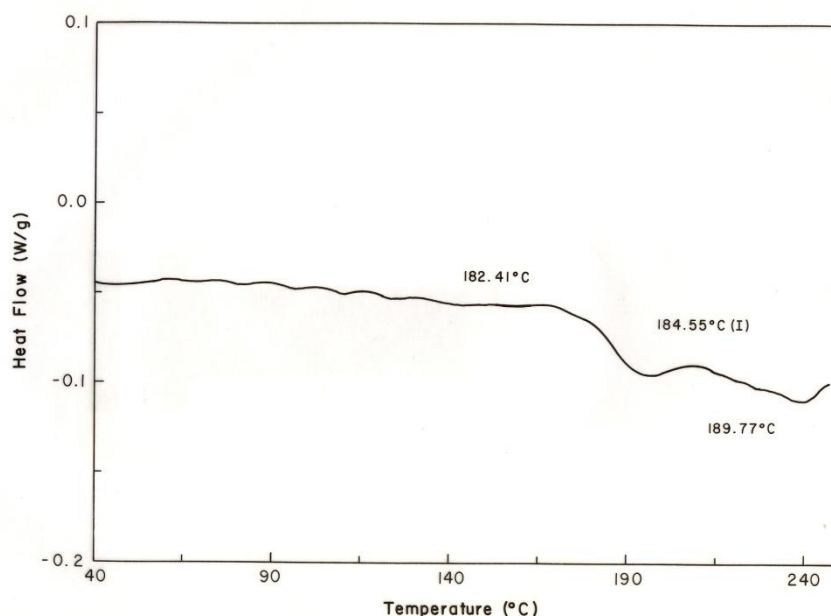


Figure 4.11. DSC graph of SPEEK (DS 68%) membrane

4.1.2 Sulfonation of PES

4.1.2.1 Effect of Actual Composition of PES Used

For the sulfonation of PEEK, sulfuric acid acted as the solvent and the sulfonating agent. The required DS values were achieved by controlling the polymer/acid ratio, time and the reaction temperature. PEEK is a polymer that can relatively be easily sulfonated. However, because of the presence of the electrophilic sulfone group in the structure of PES it can not be sulfonated easily as PEEK. The most suitable sulfonating agent is the chlorosulfonic acid (ClSO_3H ; CSA) as stated in the literature survey part. During PES sulfonation, H_2SO_4 with the same concentration (95-98%) was used as the solvent and after dissolution the necessary amount of CSA were added drop by drop (Guan et al., 2005). However, the dissolution time was a problem similar to the PEEK case. It was reported in the literature that PES dissolves nearly in 2 h at room temperature but

the PES used in this study did not. In some of the reports it was stated that the powder form was used. PES available was in pellet form and unlike PEEK it could not be ground. During the dissolution period, the size of the glass reactor, polymer-to-acid ratio and the stirring rate were critical to prevent the agglomeration of PES in sulfuric acid. The time of dissolution was decreased to several hours by optimizing these parameters.

Besides these practical problems, the first H-NMR results (Figure 4.13) were not similar to the reported ones in the literature. The expected peak at 8.3 ppm chemical shift (Figure 4.12) showing the attachment of the sulfonic acid groups to the ring was very small compared to the literature (Guan et al., 2005, Kim et al., 1999) and instead a peak that was not expected showed at around 7.4-7.5 ppm chemical shift.

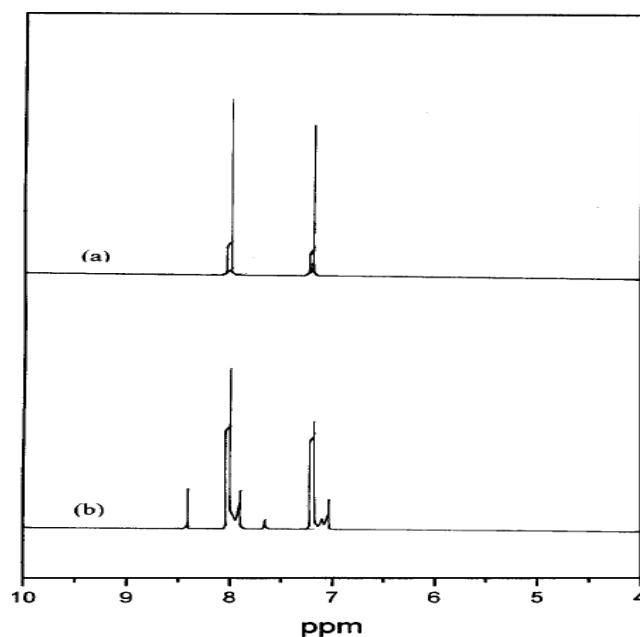


Figure 4.12. H-NMR a) PES b) SPES (Kim et al., 1999)

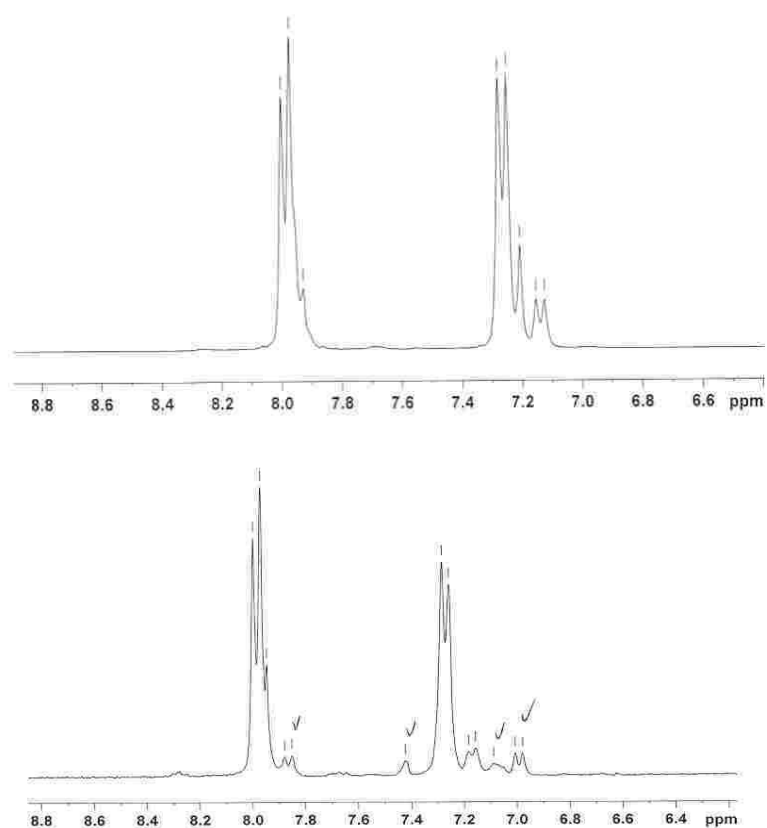


Figure 4.13. H-NMR spectra of a) PES(1) b) SPES(1)

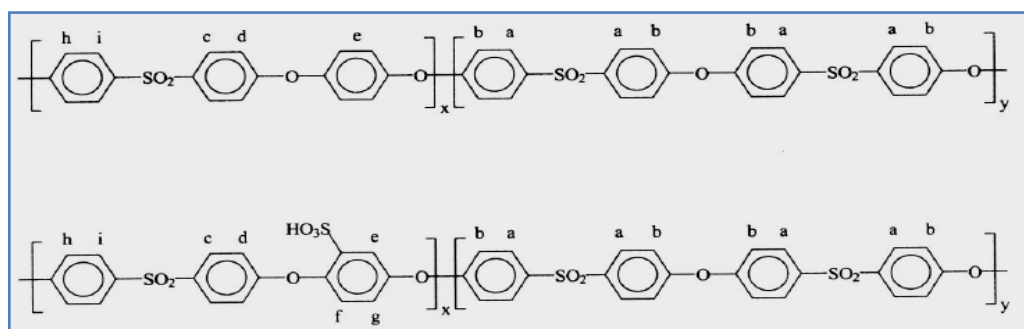
Table 4.3 summarizes the S% by weight of sulfonated PES samples prepared under different conditions from sulfur elemental analysis. M_w of PES unit is 232, theoretically each unit has one sulfone group so S% by weight is ~13.7% for unsulfonated PES, however from Table 4.3., it can be seen that there are values below this value for sulfonated samples. One reason of the low S% percentage may also be the water content although the samples were dried and kept in desiccator but from TGA results it is known that even if dried at 100 °C, sulfonated polymers bound water is lost until around 200 °C. Another reason may be some break-ups on the main chain caused by chlorosulfonic acid.

Table 4.3. Summary of characterization results for determination of DS for SPES samples sulfonated at various conditions

Sample	Elemental (S% wt)
1	15.09
2	14.27
3	12.89
4	12.82
5	11.16
6	11.66
7	11.49

From H-NMR spectra, the expected signal for sulfonic acid group at 8.3 ppm was never observed clearly even for the samples having high S% by weight from sulfur elemental analysis. Elemental results show that some of the PES samples were clearly sulfonated to some extent. S wt% greater than the theoretical S wt% for the unsulfonated PES proves the sulfonation. Another important point was the peak in the H-NMR spectra at the 7.5 ppm chemical shift. This peak was suspected to show the attached sulfonic acid group to the polymer but not at the point expected. The reason of this interesting result was explored from a different study on sulfonation.

During literature survey, to find the reason of this unexpected result, a similar spectrum obtained from samples of this study was found but for the polymer named (Polyetherethersulfone (PEES)) (Benavente et al., 2000). They sulfonated PEES with the structure given in Scheme 4.2 and characterized the sulfonated polymer with H-NMR.



Scheme 4.2. Repeating unit and proton designations of PEES and SPEES (Benavente et al. 2000)

Figure 4.14 shows the peak positions of the protons designated in Scheme 4.2 for unsulfonated PEES, 5%, 10% and 20% sulfonated PEES. From the spectra it is clear that the area of the peak at the chemical shift position around 7.4 ppm increases as the DS increases. Authors assumed that after complete conversion (sulfonation) only the x part was sulfonated and the percentage of this part can be found from the ratio of the areas from H-NMR.

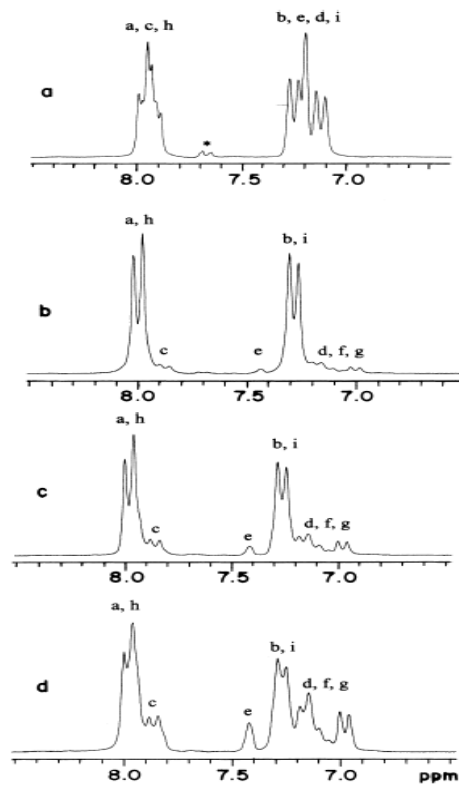


Figure 4.14. H-NMR a) PEES b) SPEES (5) c) SPEES (10) d) SPEES (20) (Benavente, 2000)

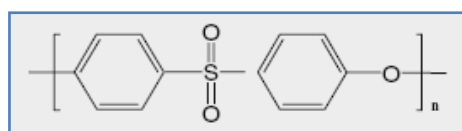
$$x + y = 1$$

$$\frac{A_{lf}}{A_{hf}} = \frac{2y}{(2y + 3x)}$$

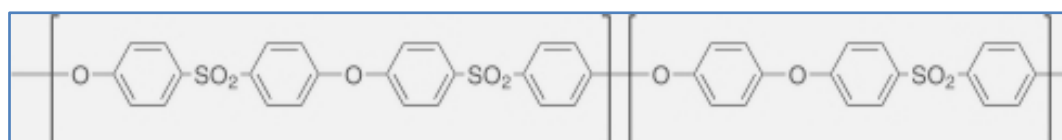
where A_{lf} is the area under the signals at low field (over 7.6 ppm) and A_{hf} is the area under the signals at high field (below 7.6 ppm).

It was surprising that the spectrum was similar to that obtained in this study, which may explain the unexpected results. After investigating the

product specifications of PES produced by Radel-Solvay it was realized that the product contains an unknown small ratio of PEES units. From both the specifications of the producer (Radel-Solvay) of the PES used (Scheme 4.3), from the preliminary H-NMR results and from Benavente et al.'s results, it was concluded that the unknown ratio of PEES units in this polymer completely changes the sulfonation behavior and therefore spectra.



a)



b)

Scheme 4.3. a) Structure of Polyethersulfone (PES) (Aldrich product) & b) Polyethersulfone (PES) (Solvay product)

More experiments were performed to observe the effect of this unit on sulfonation. As a result it was shown that this unit (PEES unit) is preferably and easily sulfonated compared to the PES unit because of the position of the electrophilic sulfone group. This sulfone group exists in both units but an additional ether linkage in PEES unit makes one phenylene ring less affected.

To observe the difference of a PES and PES containing certain amount of PEES units, PES (Solvay) and PES (Aldrich) were sulfonated under

exactly the same sulfonation conditions. 10 grams of polymer dissolved in 50 ml H₂SO₄ at room temperature (17 °C) and then 25 ml CSA were added dropwise in half an hour. After 3 hour reaction time, results in Table 4.4 showed that PES (Solvay) including certain ratio of PEES units was sulfonated more under same reaction conditions.

Table 4.4. Comparison of IEC, DS & inherent viscosity of PES polymers sulfonated at the same conditions

Sample	IEC (meq/g)	DS (mol%)	η_{inh} (dl/g)
SPES(Aldrich)	0.25	6	0.58
SPES(Solvay)	0.73	18	0.84

Note: IEC & DS calculated by titration; Inherent viscosity of PES (Aldrich) & PES (Solvay) are: 0.51 & 0.52 respectively

4.1.2.2 Comparison of Sulfonation Methods

In the literature, there are few studies on SPES compared to SPEEK because of the difficulty experienced in sulfonation of PES. Therefore different methods of sulfonation were tried to be developed for improving the DS of PES.

In the US patent 6,790,931, it was reported that using carboxylic anhydrides catalyzed the sulfonation. According to the proposed mechanism, anhydride takes the proton of chlorosulfonic acid in the presence of DCM and then sulfonates PES. In the experiment performed acetic anhydride was used. 50 ml H₂SO₄ was first cooled in ice bath and

17.5 ml CSA added dropwise to remove the absorbed water vapor in sulfuric acid. Then, 10 g dried PES(Aldrich) added. Dissolution occurred only after 7 hrs, after adding 25 ml DCM the reaction medium is cooled again to near 0 °C. 2 ml CSA was added dropwise in ½ hrs and the 4 ml acetic anhydride was added. Reaction proceeded for 2.5 hrs. It was observed that there were still some undissolved PES, this portion was removed by filtering and the solution was poured in excess of icy distilled water. N₂ gas was passed through the reaction medium during the course of reaction to keep water vapor and HCl formed away.

The sulfonated polymer was titrated for determining IEC and DS after drying at 90 °C. Since during titration experiments of SPEEK problems were encountered, 3 different procedure for titration were used for determining DS of SPES samples. In the first procedure, SPEEK sample was dissolved in 10 ml DMF and titrated with 0.1 M NaOH; in the second one sulfonated polymer was dissolved in 25 ml DMF and titrated with 0.05 M NaOH; in the third procedure, sulfonated polymer was kept in 3 M NaCl (8 hrs, 60 °C) and all titrated with and 0.1 M NaOH. The DS values calculated from 3 titration procedures were very close Table 4.5.

Table 4.5. Titration DS results of SPES (acetic anhydride catalyzed)

Procedure	M _{NaOH} (M)	V _{NaOH} (ml)	DS (mol%)	η _{inh} (dl/g)
0.5 g in 10 ml DMF	0.1	4.8	25	
0.5 g in 25 ml DMF	0.05	9.5	24	0.58
0.5 g in 50 ml NaCl (3 M) @ 60 °C	0.1	4.6	23	

To evaluate and compare effect of different procedures of sulfonation of PES, another set of experiments were performed: (1) 5 g dried PES in 25

ml H₂SO₄ was dissolved in 7 hrs, undissolved part filtered, 15 ml CSA added dropwise. In another batch (2), 10 ml CSA was first added to H₂SO₄ for dehumidification and then 5 ml CSA added. In a 3rd batch (3) additional 2 ml acetic anhydride was added which has the same procedure with 2nd. Reactions proceeded for about 2.5 hrs. All samples were treated with 1 M HCl, then put in 50 ml, 3 M NaCl for 1 day, then titrated with 0.05 M NaOH. DS% values calculated from titration were summarized in Table 4.6.

Table 4.6. Titration DS results of SPES samples sulfonated with different procedures

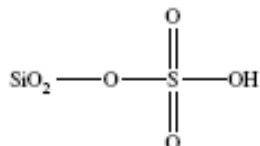
Sample	DS (mol%) (Tit)
SPES(1)	5
SPES(2)	25
SPES(3)	26

The results showed that dehumidifying acid seems to increase the sulfonation, while acetic anhydride addition effect is not so clear. Viscosity results are very important for detecting a possible main chain degradation which causes a loss of average molecular weight of the polymer. This may cause brittle membranes as well as low hydrolytic, thermal and mechanical stability during fuel cell operation.

Since the sulfonation of PES is difficult compared to PEEK sulfonation and a CSA, which may cause chain degradation and crosslinking, must be used, alternative sulfonation procedures were tried.

Hajjipour et al. (2004) reported a novel sulfonation method that enables a mild and effective sulfonation for aromatics. Authors reported that silica gel

reacts immediately with CSA giving HCl away and forming silica-sulfonic acid.



Silica-sulfonic acid

Silica-sulfonic acid was introduced as a candidate for sulfuric acid replacement in organic reactions without any limitations such as destruction of acid sensitive functional groups, and giving a heterogeneous easy work-up procedure (Hajipour, 2004). Many aromatic rings such as low molecular weight liquid organics such as benzene, and benzene derivatives were shown to be easily sulfonated with this reagent however, there was not any result about the effectiveness of this sulfonating agent on polymers. Therefore, the potential of this reagent was investigated with a set of experiments.

Silica-sulfonic acid was prepared by adding 30 ml (52.5 g, 0.45 mol) CSA drop by drop to 60 gr silica gel, stirred for 2.5 hrs, and shaken for ½ hrs. An excess of silica used in the formation of silica-sulfonic to ensure that all the CSA reacts and non-reacted CSA do not affect the comparison of the sulfonation results with that performed by CSA only.

In one experiment set, 20 g PES was dissolved in 100 ml H₂SO₄ and heated to 60 °C in 4.5 hrs. Small undissolved part filtered. Half of it (50 ml) separated and two 50 ml solution were cooled to 8 °C in ice bath. 30 ml CSA added drop by drop from the funnel in ½ hr to one of solutions. For the other set, solution was poured into silica-sulfonic prepared as described

above. Polymers were dried under vacuum before sulfonation at 100 °C for 3 hrs. The H-NMR and titration characterization results are given in Figure 4.15 and Table 4.7. Titration was performed by keeping 0.5 g polymer in 1 M-50 ml NaCl at 50 °C under stirring for 2 days and titrating with 0.1 M NaOH.

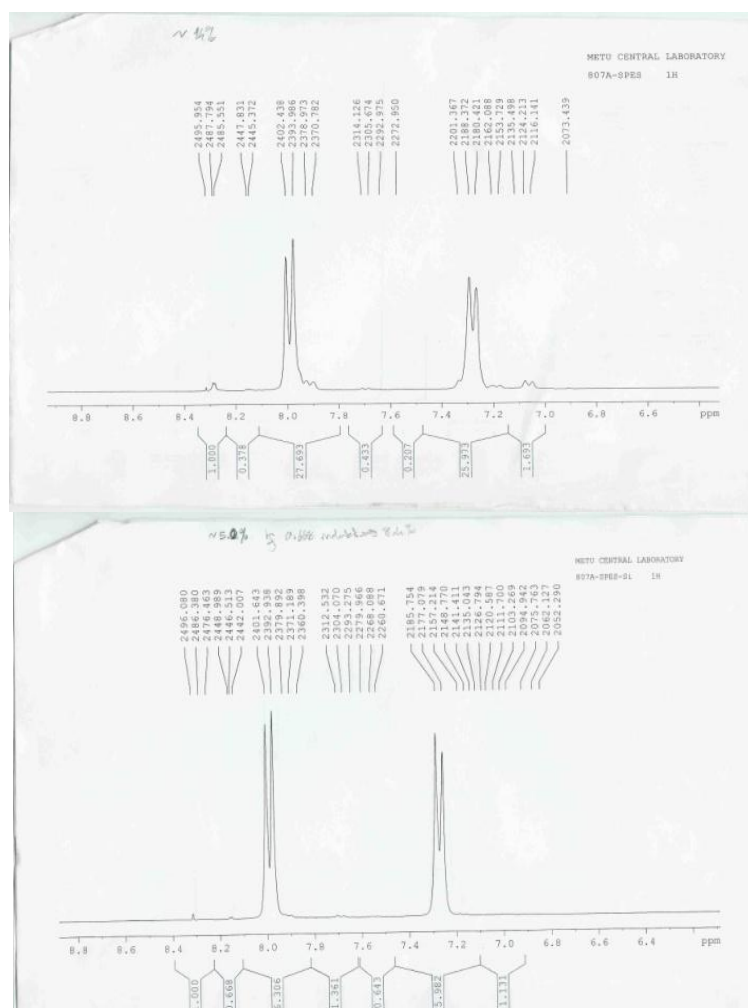


Figure 4.15. H-NMR spectra of SPES (up) & SPES(Si) (down)

Table 4.7. DS of SPES & SPES(Si)

Sample	DS (NMR)	DS (Titration)
SPES	14	13
SPES(Si)	5	3

Results show that sulfonation with silica-sulfonic acid decreases DS significantly compared to that obtained by CSA probably since heterogeneous sulfonation prevents effective contact of sulfonic acid groups with the polymer. In the literature it was reported that sulfonation with H_2SO_4 is very difficult even at high temperatures and at long reaction times. This means that the low level of sulfonation was achieved by silica-sulfonic acid. Therefore, it seems possible to sulfonate PES with this novel sulfonating agent by improving the method of sulfonation such as increasing the contact area of the sulfonating agent.

In another set, chromatographic silica gel was used to increase the contact area. PES with PEES units was also included in the experiment (PES Solvay) to see if silica-sulfonic can sulfonate PEES units. 25 ml CSA was added drop by drop and stirred at room temperature for 1 day over 50 gr. Silica beads and silica gel (chromatographic) to prepare silica-sulfonic acids. 10 g PES and PES-Solvay samples were dissolved in 50 ml H_2SO_4 (95-97 %) in 18 hrs. Since the solutions are too viscous, 50 ml more sulfuric acid was added. Silica-sulfonic acids were then added. DS of around 3% could be achieved with the chromatographic silica-sulfonic acid. Attempts of sulfonation with this novel sulfonating agent were not successful because of the highly heterogeneous medium, this approach can be adapted for PEEK for more controllable and less harmful (to the main chain) sulfonation.

PEES (Aldrich) was also used in sulfonation studies since it was shown that the PEES units were easily sulfonated. However, PEES did not dissolve in H_2SO_4 easily (after several days at room temperature). 25 g dried PEES in 125 ml H_2SO_4 was dissolved in 1 day at 50-60 C. Two reaction media were prepared, in one batch 30 ml CSA was added dropwise, and in the other silica-sulfonic acid prepared by 30 ml CSA was added and both reacted for 5 hrs. After pouring in cold water, direct CSA sulfonated one dissolved whereas silica-sulfonic acid sulfonated polymer did not. An interesting point in this experiment was that, a portion of sample taken, before CSA was added, from the first batch and poured in cold water showed swelling. However, the one sulfonated with silica-sulfonic acid did not show any swelling even after the total reaction time. This result also observed in other direct CSA sulfonation meaning either excessive sulfonation or chain decomposition. Since DS values of direct CSA sulfonated samples are generally around ~20-30, chain decomposition is more probable. In silica-sulfonic acid sulfonated samples although the DS values are very low, there were no sign of swelling indicating that there were no chain breakings. Another reason may be the desulfonation occurred when silica-sulfonic acid is used probably because of the water vapor captured by excess silica gel.

4.1.2.3 Thermal Characterization (TGA & DSC)

TGA (Figure 4.16) and DSC (Figure 4.17) curves of PES & SPES respectively are similar in character with that of PEEK and SPEEK except being totally amorphous. Glass transition temperature (T_g) of PES is around 220 °C as expected. Weight loss steps are for water, sulfonic acid group and polymer main chain respectively. Decomposition of PES starts around 500 °C.

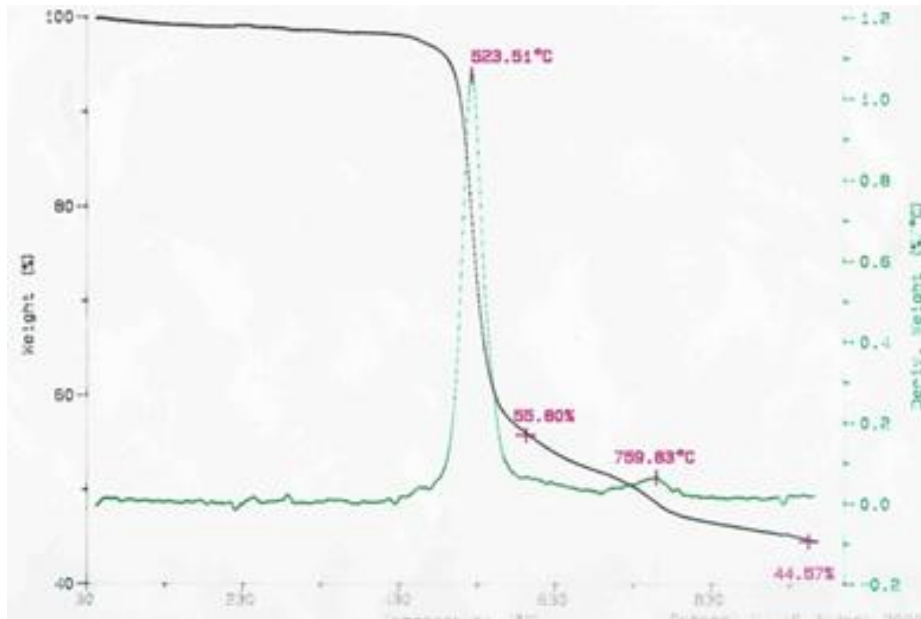


Figure 4.16. TGA of PES

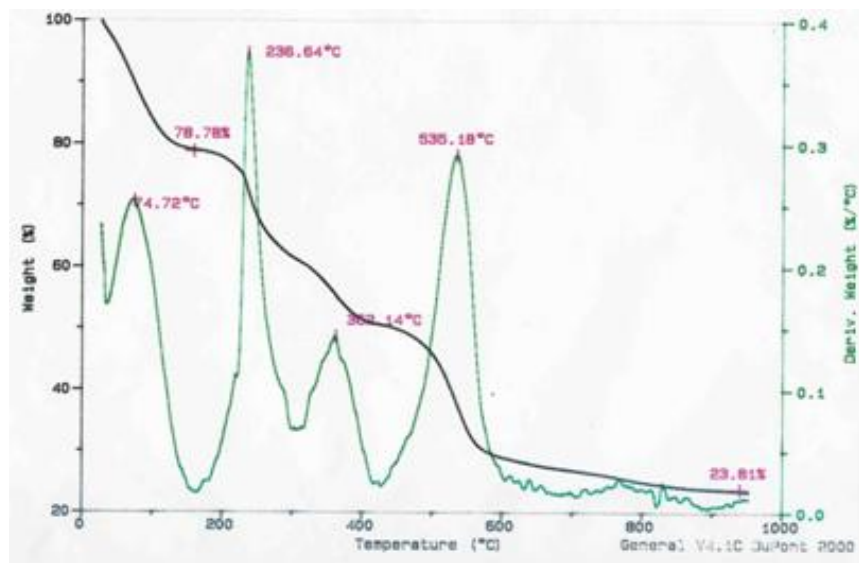


Figure 4.17. TGA of SPES

Glass transition temperatures (T_g) for PES and SPES are clearly observed from DSC curves below. T_g which is about 220 °C (Figure 4.18) for unsulfonated PES increased to about 232 °C (Figure 4.19).

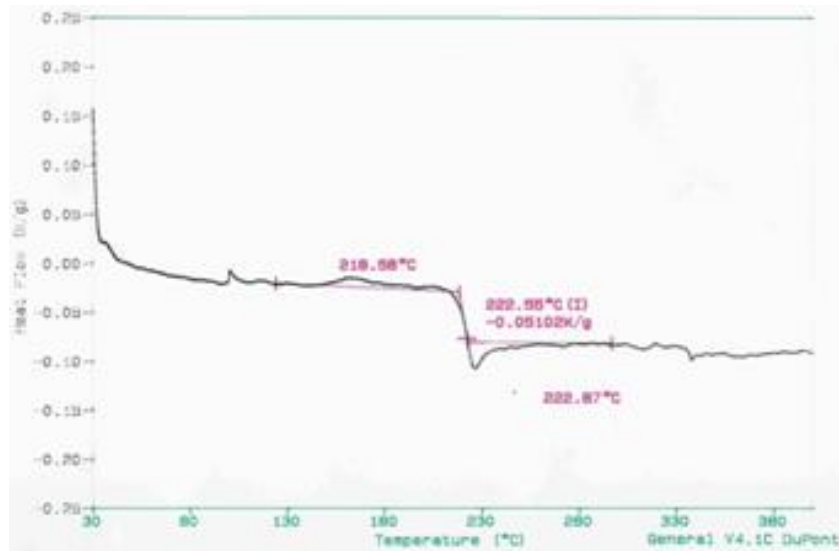


Figure 4.18. DSC of PES

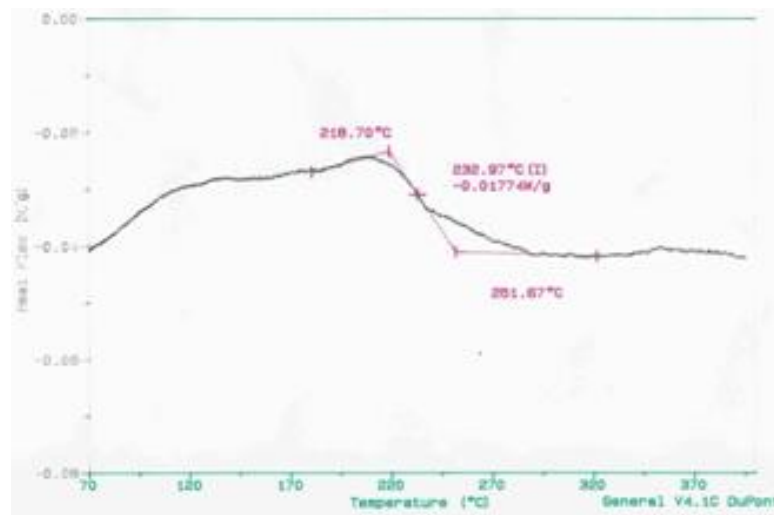


Figure 4.19. DSC of SPES

The increase in T_g with increase in DS to the case similar to SPEEK means mobility of the polymeric chains decreases with new molecular interactions introduced with $-\text{SO}_3\text{H}$ groups.

4.2 Proton Conductivity Measurements and Equivalent Circuit Modelling

As discussed before various factors affect the results of the proton conductivity measurements and causing the discrepancies in the reported results. Two important factors among them are the design of the conductivity cell and the measurement method. Therefore, these factors were also investigated during this study.

Theoretically, there are more impedance components in 2-probe (2-P) measurements compared to 4-probe (4-P) measurements, therefore 4-P measurements were suggested for more accurate results particularly for low impedance measurements (Deslouis et. al., 1995). Researchers reported that the choice of 2-P and 4-P methods for conductivity measurements might be important according to the experiment, materials and the range of measurement. For example, Zawodzinski et al. (1993) reported that for 2-probe method high frequency is needed to separate the membrane impedance from the impedance caused by interfacial capacitance; Cahan et al. (1993) reported that they measured membrane impedance separate from interfacial capacitance resistance with 4-probe and in a large frequency range and Lee et al. (2005) reported that they found 4-probe measurements always higher than that obtained with 2-probe (2-5 times).

To observe the difference between 2-P and 4-P measurements particularly for the conductivity cell and the system that was used in this study, a set of

conductivities in a large range were measured and compared exactly at the same conditions with the first conductivity cell (membrane contacting water for 100% RH). As it is clear from Figure 4.20 below, 4-P results were always higher than the 2-P results similar to the reported data in the literature reviewed in the preceding paragraph but the difference was not considerable. Again being consistent with literature, the points at high conductivities i.e. at low impedance points, the differences were more considerable.

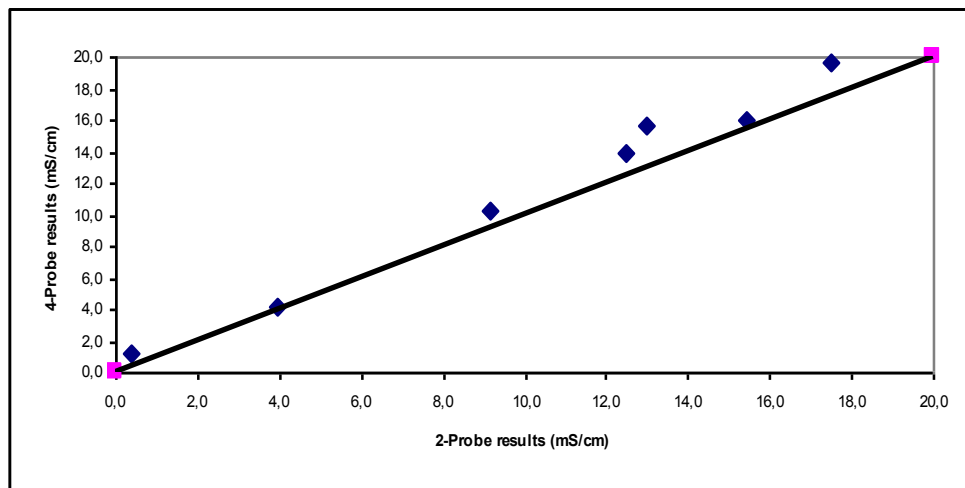


Figure 4.20. Proton Conductivities measured with 2-Probe vs 4-probe measurements for various samples

Proton conductivities given above were measured with a Agilent 4294 Impedance Analyzer that works in the frequency range of 40 Hz to 110 MHz. The solution resistances were obtained from the point where the phase angle approaches zero since the output of this equipment was Bode type. The output screen and sample calculation were given in the appendix.

An equivalent circuit model, which fits the data, may suggest a chemical model, process, or mechanism that can be proposed and tested. EIS data and the equivalent circuit model can provide useful data about the physical system. However, fitting the data may result also in physically meaningless results. Generally the equivalent circuit modeling is started with the simplest available models such as Randles circuit described in the literature survey section and then more components that may be physically meaningful can be added until perfect fit is obtained.

For plotting Nyquist and Bode plots and for equivalent circuit fitting, Gamry Echem Analyst Software using Levenberg-Marquardt and Simplex algorithms was used. Both algorithms adjust the parameter values of the elements used in the model to find the best fit. For fitting equivalent circuits constructed, logical seed values must be entered since the program require initial values within a decade or two of their final values before it can fit properly. For these guesses, resistances where the phase angle is zero representing the solution resistance at high frequency intercept, and the polarization or charge transfer resistance calculated from low frequency intercept and the true capacitances calculated from the top of the semi-circles were used.

In the first part of this study, conductivities were measured by using the first conductivity cell (in water) with 4-probe method with slightly thicker platinum electrodes ($D \sim 0.5$ mm) compared to second cell ($D \sim 0.3$ mm). All the Nyquist plots obtained were similar in shape (linear without a semicircle). Both Nyquist and Bode plots were given below in Figure 4.21 for Nafion 115. The membranes ionic resistances were read from the point where the impedance curve intersects the real axis in Nyquist plots or from the Bode plots where the phase angle is zero (plateau at high frequencies), and proton conductivities were calculated from this resistance as described before.

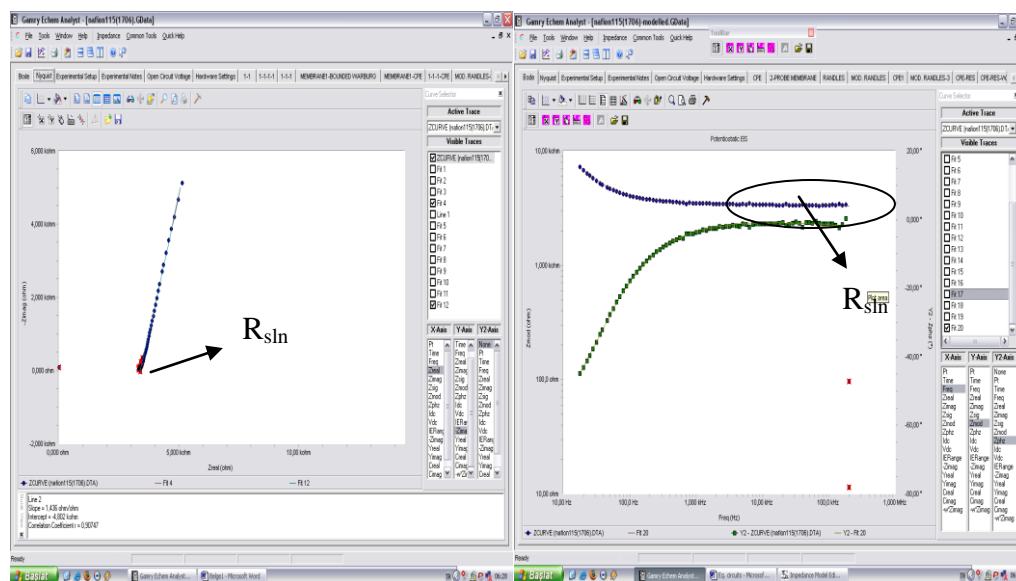


Figure 4.21. Nyquist (left) and Bode (right) plots of Nafion 115 (first cell; in water)

When the Nyquist plots obtained from Gamry Echem Analyst Software were investigated, the first point that can be noticed is the lack of semi-circle typical to Randles type systems showing double layer or charge transfer resistance (Figure 4.21). At first look the Nyquist plot is similar to a Warburg resistance showing a dominant diffusion resistance of charge carriers, however when more resistant membranes were investigated it was understood that this is not the case. This was probably because of the conductivity cell design used. Thin platinum wire electrodes placed with 2.5 cm distance and 4-probe measurement had probably diminished the capacitive effect observed with planar electrodes such as platinum sheets. Actually the capacitive and polarization resistance components are too high compared to solution resistance and not seen in the frequency domain. This semi-circle has also been observed in the systems in which the membrane is sandwiched generally between two stainless steel electrodes and the conductivity is measured through-plane.

At this point it should be noted that although through-plane measurements may be meaningful for non-isotropic structures, obtaining 100% R.H. is very difficult when the membrane is sandwiched between two planar electrodes. Since a small change in R.H. significantly affects the proton conductivity, especially for the membrane types investigated in this study of which their proton conductivity strongly depends on hydration, in-plane measurements were preferred.

Below, in the Nyquist plots of PES and 25% SPEEK/PES blend resistive/capacitive effect indicated by a semi-circle can be observed (Figure 4.22). Curves in Bode plots of the conductive membranes and resistive membranes are symmetrical. The plateau on which the impedance does not change with frequency and showing the solution resistance is on the left side (at low frequencies) for resistive membranes, whereas it is on the right side of the curve (at high frequencies) for conductive membranes. These typical shapes of Nyquist and Bode plots enable us to determine the membrane's ionic conductivity character at a first glance.

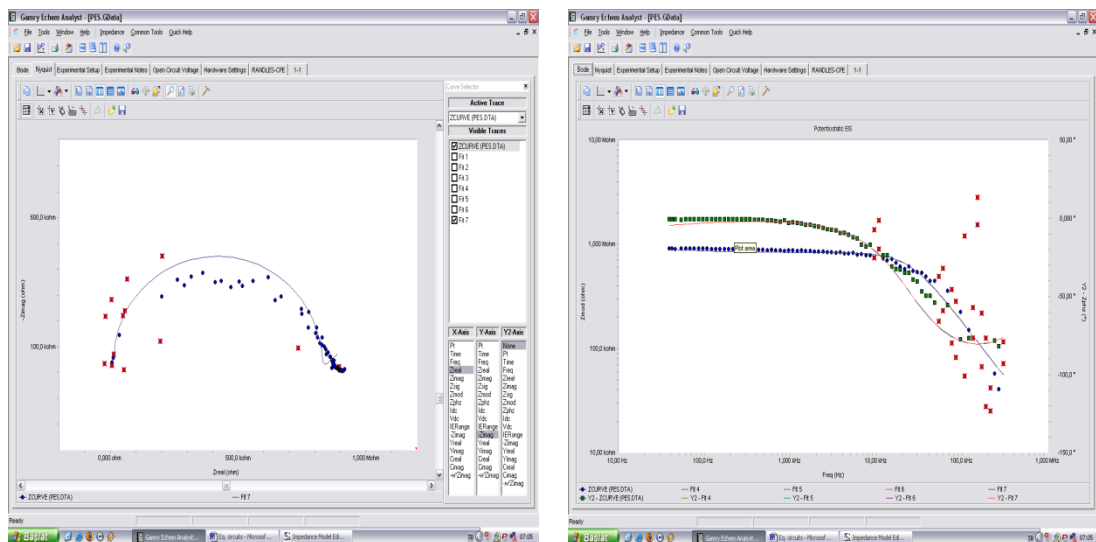


Figure 4.22. Nyquist (left) and Bode (right) plots of 25% SPEEK/PES blend (first cell; in water)

Since the solution resistances of most of the membranes investigated were very low compared to the other component resistances such as contact resistance and Warburg resistance, the conductivity results obtained by 2-P, 4-P, in-water, and in-vapor were very close. This means that as the proton conductivity increases the effect of the measurement method and the environment diminishes. One of the reasons is the large cell constant (k) that can be defined as the ratio of distance (L) of flow to the cross-sectional area (S). In through-plane measurements where membrane is sandwiched between two planar electrodes this constant is very small since L is the thickness of the membrane in the order of microns and the other resistances starts to appear. If the objective is to measure ionic conductivity precisely than large cell constant is preferable but if the other components are also needed such as the Warburg resistance to calculate proton diffusion constants the frequency range is not sufficient.

$$\text{Ionic Conductivity: } \sigma = \frac{L}{R \cdot A}; \quad \text{cell constant: } k = \frac{L}{A}$$

The 4-P impedance spectra of the membranes gave only the solution resistance similar to the results of Sone et al. (1996) given in the literature section. To observe the effects of other components 2-P results were used. A comparison of 2-P and 4-P spectra is given below for the same membrane.

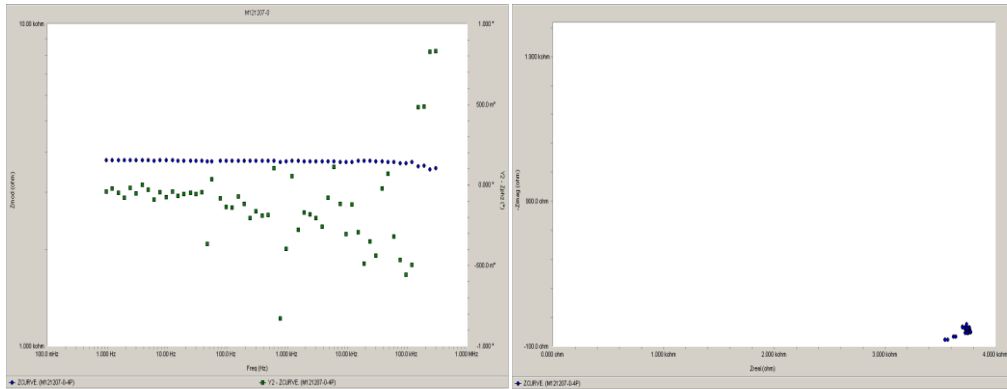


Figure 4.23. Bode (let) & Nyquist (right) Plots of SPEEK (DS=68) (4-P; in vapor; RT)

The resistance varies between 3.7 and 3.8 k Ω in the whole frequency range (1 Hz-300kHz) which means 4-P measurement with a large cell constant gives very precise ionic conductivity results regardless of the frequency. Below in the Bode and Nyquist Plots of the same membrane with 2-P, the capacitance of the cell becomes detectable, but the resistance read from the real axis intercept is 3.9 k Ω which is very close to the 4-P result.

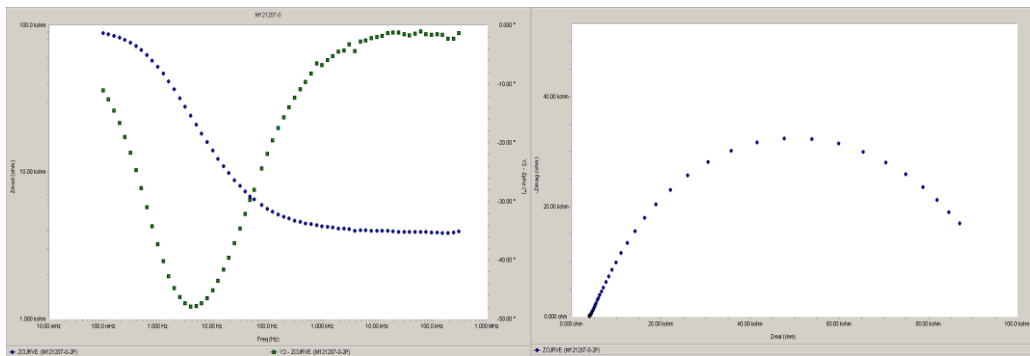



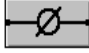






Figure 4.24. Bode (left) & Nyquist (right) Plots of SPEEK (DS=68) (2-P; in vapor; RT)

The equivalent circuits including a constant phase element (CPE) are generally more capable of identifying the system. A CPE is a distributed

element meaning distributing the nonidealities of the system. For example, at the electrode-membrane interfaces there may be nonuniformities caused by the defects on the surface of the electrode, or the porosity of the membrane may have similar effects. A CPE counts these effects by using a non integer power, n . Actually when $n=1$ CPE is a capacitor, and when it is $\frac{1}{2}$ it is Warburg diffusion element as can be followed from Table 4.8

Table 4.8. Circuit Elements Used in the Models

	Equivalent element	Admittance	Impedance
	Resistor (R)	$1/R$	R
	Capacitor (C)	$j\omega C$	$1/j\omega C$
	Inductor (L)	$1/j\omega L$	$j\omega L$
	Constant Phase Element (Q)	$Y_0(j\omega)^n$	$(1/Y_0)/(j\omega)^n$
	Infinite Warburg (W)	$Y_0\sqrt{j\omega}$	$(1/Y_0)/\sqrt{j\omega}$
	Porous Bounded Warburg (O)	$[Y_0\sqrt{j\omega}] \coth\{B\sqrt{j\omega}\}$	$[(1/Y_0)/\sqrt{j\omega}] \tanh\{B\sqrt{j\omega}\}$
	Bounded Warburg (T)	$[Y_0\sqrt{j\omega}] \tanh\{B\sqrt{j\omega}\}$	$[(1/Y_0)/\sqrt{j\omega}] \coth\{B\sqrt{j\omega}\}$
	Gerischer Impedance (G)	$Y_0\sqrt{K_A + j\omega}$	$(1/Y_0)[1/\sqrt{K_A + j\omega}]$

Since the capacitive effect could be easily observed with the second cell for the measurement of conductivity in vapor when 2-P method was used (Figure 4.25), equivalent circuit fitting can be utilized. A Randles circuit in which the capacitance was replaced with a CPE was used and Randles circuit fitting was also added for comparison with a CPE in Figure 4.25.

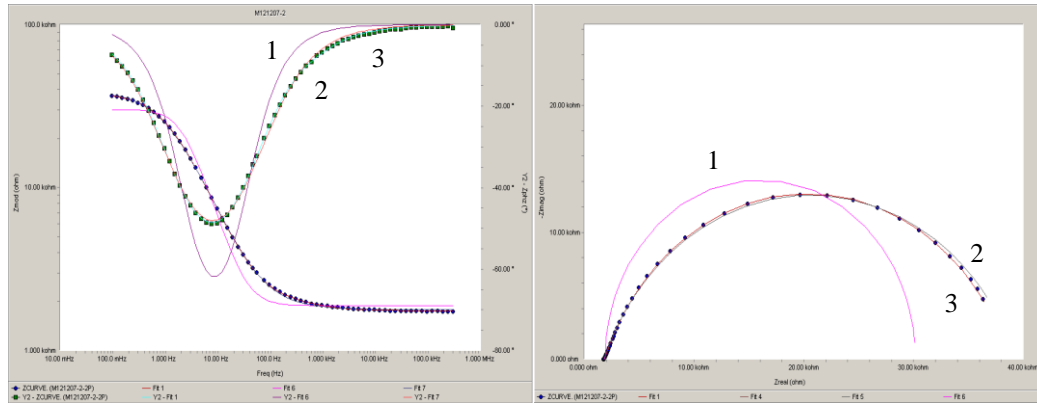


Figure 4.25. Bode (left) & Nyquist (right) Plots of a Composite/blend Membrane with Equivalent Circuit Fittings

Three equivalent circuits used for fitting the data and the parameters were summarized in Table 4.9 below. When more components are added a perfect fit is possible but as discussed in the literature part these circuits may be physically not meaningful.

Table 4.9. Equivalent Circuits Fitted for a Composite/Blend Membrane

Circuit Number	Circuit Definition	Circuit Components
1	Randles	
2	Randles with CPE	
3	Randles in series with porous Warburg	

Table 4.10. Parameter Values for Equivalent Circuits Fitted for a Composite/Blend Membrane

1			2			3		
Param.	Value	Error	Param.	Value	Error	Param.	Value	Error
R_u (k Ω)	1.89	7.51 Ω	R_u (k Ω)	1.78	449.8 Ω	R_u (k Ω)	1.74	542.9 Ω
R_p (k Ω)	28.29	206.1 Ω	R_p (k Ω)	37.65	8.9 8 Ω	R_p (k Ω)	36.85	13.46 Ω
C_f (μ F)	2.614	20.86 Nf	Y_0 (Ss $^\alpha$)	6.2×10^{-6}	123×10^{-9}	Y_0 (Ss $^\alpha$)	5.886×10^{-6}	158.5×10^{-9} (Ss $^\alpha$)
			α	0.766	0.0044	α	0.784	0.0071
						Y_{06} (Ss $^\alpha$)	-160.9e-6 Ss $^{(1/2)}$	42.14×10^{-6} Ss $^{(1/2)}$
						B7	-22.5x10 ⁻³ sec ^(1/2)	6.05×10^{-3} sec ^(1/2)
Goodness of Fit	26.6×10^{-3}		Goodness of Fit	348×10^{-6}		Goodness of Fit	34.3×10^{-6}	

From the plots and the goodness of fit values the perfect fit is with circuit 3, however a series Warburg component as well as the negative parameters are physically not meaningful. This circuit was added to the analysis to show how easily impedance data interpretation can be misleading. Randles circuit is not suitable since the phase shift must be -90° theoretically but the maximum phase shift is around -50° as can be seen in Figure 4.25 and also from the poor fit. The best equivalent circuit for describing the system among three is the Randles with A CPE. Alpha value of 0.766 which is close to one is meaningful for the reasonable deviation from a complete capacitance effect indicating the nonuniformities of the electrode surface and porous structure of the membrane possibly. R_u obtained from circuit fitting is 1.78 k Ω and close to the value of 1.72 k Ω read from the high frequency intercept of the real axis in the complex plane.

When the resistance of the membrane increases, other components can be observed in the frequency domain available with the system (0.1Hz-300kHz). An example to this is the blend membrane with 75%SPES (DS~20) and SPEEK (DS=68). Since the resistance of solution is high, polarization and Warburg resistances dominates in the low frequency part. The equivalent circuit used by Ciureanu et al. (2003) was fit but its modified form with a CPE instead of the capacitor gave a perfect fit.

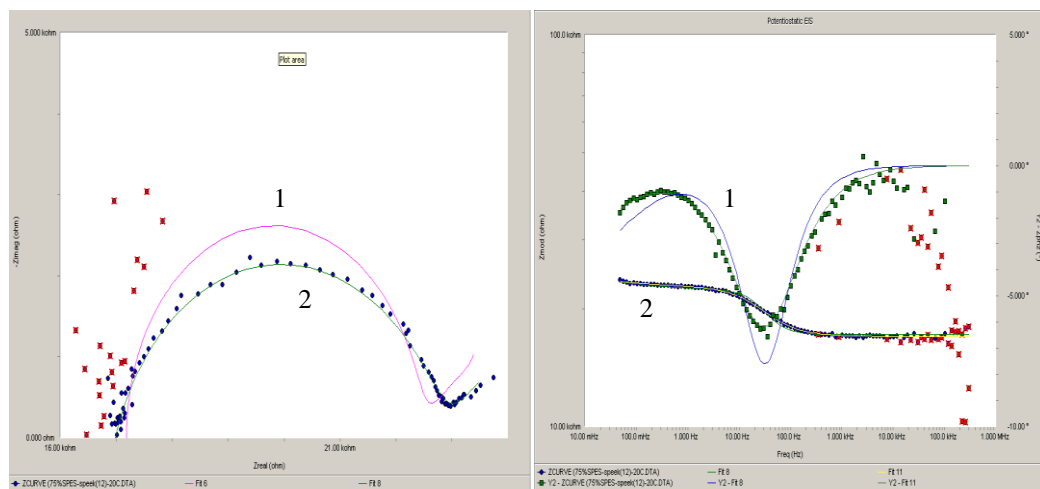


Figure 4.26. Bode (left) & Nyquist (right) Plots with Equivalent Circuit Fittings for 75 %SPES/SPEEK Blend

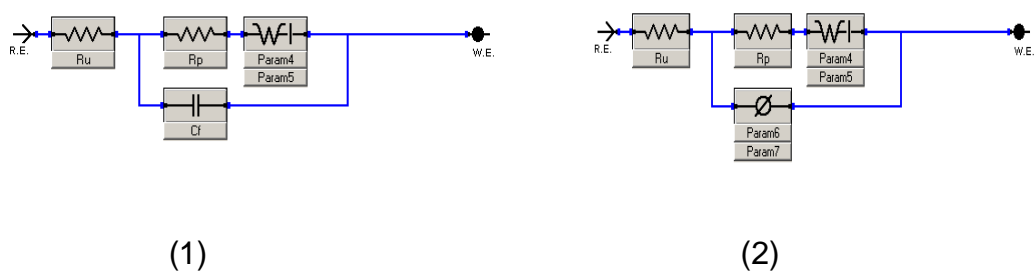


Figure 4.27. Equivalent Circuit Fittings used for SPES/SPEEK Blend: (1) Randles Type with Bounded Warburg Element (2) Randles Type with Bounded Warburg Element and CPE.

Table 4.11. Parameter Values for Equivalent Circuit (2) of Composite/Blend Membrane with Equivalent Circuit Fittings for 75 %SPES/SPEEK Blend

Parameter	Value	Error
R_u	16.98 (Ω)	112.2 (Ω)
R_p	5.862 (Ω)	361.2 (Ω)
Param4	1.976 Ms	1.081 Ms
Param5	6.320 $\text{sec}^{1/2}$	199.5 $\times 10^{-3}$ $\text{sec}^{1/2}$
Param6	2.935 μS	754.0 Ns
Param7	799.5 m	47.60 m
Goodness of Fit	75.98 $\times 10^{-6}$	

R_u from the fitting is in excellent consistency with the value read from the intercept, alpha value of CPE which is parameter 7 is about 0.8 again a logical value close to 1. It was demonstrated in this section that equivalent circuit fittings can be useful for obtaining more information rather than calculating conductivity only. However, the choice of the cell parameters is important if all the resistive components are needed to be evaluated .

4.3 Pristine Membranes (SPEEK & SPES)

4.3.1 Effect of Degree of Sulfonation (DS)

As the sulfonic acid moiety increases in the polymer, proton conductivity increases by the help of both increased ion-exchange capacity and increased water uptake, which is responsible for the transport of protons. The relationship between conductivity and DS is nearly linear for the range of DS, which is between 50 and 75 % (Figure 4.28).

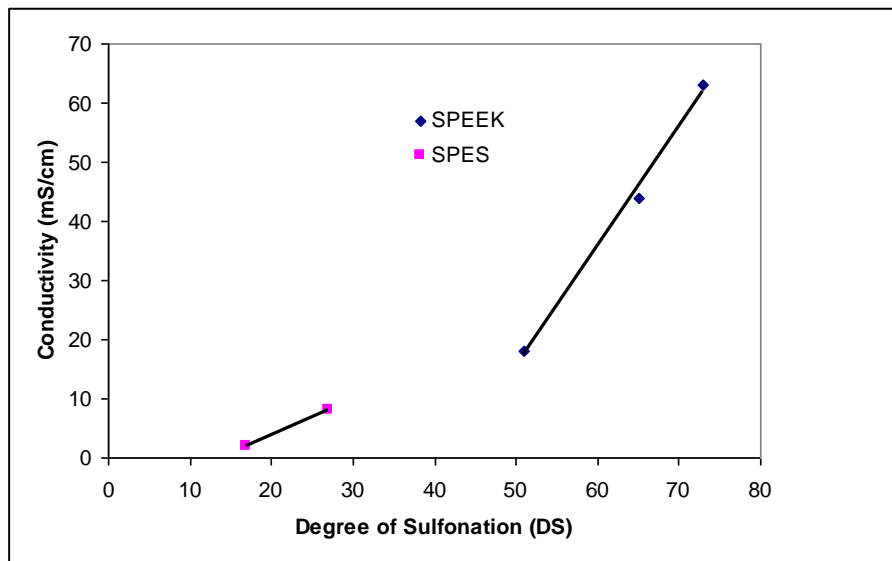


Figure 4.28. Proton Conductivity vs Degree of Sulfonation (DS) for SPEEK & SPES

The conductivity of SPEEK sulfonated to around 70 % is comparable to Nafion 112 which was also around 70-80 mS/cm and it is obvious that above 70 % sulfonation SPEEK conductivity can exceed Nafion. However, as will be discussed later the hydrolytic stability of SPEEK above this DS decreases sharply. Conductivity of SPES also increases as DS goes up, however since achieving high DS with post-sulfonation for PES is difficult, the DS values are low compared to SPEEK (Figure 4.28). A 10 % increase only in DS caused a 4-fold increase in proton conductivity for SPES. Although the conductivities were low, the hydrolytic stability of SPES membranes were excellent, therefore this picture brought the idea to combine high conductivity of SPEEK with good stability of SPES and this blending approach will be explained later.

4.3.2 Effect of Pre-treatment of the Membrane

Both the temperature and acid treatment were found to be effective on proton conductivity as can be followed from Table 4.12. Membranes were first dried for 12 hours at 80 °C, then further 12 hours at 150 °C. Acid treatment was performed using 1 M sulfuric acid. As it will be shown in single cell performance tests, treatment of the membrane has also a significant effect on the overall performance. From Table 4.7, it can be seen that treatment of the membrane with 1 M H₂SO₄ for 1 day approximately doubles the proton conductivity both for 80 °C and 150 °C cast membranes. Thermal treatment at a high temperature decreased the conductivity possibly by influencing the structure of the polymer. Water uptake of the thermally treated membranes also decreased. Reason of this could be the shrinkage of the pores.

Table 4.12. Effect of Casting Temp. and Acid Treatment on SPEEK-72

Sample	T (°C)	R (kΩ)	Thickness (micron)	Proton Conductivity (mS/cm)
80 °C (untreated)	20	14	70	21
150 °C (untreated)	19	22	64	14
80 °C (treated)	19	7	70	40
150 °C (treated)	20	8	73	33

4.3.3 Effect of Casting Solvent

The effects of three common casting solvents were investigated for SPEEK with a DS of 72 %. From Table 4.13, it is apparent the best conductivity was obtained with DMAc, and most of the membranes were casted with this solvent therefore. DMF generally gives the poorest

conductivity. Similar results were reported by Kaliaguine et al. (2003) and DMF was suspected to react with sulfonic acid groups of the polymer which results in deactivation of some of these sites under the scope of H-NMR results in their study.

Table 4.13. Casting solvent effect on proton conductivity

Sample	Thickness (μm)	$\sigma(\text{mS/cm})$		
		Water (1 st cell)		Vapor (2 nd cell)
		BT	AT	AT
SPEEK-DMF	70	32	57	39
SPEEK –DMAc	70	43	76	53
SPEEK- NMP	70	43	54	51
Nafion115	130	77	88	75

4.4 Zeolite Beta Composites

4.4.1 Synthesis of Zeolite

Zeolite Beta fillers with different $\text{SiO}_2/\text{Al}_2\text{O}_3$ ratios were synthesized and characterized by fuel cell research group members during their M.S. studies (Gür, 2006; Erdener, 2007). The general formula was 2.2 Na_2O : 1.0 Al_2O_3 : x SiO_2 : 4.6 $(\text{TEA})_2\text{O}$: 440 H_2O . By varying x Si/Al ratio was controlled. The structure of the zeolites were confirmed by XRD analysis. The characteristic peaks of zeolite beta crystals (Figure 4.29) were observed at $2\theta \sim 7.8^\circ$ and $2\theta \sim 22.4^\circ$ as stated in literature for zeolite beta samples synthesized at $\text{SiO}_2/\text{Al}_2\text{O}_3$ in the range of 20-50 (Holmberg, 2005).

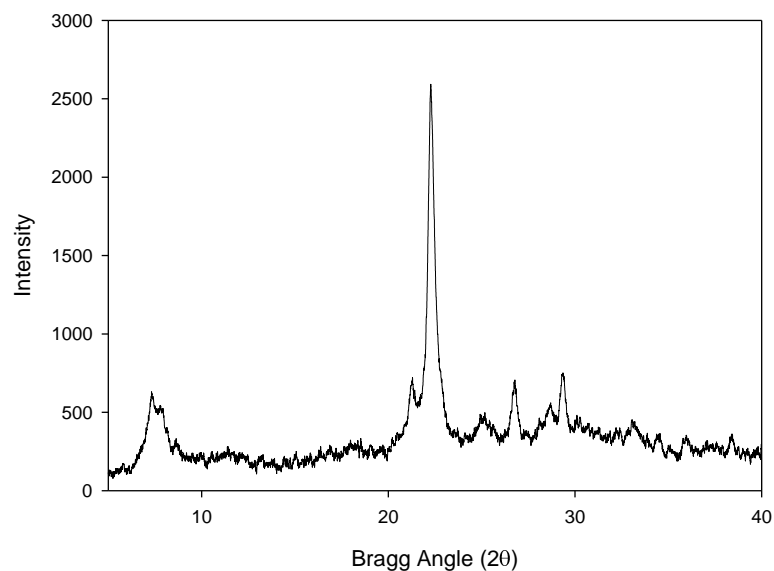


Figure 4.29. XRD pattern of as synthesized zeolite beta ($\text{SiO}_2/\text{Al}_2\text{O}_3=20$)

The resistance of zeolite beta crystals to the acid environment was investigated since the fuel cell environment is highly acidic and found to be stable in acid environment. The characteristic peaks of zeolite beta were identified in the same position after the acid treatment with strong sulfuric acid solution of 95-98 wt% as can be seen in Figure 4.30. However, $\text{SiO}_2/\text{Al}_2\text{O}_3$ ratio was found to be changed probably because of dealumination observed from ICP analysis. Guisnet et al. (1997) reported that acid treatment of zeolite Na-Beta caused it to be converted to H-Beta and to be dealuminated.

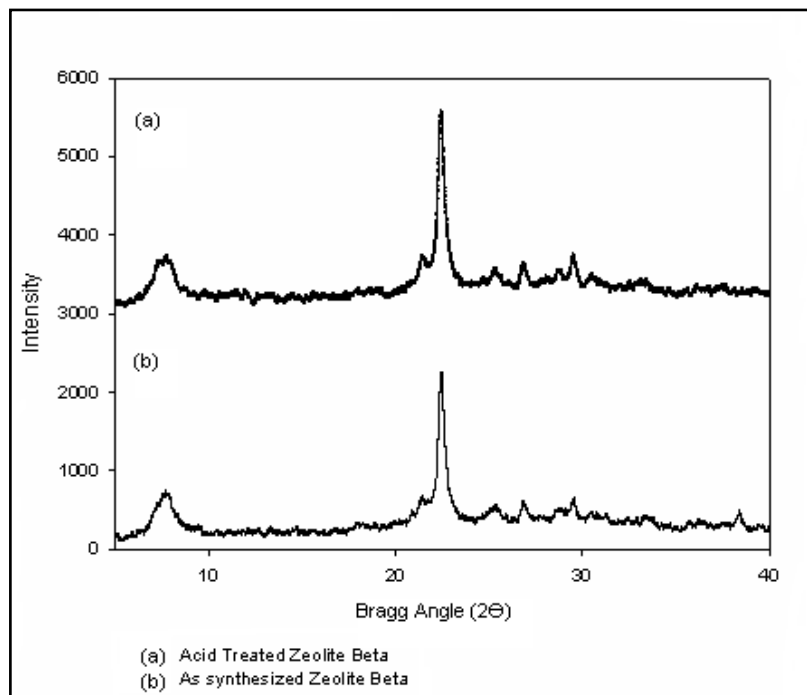


Figure 4.30. XRD pattern of zeolite beta treated with 95-98 wt% H₂SO₄

Thermal stability of zeolite beta samples synthesized were investigated with thermo-gravimetric analyses (TGA) and showed that the first weight loss was around 465°C (Figure 4.31) and it corresponds to the removal of the structure directing agent (SDA) from the zeolite structure. Therefore, zeolite crystals should be calcined at higher temperatures to remove SDA completely. The thermal decomposition temperature of zeolite beta particles was around 850 °C.

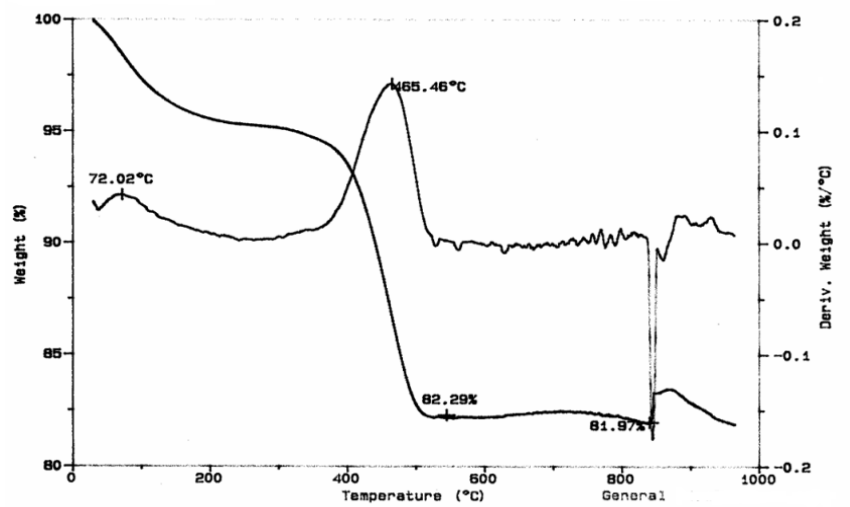
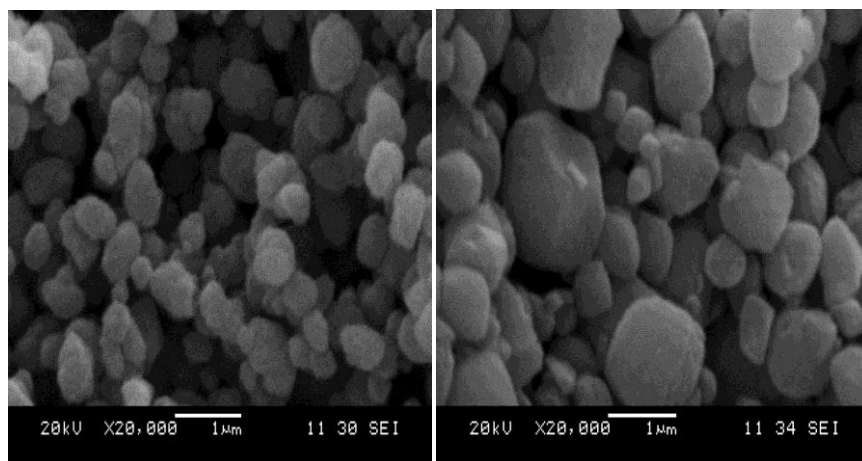


Figure 4.31. TGA graph of zeolite beta crystals

The range of the particle size and morphology of the synthesized zeolite particles can be seen in Figure 4.32 showing the scanning electron microscopy (SEM) SEM micrographs. The largest synthesized zeolite particle size was around 1µm.



a) Si/Al= 20.5, 150 °C

b) Si/Al= 30, 150 °C

Figure 4.32. SEM micrographs of synthesized zeolite beta crystals

4.4.2 Loading Effect

The effect of zeolite beta loading (wt %) was investigated using SPEEK (DS=68) as the host polymer. Loadings were 5, 10 and 20 % respectively. From Figure 4.33, it can be followed that 10% was found to be the optimum loading, the negative effect of higher loading was more pronounced at the temperature of 70 °C which is the regular operating temperature of a PEM fuel cell.

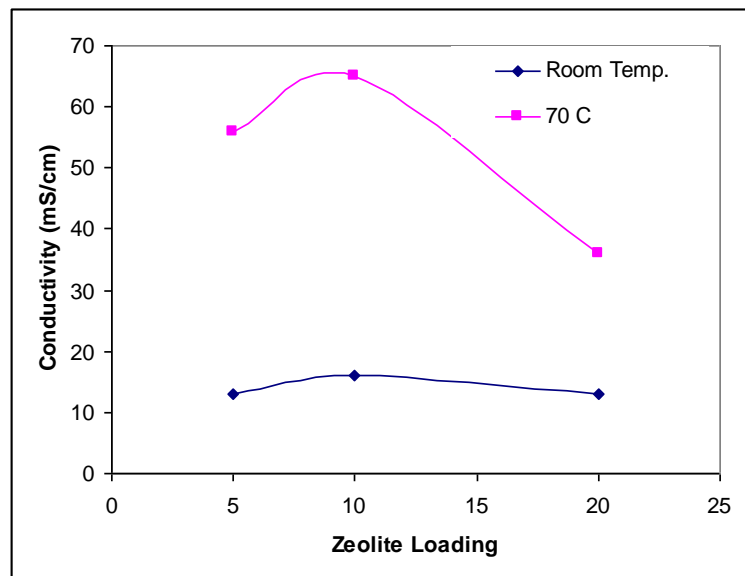


Figure 4.33. Effect of zeolite loading wt % on proton conductivity of SPEEK/Zeolite beta composites

4.4.3 Effect of Si/Al Ratio

Proton conductivity measurements performed at room temperature to investigate the effect of loading zeolite beta fillers showed no solid trend

for increase or decrease on conductivity. For the 10 wt% loaded SPEEK only a slight enhancement on proton conductivity was observed, however at high temperatures close to the operating temperature of PEM fuel cell, this enhancement was more pronounced as can be followed from Figure 4.34.

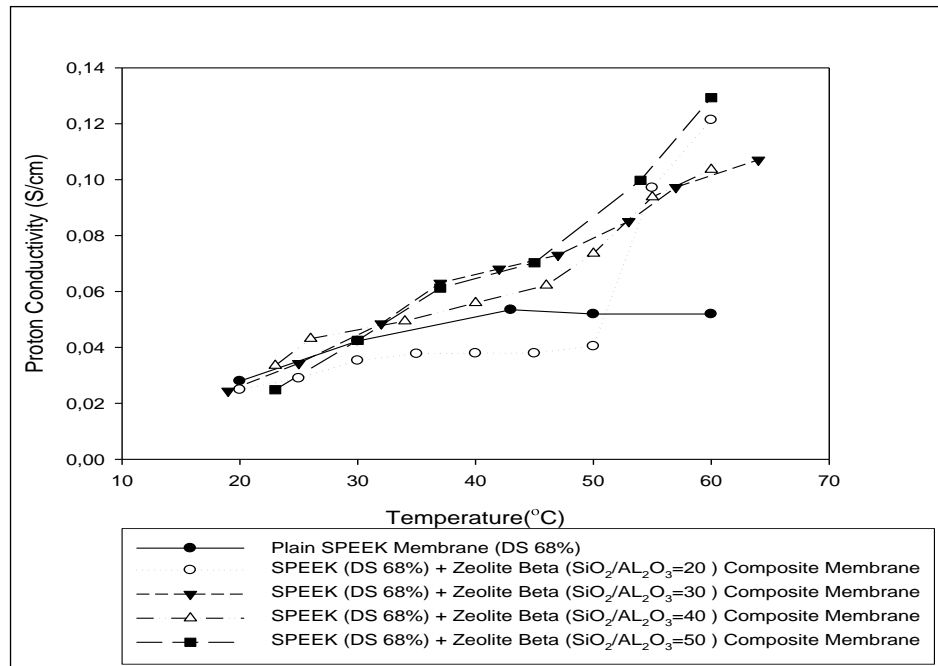


Figure 4.34. Effect of zeolite loading wt % on proton conductivity of SPEEK/Zeolite beta composites (Erdener, 2007)

Figure 4.34 actually shows the results of conductivity measurements for investigating the effect of Si/Al ratio of zeolite beta. Study was performed by using 10 wt% zeolite loading and 68% sulfonated SPEEK as the polymer matrix in our research group. Si/Al ratios selected were 20, 30, 40 and 50. In spite of the fact that there is no clear correlation between Si/Al ratio and conductivity, among the Si/Al ratios investigated, the best conductivity at all temperatures was achieved with the highest Si/Al ratio which was 50.

4.5 SPEEK Based Blends

Effect of Blending Polymer and its loading:

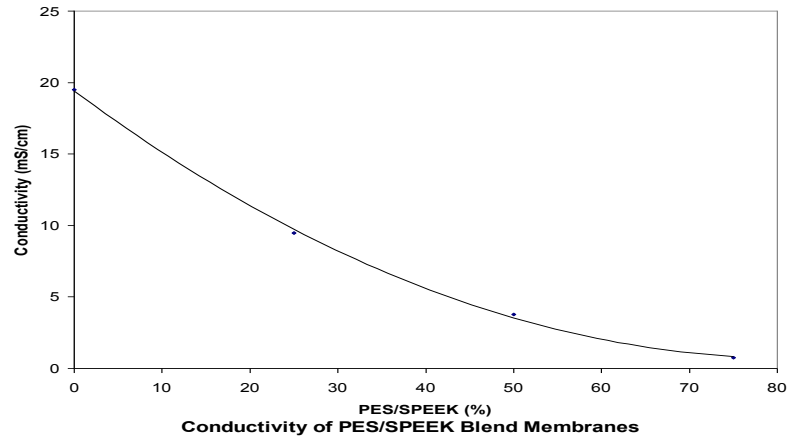


Figure 4.35. Proton Conductivities of PES/SPEEK ratios (25, 50, 75 wt%)

In the previous discussions it was commented on the high conductivity that can be achieved for SPEEK at high DS values for ease of sulfonation with the penalty of low hydrolytic stability. The case is the opposite for SPES; its sulfonation was difficult but the thermohydrolytic stability was perfect. Therefore combining these two properties was a good idea. To investigate the potential of this approach, and see if these two polymer families were compatible, i.e. do not form a phase separation, 25, 50 and 75 % PES blend ratios were prepared. As expected the conductivities decreased but nonlinearly, with an exponential decrease (Figure 4.35). The hydrolytic stabilities were tested under vapor at 80 °C and blends were stable hydrolytically as expected. However, the decrease in conductivity even at 25 % was not acceptable so lower blend ratios were tried.

Table 4.14 below shows the proton conductivities of various blend membranes. 10 wt% blends have higher conductivities than the pristine SPEEK-57 membrane. In addition, the negative effect on proton conductivity of higher casting temperature can be observed in this table. This decrease was probably a result of crosslinking and deactivation of some exchange sites at high casting temperatures.

Table 4.14. Conductivity Results of SPEEK-57 based Blends

25% Blends	Casting T/Treatment	
	150C-treat.	80 C-treat.
Sample	Conductivity (mS/cm)	
None	2	3
PES	5	15
PES/PEES	2	9
PEES	3	7

10% Blends	Casting T/Treatment	
	80C-not treated	80C-treated
Sample	Conductivity (mS/cm)	
None	2	6
PES	6	18
PES/PEES	7	15
PEES	6	22

In a set of experiments for investigation of the blending effects on conductivity, SPEEK with a DS of 57% was used as basis. DMAc as casting solvent was used in a ratio of 1:50 (g/ml). PES, PES(Solvay) and PEES were added in determined ratios and both mechanical and ultrasonic mixing were utilized for at least 1 hr. Membranes were dried at 80 °C and 140 C in oven. After removing from petri dishes by swelling in deionized water they were treated in 1 M H₂SO₄ for 1 day to protonate the cation exchange sites. In Table 4.15, the effect of 20 % blend ratio of different polysulfones (PES, PES (Solvay) & PEES) can be observed.

Among the blend membranes 15% sulfonated PES (Solvay) blend has the highest conductivity as expected.

Table 4.15. Conductivity & Water Uptakes of SPEEK-72 Based Membranes (Casting Temp= 80 C)

Sample	T(°C)	R (kΩ)	Thick. (micron)	Cond. (Ms/cm)	Uptake% (80 C)	Uptake% (150 C)
SPEEK-72	19	7	70	40	43	30
PES (20%)	21	21	57	17	29	18
Solvay (20%)	21	17	57	20	28	17
PEES (20%)	21	12	63	27	30	21
Solvay-15 (20%)	21	9	73	32	38	24

4.6 Comparison of Inorganic Fillers

4.6.1 Metal Oxides-Clays-Aluminosilicate (zeolite)

Metal oxides, clays and zeolite as an aluminasilicate were compared for their potential to enhance the proton conductivity with their various characteristics such as retaining water, helping conduction directly by adding extra acidic sites or introducing new conduction pathways/mechanisms. Titanium dioxide (TiO₂) which was selected from the metal oxide family, montmorillonite (MMT) from the clay family and zeolite beta with two different Si/Al ratios (75 & 150) from the aluminosilicates were used as the fillers.

In Table 4.16 a set of conductivities of pristine SPEEK (DS=61), montmorillonite (MMT), TiO₂, zeolite 75 and zeolite 150 (Si/Al=75 & 150

respectively) composite membranes were summarized. All the composites were prepared by using 10% inorganic fillers by weight, sulfonated polymer (SPEEK, DS=61%) and NMP as the casting solvent. Measurements were performed with the first conductivity cell which enables the membrane contact with water for full hydration (aqueous medium). Nafion 112 was included for comparison. TiO₂ composite membrane showed the highest conductivity among composites in this set and all other fillers seemed to decrease the conductivity a little; Zeolite Beta composite with Si/Al ratio of 150 gave a higher conductivity than that of with 75. Water uptakes of the composites increased from 15% to 24% with the incorporation of inorganic fillers of which all are known as hygroscopic materials. Highest increase was observed with zeolite composite with Si/Al ratio of 150.

Table 4.16. Comparison of proton conductivities of composite membranes

Membrane	Thickness		Water Uptake	
	(μm)	R (k Ω)	σ (mS/cm)	(%)
SPEEK (DS=61)	140	9,2	19	15
SPEEK-MMT	170	9,0	16	18
SPEEK-TiO ₂	145	8,0	21	21
SPEEK-Zeolite beta75	110	22,0	10	22
SPEEK-Zeolite beta150	140	11,0	16	24

Since TiO₂ gave the best conductivity value at room temperature in the experiment that compares inorganic fillers of different families, loading effect of this filler was further investigated. Table 4.17 shows that if non-treated (BT: before treatment) membranes are taken into consideration, conductivity increases with increasing loading upto 20% which was the highest loading, however for treated membranes (AT: after treatment) 5 wt% was the best with 52 mS/cm conductivity. What was important in this set of experiment is that all titanium dioxide composites gave higher

conductivities than the pristine SPEEK membrane. Treatment of the membranes was performed by keeping membranes in 1 M sulfuric acid for 1 day.

Table 4.17. Loading Effect of TiO₂ on Proton Conductivity

TiO ₂ wt%	Proton Conductivity (mS/cm)	
	BT	AT
0	20	43
3	21	49
5	33	52
10	33	43
20	36	44

BT & AT refers to before and after acid treatment conditions. All the measurements were conducted at room temperature (24 °C) in water and by 2-probe method.

4.6.2 Heteropolyacid (HPA) Composites

HPAs are known to be excellent solid proton conductors. Therefore HPA composites are expected to perform better than the pristine SPEEK membranes sulfonated to a value that is not sufficient for the PEM operation but have required thermohydrolytic stability. However, HPAs are suspected to leach since they are water soluble. To investigate the potential of HPA composites and to investigate also the HPA loaded zeolite-beta composites as a support used in this study, a set of composite membranes were prepared. SPEEK with a DS of 68 was selected as the polymer matrix and two HPAs (Tungstophosphoric acid (TPA) & Silicotungstic acid (STA)) were incorporated directly or after loading on zeolite-beta (Si/Al=25) as the supporter. Details of preparation were explained in the experimental section. Loading of HPAs were fixed at 5

wt% of the sulfonated polymer and loading of HPA on zeolite was 50% theoretically. Since the aim was to compare the effect of HPA on conductivity with and without zeolite as a support, HPA loading was kept constant in all membranes. In Table 4.18 thickness, proton conductivity and water uptakes of these composite membranes were given.

Table 4.18. Proton Conductivity and Water Uptakes of HPA Composites

Membrane	Thickness (μm)	Conductivity (mS/cm)		Water uptake (wt%)
		Untreated	Untreated	
SPEEK-68	110	22	42	44
TPA Comp. (5%)	95	35	62	46
STA Comp. (5%)	115	40	52	46
TPA-Zeolite Comp.	100	21	43	46
STA-zeolite Comp.	115	17	42	43
Zeolite Comp. (10%)	115	22	35	44

All measurements were performed at room temperature ($T \sim 19^\circ\text{C}$); membranes were dried at 80°C 12 hrs; DMAc used as casting solvent; equilibration at 100 % RH at about 2 hrs.

The highest conductivity among the HPA composites was achieved with TPA/SPEEK composite at room temperature among the acid treated membranes. Zeolite supported HPA composites showed no enhancement of conductivity. 5% HPA incorporation did not change the water uptake at room temperature but increased the proton conductivity by a considerable amount. This shows that the increase in proton conductivity was not caused by water uptake increase but directly by the increase in acidity and increase in proton conducting sites. However, mechanical and

thermohydrolytic stability of these composite membranes were not sufficient enough for a long term operation in fuel cell environment.

Table 4.19. Proton Conductivity of HPA Composites (Loading)

Membrane	Thickness (μm)	Conductivity (mS/cm)
SPEEK (DS=70)	80	42
TPA (5%)	90	58
TPA (10%)	100	73
TPA (20%)	150	77
TPA/Zeolite (20%)	115	46
TPA/Zeolite (40%)	120	52
STA (20%)	80	60
STA-zeolite (40%)	110	44
Zeolite (20%)	150	57
Nafion-112	51	71

As it was discussed in the previous thermal analysis results, SPEEK's single decomposition temperature is around 580 °C which was observed from the only step loss in TGA curve. After sulfonation, at least three step losses were observed: First one is the weight loss of bound water until about 200 °C, second loss corresponds to the sulfonic acid group loss starting around 300 °C until about 450 °C, and third loss corresponds to the main chain decomposition starting around 450 °C. To investigate the effect of HPA fillers, pristine SPEEK, 20% TPA, SPA and TPA/Zeolite Beta composites were selected and compared for their thermal behavior in Figure 4.36. The first step is similar in all composites showing that the water uptake capacities were not changed considerably. However, comparison of second step losses shows that sulfonic acid group loss is the highest for pristine SPEEK and decreased for composites. To investigate these, weight losses and DS values calculated from TGA

curves were tabulated in Table 4.15. DS value calculated from H-NMR for SPEEK was 70% and that from TGA is 73% which is very close to the value obtained from H-NMR. The decrease around 10% in sulfonic acid group for composites of TPA and STA may be attributed to an interaction between the heteropolyacids and these sulfonic acid groups. As reported and discussed before, HPA loaded zeolites did not give proton conductivities as expected and were lower than the HPA only composites. This was attributed to possible prevention of HPAs interacting with sulfonic acid groups directly by cage-like zeolite structure. TGA results seem to support this hypothesis since TPA/Zeolite composite's DS is close to pristine SPEEK. The interesting point here is that although the HPA incorporation seems to deactivate some of the sulfonic acid groups, the conductivity of these composites increased by a considerable amount indicating a more effective proton pathway created by these inorganic solid acids. TGA curves showing the weight losses can be found in Appendices.

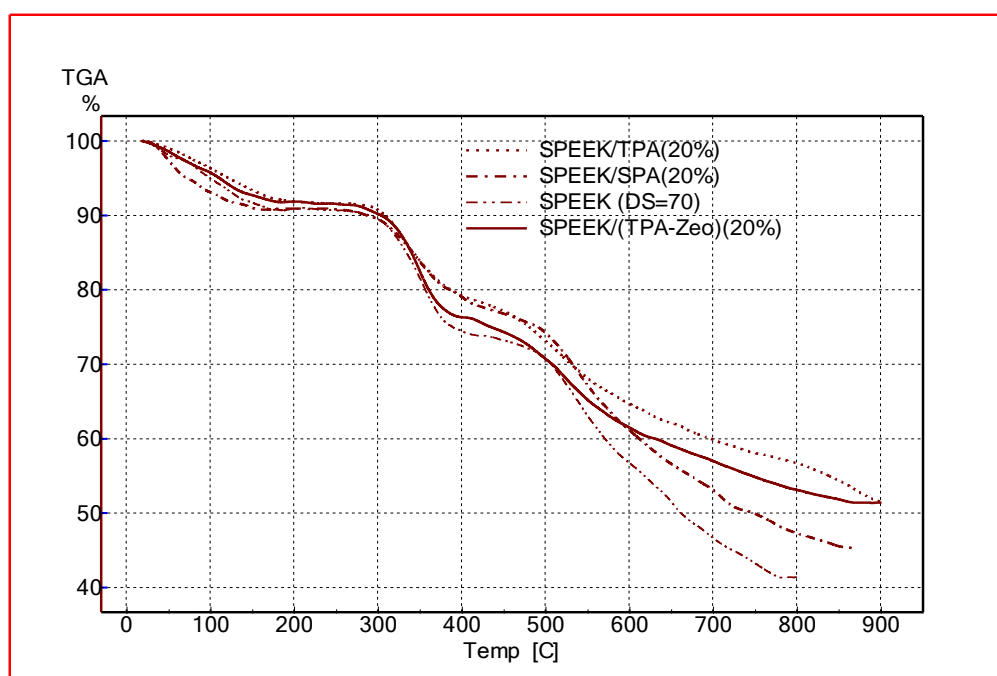


Figure 4.36. TGA curves of HPA composites

Table 4.20. DS and Weight Losses of HPA-Composite Membranes Calculated from TGA Curves

Sample	DS% (TGA)	$W_{\text{lost}} \%$ (2 nd :250-450 °C) (-SO ₃ H)	$W_{\text{lost}} \%$ (1 st : up to 250 °C) (Water)	$W_{\text{lost}} \%$ (2 nd)-Corr.	T _d (°C)
SPEEK (DS=70)	73	17.0	9.3	18.7	~450
TPA (20%)	61	14.6	8.2	15.9	~450
TPA/Zeolite (20%)	75	17.5	8.1	19.0	~450
STA (20%)	59	14.2	8.9	15.6	~450

4.7 Blend/Composites

The thermohydrolytic stability of HPA composites were not sufficient at around 80 °C which is close to the operating temperature of the PEM fuel cell. Crosslinking and/or blending may increase the stability of these membranes as discussed before. Blending with PBI, which is a basic polymer intrinsically, may result in crosslinking with the help of its amine groups. 10% PBI blends were prepared with the same SPEEK (DS~70%), and also with 50% TPA. Results showed that blending only with 10 wt% PBI decreased the conductivity nearly 4-fold, but the hydrolytic stability of the blend membrane increased considerably and was excellent (Table 4.21). TPA incorporated to compensate the decreased proton conductivity resulted in an increase more than 3-fold compared to the blend but the stability of the membrane was not sufficient. High acid loading caused deterioration in mechanical stability. Since the 10% blending decreased conductivity and 50% TPA decreased the mechanical stability both percentages were halved in the next experiment to 5% and 25%. The conductivity and thermo-hydrolytic stability results showed that 5% PBI blend still had good hydrolytic stability with 3-fold sacrifice in conductivity. 25% TPA seems to close this conductivity gap. From these results, it can

be concluded that it is possible to achieve high conductivity and stability at the same time by combining blending and composite approaches.

Table 4.21. Proton Conductivities of PBI/SPEEK blends and their TPA Composites

Membrane	Thick. (micron)	Conductivity (mS/cm)	Chemical Stability	Hydrolytic Stability
SPEEK	80	42	--	--
PBI(10%)/SPEEK Blend	100	11	++	++
PBI(10%)/SPEEK/TPA (50%) Blend/Composite	110	24	++	--
PBI(5%)/SPEEK Blend	100	15	++	+
PBI(5%)/SPEEK/TPA (25%) Blend/Composite	100	41	++	--

Note: Hydrolytic stability test was performed by keeping membranes at 80 °C in a fully humidified vacuum oven for 1 day.

To investigate the stability of blend composite membranes especially for TPA stability, PBI(10%)/SPEEK/TPA (50%) Blend/Composite membrane was kept in 3% H₂O₂ and 4 ppm Fe⁺⁺ ion at 60 °C for 12 hours. Contrary to the case of pristine SPEEK and HPA only composites this membrane was chemically stable after peroxide test. For investigating the loss in ionic conductivity, proton conductivity was measured again and 27 mS/cm was found. This result shows that TPA did not leave the structure during the acid treatment, washing and peroxide test. However, a leaching study with continuous flow similar to the fuel cell environment is necessary for simulating long term performance. A slight increase in conductivity may be because of the experimental conditions or because of the removal of metal and organic impurities during this chemical stability test.

4.8 Temperature Dependence of Proton Conductivity (Activation Energies)

The proton conductivity is temperature dependent and the relationship is Arrhenius-like. This behavior is important for comparison among the membranes and for calculating the activation energy for proton transfer and to comment on the proton conductivity mechanism. Activation energies of the various membranes were calculated and compared, results were given below. The dependence of membrane's conductivity on temperature can be expressed by the Arrhenius relationship:

$$\sigma = A \exp\left(-\frac{E_a}{RT}\right)$$

where σ : proton conductivity

A: frequency factor

E_a : activation energy for proton conduction (J/mol)

R: gas constant (J/mol.K)

T: absolute temperature (K)

So plotting the conductivity vs temperature data in logarithmic form gives the activation energies as follows:

$$\ln\sigma = \ln A - \left(\frac{E_a}{R}\right) \frac{1}{T}$$

This equation indicates that the conductivity of the membrane should increase as temperature increases. This temperature dependence becomes more significant when the activation energy is high. It has been well reported that Nafion membranes have relatively small values of the activation energies, suggesting the Grotthus mechanism (hopping) for proton transport (Ye, 2006)

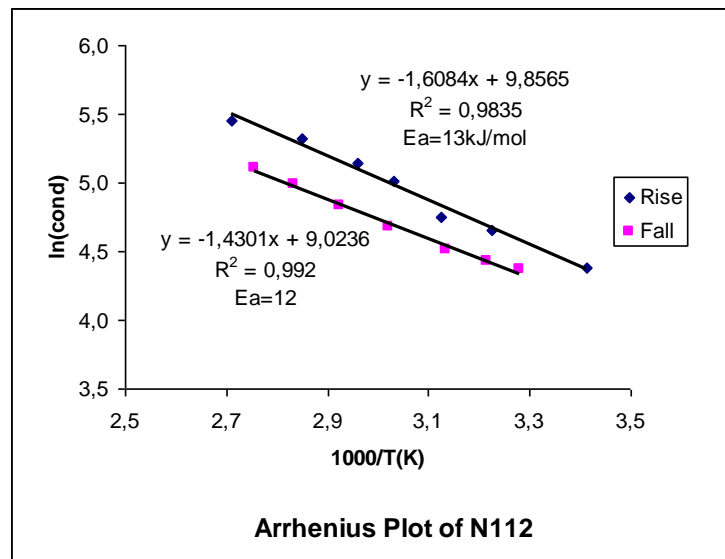


Figure 4.37. Arrhenius behavior of Nafion 112

The measurements were performed with the conductivity cell in vapor medium (100% humidity), and using 4-P AC-EIS. The activation energies (E_a) for Nafion 112 (Figure 4.37) which is 13 kJ/mol and 18.2 kJ/mol for SPEEK (DS~60%) (Figure 4.38) are consistent with literature values. The difference in conductivities during the rise and fall of temperature was observed also for other membranes.

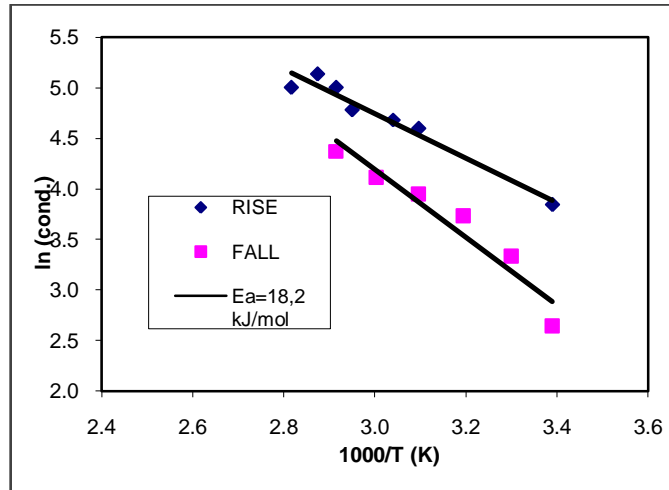


Figure 4.38. Arrhenius behavior of SPEEK

E_a is a measure of the energy barrier for proton conduction and also a measure indicating the dependence of the conductivity to temperature, therefore important for evaluation of the proton conductivity behaviors of alternative membranes. Therefore, activation energies for proton conduction of various pristine, blend and composite membranes were compared as can be followed from the Figure Figure 4.39 below.

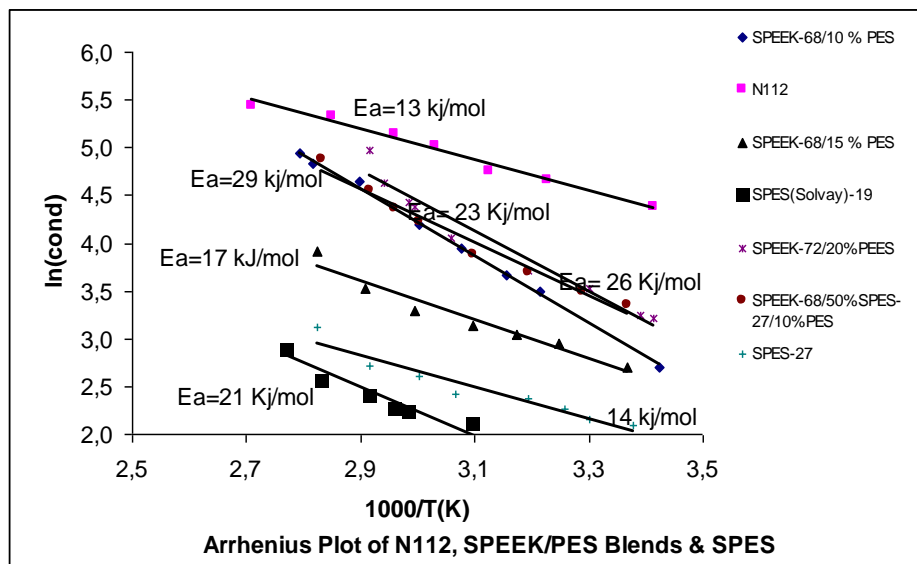


Figure 4.39. Activation energies for proton conduction of various pristine, blend and composite membranes

4.9 Mechanical Stabilities

Mechanical Characterization (DMA):

Table 4.22. Mechanical Analysis Results of Composite & Blend membranes

Sample	Tensile Strength (MPa)	Elongation at Break (%)
N112 (Dry)	12	58
N112 (Wet)	12	111
SPEEK-59	38	50
SPEEK-59/PES(20%)	50	44
SPEEK-72	34	55
SPEEK-72/20%PES/10%Cloisite25A	21	10
SPEEK-72/20%PES/10%SiO ₂	29	7
SPEEK-72/20%PES/10%TEOS	12	9
SPEEK-72/20%PES/10%BPO ₄	27	63

Although hydrolytic stability is more meaningful for the purpose of this study, tensile strength is also an important parameter showing the mechanical strength of the material exposed to a stress. Therefore, tensile strengths (MPa) of some of the composite and composite/blend membranes were measured to give an idea about the mechanical strength of the membranes studied. From the results (Table 4.22), it can be concluded that all the polymers studied have higher tensile strengths than Nafion 112. Blending with 20% PES increased the tensile strength of the SPEEK with a DS of 59. All the composites prepared with clay, silica and BPO₄ decreased the tensile strength compared to pristine SPEEK with a DS of 72.

4.10 Methanol Permeability

For DMFC type fuel cells methanol permeability is as important as proton conductivity since permeation of methanol from anode side to cathode side causes a decrease in OCV. Nafion's methanol permeability is very high decreasing the maximum power that can be obtained despite its very high conductivity. Therefore, to investigate the potential of developed membranes in DMFC type fuel cells, methanol permeability tests were conducted as explained in the experimental section. To compare membranes DMFC potential a selectivity parameter (S) can be defined by taking the ratio of proton conductivity to methanol permeability.

$$S = \frac{\sigma}{P}$$

Methanol permeabilities were measured and calculated with the permeability cell and method as described in the experimental part. The methanol permeability of Nafion 112 (N112) with a thickness of 51 μm was calculated to be $9.62 \cdot 10^{-7} \text{ cm}^2/\text{s}$ from the slope of the concentration vs. time graph (Figure 4.40) which is consistent with the literature.

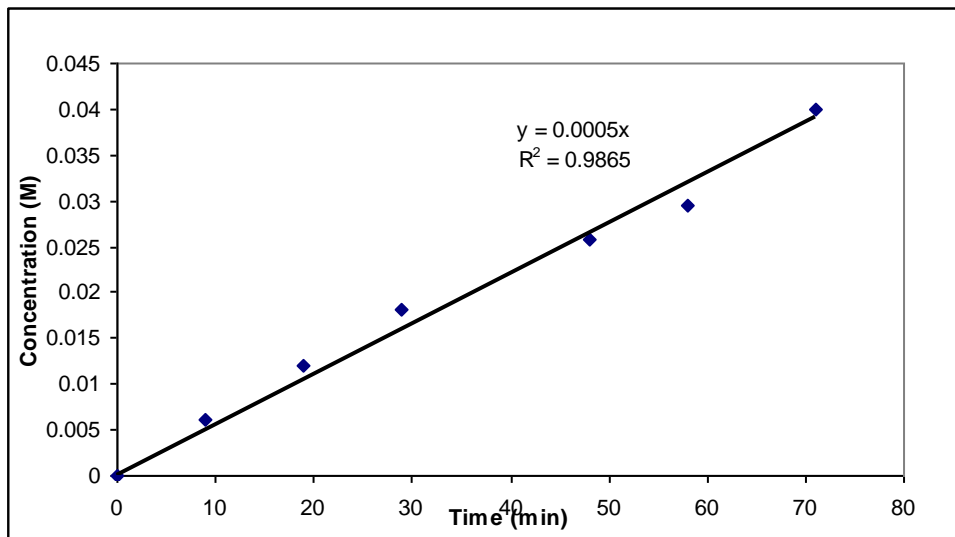


Figure 4.40. Methanol Concentration Change in Compartment B with respect to Time for N112

The effect of zeolite beta fillers on methanol permeability was investigated for 10% and 20% loading on SPEEK (DS=59) and compared with Nafion 112 as shown in Figure 4.41. The methanol permeabilities calculated from the slopes and selectivity values were summarized in Table 4.23. Zeolite fillers clearly decreased the methanol permeability, however the selectivity values were still less than that of Nafion 112. But it should be noted that the composite membranes tested were prepared with SPEEK with a low DS for retaining the mechanical and hydrolytic stability as discussed in the preceding sections so their conductivities were also low.

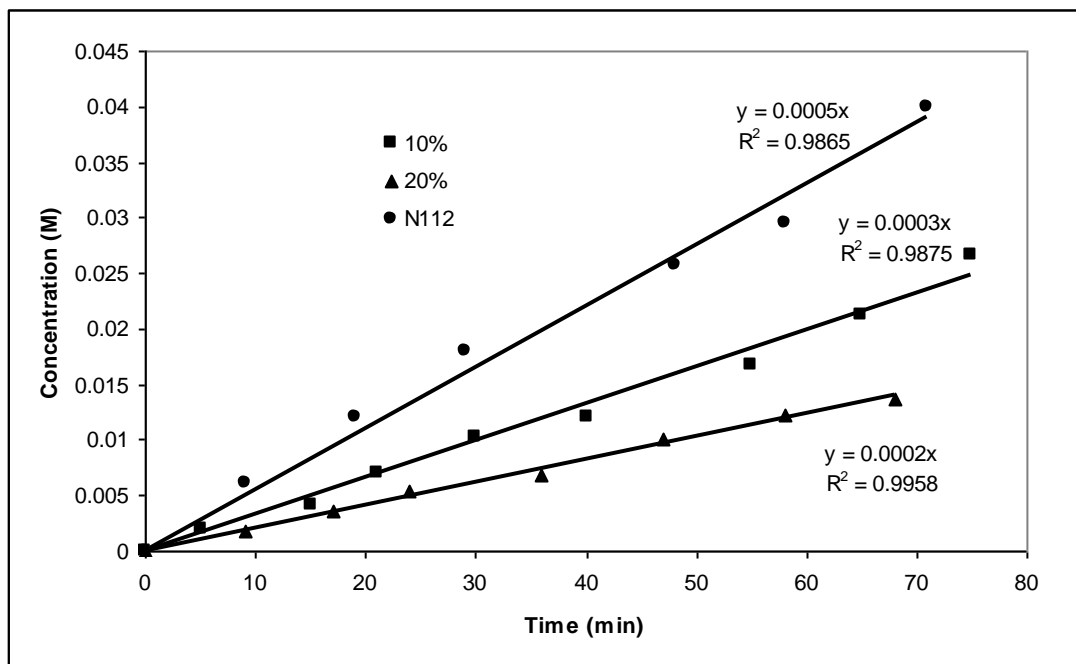


Figure 4.41. Methanol Permeabilities of N112 and Zeolite Beta Composites

Table 4.23. Conductivity, Methanol Permeability & Selectivity (S) of N112 and Zeolite Beta Composites

Membrane	Conductivity (mS/cm)	Methanol Permeability (cm ² /s)	Selectivity (S)
N112	71	9.6*10 ⁻⁷	7.3*10 ⁷
10% Zeo Comp.	13	7.4*10 ⁻⁷	2.2*10 ⁷
20% Zeo. Comp.	16	6.8*10 ⁻⁷	1.9*10 ⁷

The potential of composite/blends which were shown to perform better than both pristine sulfonated and composite only membranes for their proton conductivity and mechanical/thermohydrolytic stability were also investigated for DMFC potential. From this family two membranes were selected, one with PBI as blending component and TPA as inorganic

proton conductor filler and one with PES as blending component and TiO₂ as hygroscopic inorganic filler.

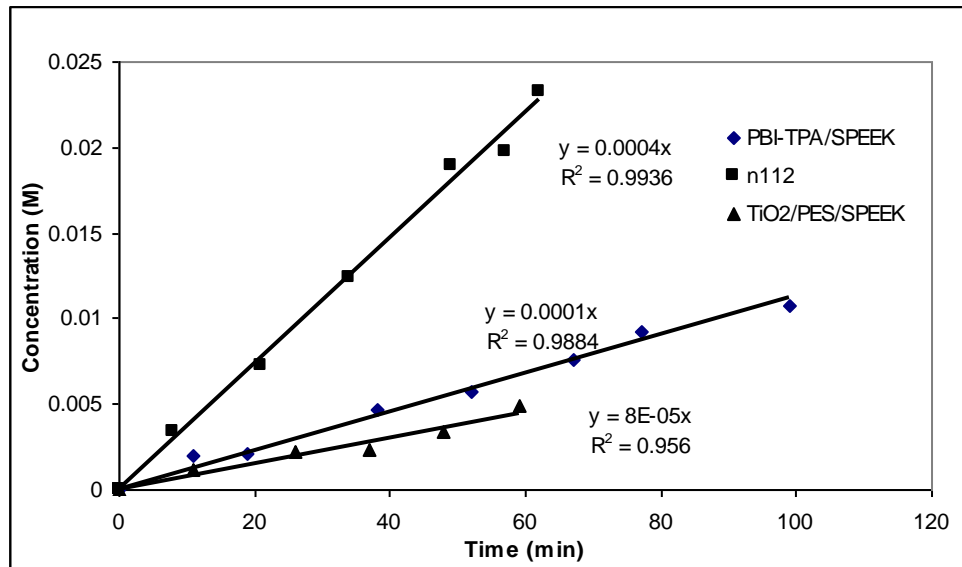


Figure 4.42. Concentration vs Time for Methanol Permeabilities of N112 and Selected Composite/Blends

Table 4.24. Conductivity, Methanol Permeability & Selectivity (S) of N112 and Selected Composite/Blends

Membrane	Conductivity (mS/cm)	Methanol Permeability (cm ² /s)	Selectivity (S)
N112	71	9.6*10 ⁻⁷	7.3*10 ⁷
SPEEK12/PBI(10%)-TPA(50%)	24	4.34*10 ⁻⁷	5.5*10 ⁷
10%PES/10% TiO ₂	24	2.57*10 ⁻⁷	9.3x10 ⁷

Composite/blends decreased methanol crossover more than the pristine and zeolite composites. PES/TiO₂ membrane's selectivity exceeded Nafion 112 selectivity. The proton conductivities of these composite/blends are not the highest ones among the many tested composite and/or blend

membranes, but the most durable ones. Actually, the typical operating temperature of DMFC is around 60 °C, therefore composites or composite/blends with sufficient stability and having higher proton conductivity will definitely be much more selective in other words better in overall performance than Nafion in DMFC.

4.11 Single Cell Tests

The final and actual evaluation of performance of fuel cell membranes comes from the single cell tests. Since for each test a MEA (membrane electrode assembly) must be prepared by spraying the catalyst layer onto the carbon paper followed by hot pressing, and hydrogen and oxygen gases are consumed, this is an expensive (Pt is also consumed) and time consuming task. Therefore, testing each membrane candidate in a single cell is not feasible. As discussed before in the previous sections, membranes were first characterized and tested with preliminary methods such as proton conductivity measurement, chemical, mechanical and thermohydrolytic stability, ion exchange capacity (DS) etc. Finally, the best ones were tested in fuel cell. Actually, the weak thermohydrolytic stability of pristine SPEEK was also realized in one of the first single cell tests. After that, low DS SPEEK was tried to be used as the host matrix for composite membranes. However, as the temperature increased from 60 °C to 70 °C the mechanical integrity of this membrane was lost after a short time of operation. This is clear from the decrease in both OCV and also from the loss of performance after 70 °C (Figure 4.43 and Figure 4.44). There is a considerable increase in performance from 60 °C to 70 °C, and further increase is expected at 80 °C but instead performance curve is between 60 and 70 °C. This result was confirmed from the visual examination of the MEA after test; the membrane swelled and lost its integrity.

The composite membrane with 5% TiO₂ incorporated in SPEEK with 65% DS showed a similar behavior. After an increase of performance from 50 °C to 60 and 70 °C, after a short time OCV dropped to 0.75 V from 0.92 V. The temperature at which the stability loss was observed decreased probably because of the higher DS of SPEEK, the inorganic component clearly has little or no effect on thermohydrolytic stability.

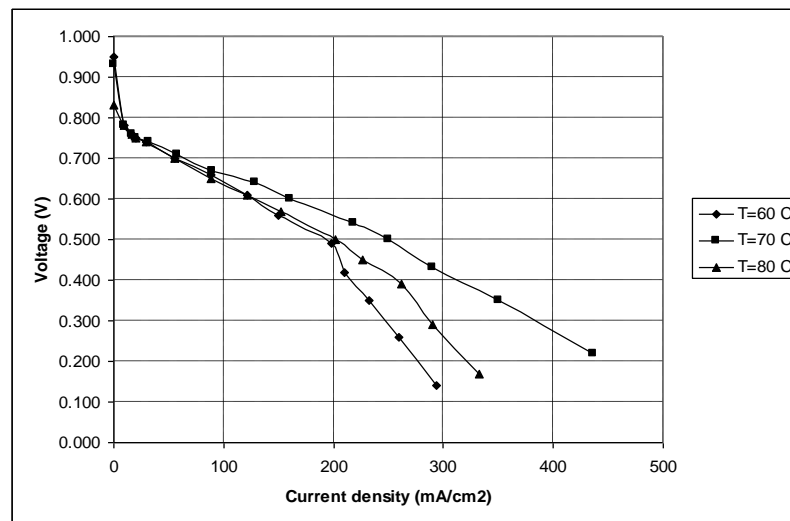


Figure 4.43. Polarization (V-I) curves of SPEEK (DS=56) at various temperatures

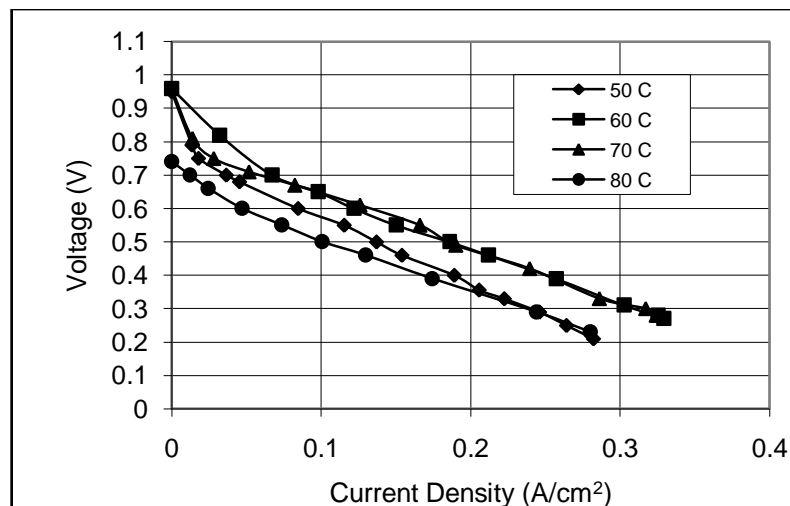


Figure 4.44. Polarization (V-I) curves of SPEEK (DS=65)/5% TiO₂ composite at various temperatures

After similar conclusions about the mechanical stability of the membrane from both previous chemical and thermo-hydrolytic stability tests together with single cell results, blends with a stable unsulfonated or less sulfonated polymer were investigated for increasing dimensional stability which is necessary for long term operation. For this purpose blends with unsulfonated PES, SPES with DS around 20% and PBI were tested. Since blending with unsulfonated hydrophobic polymers or with basic polymers such as PBI was shown to decrease proton conductivity in impedance spectroscopy measurements, composite/blend membranes were investigated for their single cell performance. Figure 4.45 shows the performance curve of 5%PBI/10%TiO₂/40%TPA/SPEEK (DS=59) composite/blend membrane. The three temperatures are the cell temperature, anode and cathode humidifier temperatures respectively. For 100% R.H. these temperatures were varied during the tests probably since water management characteristics of each membrane differ from one to another. Curves show clearly that the performance increases with increasing temperature, also the mechanical integrity of the membrane after operation of 1 day was very good. The maximum current density obtained at 0.5 V was around 220 mA/cm² at 75 °C, which was also above the pristine SPEEK and composites tested before. The shapes of the curves were all similar with a sudden drop of current density after 0.4 V probably showing flooding (difficulty in mass transport) or a problem in water management. The performance decreased a little at 80 °C and more at 90 °C which is not shown.

The same composite/blend membrane without the heteropolyacid that is suspected to leach during the operation performed even better surprisingly (Figure 4.46). The performance again increased continuously with temperature and at 90 °C increased more steeply to around 300 mA/cm² at 0.5 V. Nafion 112 performance decreases suddenly at 90 °C, therefore

this result becomes more important showing the possibility of operating at higher temperatures.

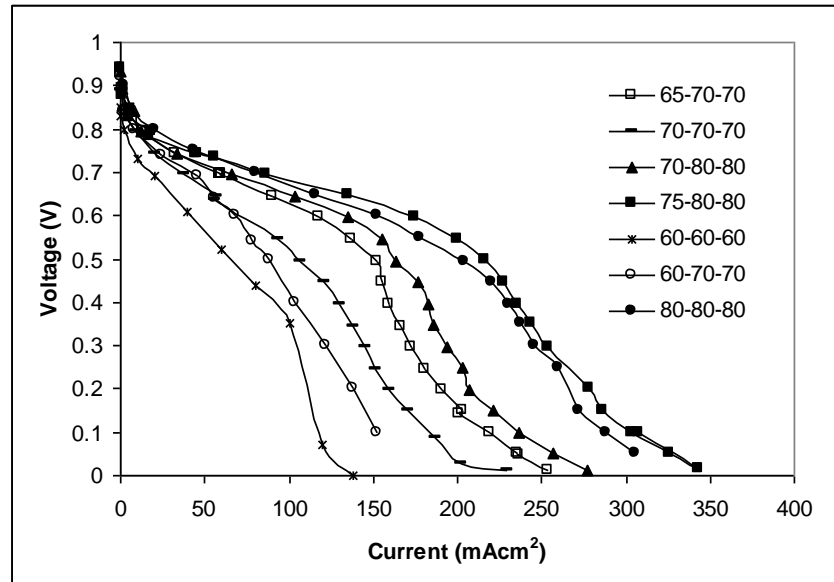


Figure 4.45. Polarization (V-I) curves of 5%PBI/10%TiO₂/40%TPA/SPEEK (DS=59) at various temperatures

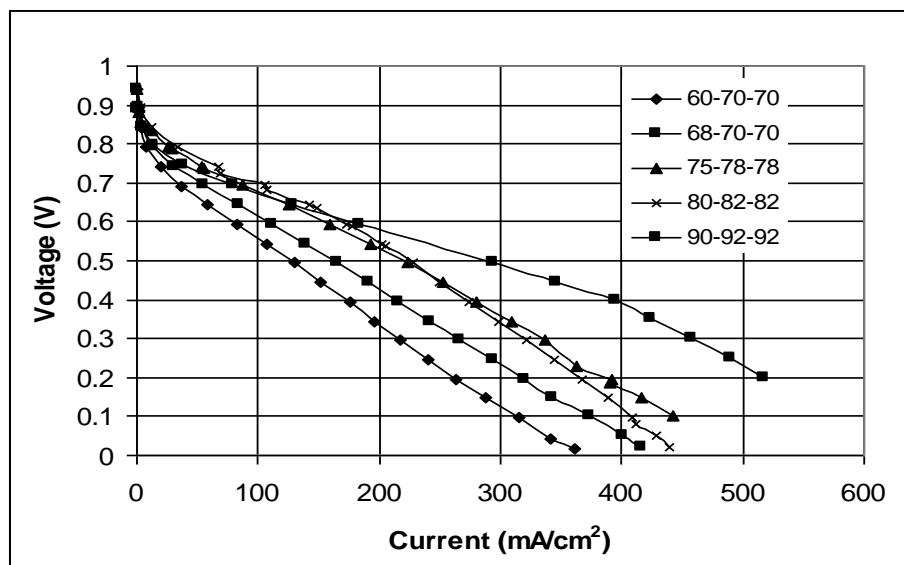


Figure 4.46. Polarization (V-I) curves of 5%PBI/10%TiO₂/SPEEK (DS=59) at various temperatures

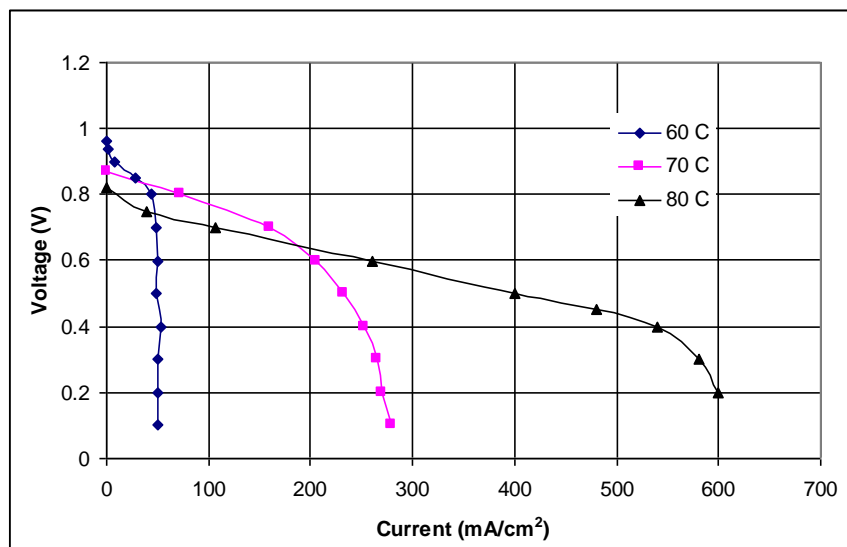


Figure 4.47. Polarization (V-I) curve of 25%SPES()/TPA(20%)/SPEEK (DS=74) at various temperatures

The first blend membrane which performed better than the pristine ones was a 10% PES blend not shown here. However, since during the thermohydrolytic stability tests they showed still excessive swelling although not dissolved completely like pristine SPEEK at 80 °C, they were not investigated so far. But increasing PES or low DS SPES blend ratio from 10 to 25% could be investigated. Therefore, a composite/blend with 25% SPES (DS~20) and 20% TPA with SPEEK (DS=74) was tested (Figure 4.47). Proton conductivity was measured to be 50 mS/cm which is good compared to previous samples. The single cell performance at 80 °C was interesting and gave the highest current density among all composite and composite/blend membranes but after 80 °C performance was lost. This membrane should be further investigated. If the reason is the mechanical integrity, than a crosslinking approach preferably with PBI blending might give good results. Another important observation is that membranes with TPA incorporated for increasing the proton conductivity

Below in Figure 4.48, the performances of various membranes were compared in the same plot and also with the best performance of Nafion 112 obtained in this test station. The membranes prepared and tested at the beginning of this study were also included to show the improvement over time. The explanations of the membranes were given in Table 4.25.

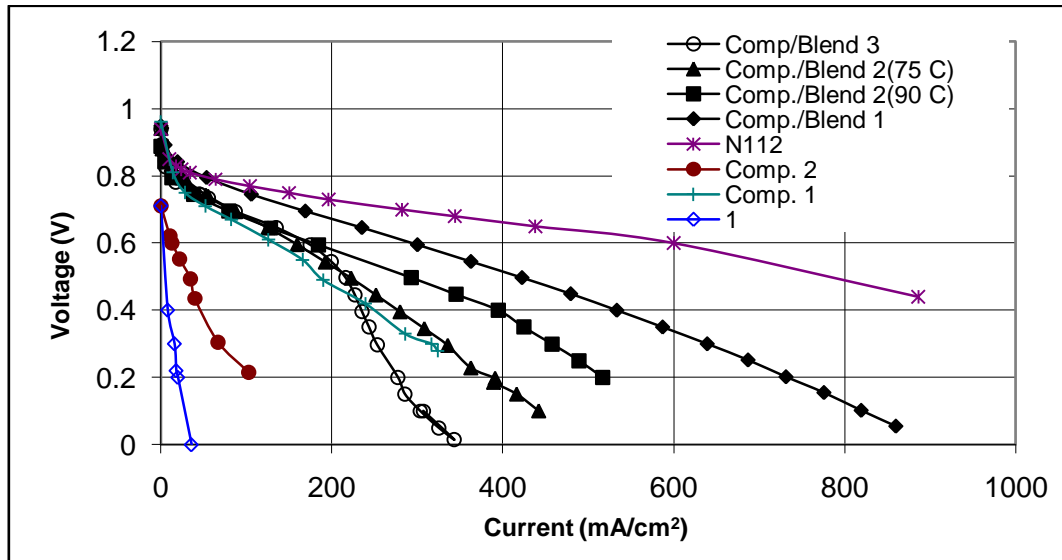


Figure 4.48. Comparison of fabricated composite and composite/blend membranes with Nafion 112 performance

Table 4.25. Summary of Membranes Tested in a Single Cell

Sample	Basis Polymer	Blending Polymer	Inorganic Fillers
Comp./Blend 3	SPEEK (DS=59)	PBI (5%)	TiO ₂ (10%)/TPA (40%)
Comp./Blend 2(75 °C)	SPEEK (DS=59)	PBI (5%)	TiO ₂ (10%)
Comp./Blend 2(90 °C)	SPEEK (DS=59)	PBI (5%)	TiO ₂ (10%)
Comp./Blend 1	SPEEK (DS=68)	PBI (5%)	TPA (25%)
Comp. 2	SPEEK (DS=40)	None	Zeolite Beta (10%)
Comp. 1	SPEEK (DS=65)	None	Zeolite Beta (5%)
1	SPES(DS=20)	None	None

Figure 4.48 also shows the improvement in performance of the developed membranes over time. As stated before, the high DS values results in high proton conductivities but this does not mean a high power performance in fuel cell. The reason of this is that high swelling may cause flooding at the cathode side and also the pinholes or cracks during drying may decrease the open current voltage. Therefore, the mechanical and hydrolytic stability of the membranes are very important. Stability tests showed that blending with hydrophobic polymers (not sulfonated or less sulfonated) improves the stability but decreases proton conductivity sharply. Blending with PES or SPES (low DS) increased the hydrolytic stability but not at the level desired, however, blending with basic PBI at low levels improved stability to the desired point. Figure 4.48 also shows that the best performances were achieved with these blends. A more striking result from this figure is that the performance of the composite/blend 2 prepared with SPEEK (DS=59); 5% PBI; and 10% TiO₂ increased appreciably when the temperature was raised from 80 °C to 90 °C most probably with the help of hygroscopic titanium dioxide incorporated. The mechanical stability of this membrane was also very good since the DS of SPEEK was optimum and blended with 5% PBI. Since the performance of Nafion decreases sharply after 80 °C the results above are promising.

CHAPTER 5

CONCLUSIONS

The aim of this study was to develop and characterize novel proton exchange membranes for fuel cell applications particularly for PEM and DMFC types. A systematic development and characterization methodology was also aimed to be established during the study period.

Fabricating a composite membrane is a tedious task including several critical steps: Sulfonation of the polymer, incorporation of inorganic fillers with suitable method, fabricating the membrane and at any step using the characterization methods.

Sulfonation studies of PES and PEEK were performed and investigated separately since their sulfonation behavior is different. For PEEK optimum sulfonation level (50-70%) for mechanical stability and the reaction parameters for this range was found to be 3-4 hours of reaction with sulfuric acid at around 50 °C. However, even at these low DS values SPEEK showed excessive swelling and problems in hydrolytic stability and therefore blending approach was utilized.

Various procedures of sulfonation were tried to increase the DS of SPES, however because of the electrophilic sulfone group DS of ~30% could not be exceeded. Therefore, PES and SPES with low DS were used as a blending agent since their mechanical stability is very good. During the sulfonation studies of PES it was found that a small ratio of PEES units existing in the polymer changed sulfonation behavior completely. These

units were found to be sulfonated primarily and possibly preventing the sulfonation of PES units.

Post sulfonated polymers were characterized with H-NMR, sulfur elemental analysis and titration to calculate the degree of sulfonation (DS) values and with TGA and DSC for thermal stability and glass transition temperature (T_g). Chemical stabilities were evaluated by hydrogen peroxide tests. Proton conductivities measured by electrochemical impedance spectroscopy (EIS)

Almost all the parameters in the fabrication period were investigated for their effect on proton conductivity and stability. Casting temperature and acid treatment were shown to be effective. As casting temperature was increased (from regular temperature of 80 °C to 120 & 140°C) mechanical stability increased possibly by some crosslinking but conductivity decreased. Acid treatment always increased conductivity and this step is necessary before measurements for complete protonation.

After introducing a standard method for sulfonation and characterization of polymers, suitable methods for both blend and composite membrane fabrication by incorporation of various fillers (metal oxides (SiO_2 , TiO_2), zeolite) were used to fabricate the composite membranes. The effect of many variables such as degree of sulfonation of the host polymer, inorganic type and loading, blending polymer type and loading were also investigated for their effect on proton conductivity. Among the inorganic fillers TPA and TiO_2 generally resulted in higher proton conductivities at room temperature. But the effect of fillers on the mechanical and thermo-hydrolytic stability was not found to be considerable.

A systematic development and characterization route was established and it was showed that by optimizing proton conductivity and thermal/chemical stability with blending/composite approaches it is possible to produce

novel high performance proton exchange membranes for fuel cell applications.

Chemically and thermo-hydrolytically stable composite/blend membranes such as 25%TPA/SPEEK(DS=70)/PBI with single cell performances close to Nafion-112 ($\sim 400 \text{ mA/cm}^2$ @ 0.5 V) were developed.

The performance of the composite/blend membrane prepared with SPEEK (DS=59); 5% PBI; and 10% TiO_2 increased appreciably when the temperature was raised from 80 °C to 90 °C most probably with the help of hygroscopic titanium dioxide incorporated. The mechanical stability of this membrane was also very good since the DS of SPEEK was optimum and blended with 5% PBI. Since the performance of Nafion decreases sharply after 80 °C the results above are promising

Selectivities (conductivity/methanol permeability) greater than Nafion 112 for DMFC were observed for composite/blend membranes.

CHAPTER 6

RECOMMENDATIONS

In this study it was shown that every step and parameter is critical for the final performance of a developed proton exchange membrane for fuel cells.

Proton conductivity measurements are particularly important since there are discrepancies in the reported values in the literature. As shown in this study special care should be given to conductivity measurements. For example, keeping membranes in distilled water and then measuring the conductivity may yield inconsistent results. The conductivity should be measured just after protonation with acid. Four probe (4-P) measurements with a large cell constant (L/S) gives accurate proton conductivity results. However, for investigating other components such as diffusional resistance (Warburg) frequency domain should be large and the cell constant should be small.

Inorganics were proven to be useful for increasing proton conductivity in this study parallel to the literature, however in literature little information were given related to the critical thermo-hydrolytic stability. Inorganic fillers have not a considerable effect on improving this stability of SPEEK particularly. Therefore, crosslinking or blending with stable polymers is crucial. PBI is a good candidate for blending but not as compatible as PES with SPEEK. For both inorganic composites and polymer blends compatibilizers can be utilized.

Particle size was shown to be important for better interaction with polymer host matrix, nano-sized fillers can be prepared with well established sol-gel procedures. An even better approach could be the preparation of composites with in-situ sol-gel during casting step. Chelating agents can be investigated for this purpose.

PBI/SPEEK composites with solid inorganic proton conductors such as tungstophosphoric acid was shown to be successful in PEMFC single cell tests. The methanol permeabilities of this kind of blend/composites are also low compared to Nafion, therefore DMFC tests are recommended for these novel membranes.

REFERENCES

- Akata B., Yilmaz B., Jirapnoghphan S. S., Warzywoda J., Sacco, Jr., A.. "Characterization of zeolite Beta grown in microgravity," *Microporous and Mesoporous Materials*, 71, 1-9, 2004.
- Appleby, A. J., "The Electrochemical Engine for Vehicles", *Scientific American*, 74-79, July 1999.
- Bac, N., Nadirler, S., Ma, C., Mukerjee, S., Proceedings International Hydrogen Energy Congress and Exhibition IHEC 2005 Istanbul, Turkey, 13-15 July 2005
- Baradie, B.; Poinson, C.; Sanchez, J.Y.; Piffard, Y.; Vitter, G.; Bestaoui, N.; Foscallo, D.; Denoyelle, A.; Delabouglise, D. and Vaujany, M. J. *Power Sources*, 74, 8, 1998.
- Barsoukov, E., Macdonald, J., R., "Impedance Spectroscopy: Theory, Experiment, and Applications", Wiley-Interscience, 2nd edition, 2005
- Barbir F., "PEM Fuel Cells theory and Practice", Elsevier Academic Press, 2005.
- Bayrakceken, A., Erkan, S., Türker, L., Eroğlu, İ., "Effects of membrane electrode assembly components on proton exchange membrane fuel cell performance" *International Journal of Hydrogen Energy*, Vol. 33, 165-170, 2008
- Bishop, M. T., Karasz, F.E., Russo, P.S. Langley, K.H., *Macromolecules* 18 86, 1985
- Bonnet, B.; Jones, D.J.; Roziere, J.; Tchicaya, L.; Alberti, G.; Casciola, M. Massinelli, L.; Baner, B.; Peraio, A. and Ramunni, E., *J. New Mater. Electrochem. Sys.*, 3, 87, 2000.
- Byun, I. S., Kim, I. C., Seo, J. W., "Pervaporation Behavior of Asymmetric Sulfonated Polysulfones and Sulfonated Poly(ether sulfone) Membranes", *Journal of Applied Polymer Science*, Vol. 76, 787-798, 2000
- Cahan, B. D., and Wainright, J. S., *J. Electrochem. Soc.*, 140, L185., 1993

Chang J-H, Park P. J. H., Park G-G, Kim C.-S., Park O.O., Proton-conducting composite membranes derived from sulfonated hydrocarbon and inorganic materials, *Journal of Power Sources*, 124, 18-25, 2003.

Ciureanu, M., Mikhailenko, S.D., Kaliaguine, S., " PEM fuel cells as membrane reactors: kinetic analysis by impedance spectroscopy", *Catalysis Today*, 82, 195–206, 2003

Deslouis, C., Musiani, M. M., and Tribollet, B., *J. Phys. Chem.*, 98, 2936 (1994)

Eikerling, M., Kharkats, Y. I., Kornyshev, A. A., Volkovich, Y. M., "Phenomenological Theory of Electro-osmotic Effect and Water Management in Polymer Electrolyte Proton-Conducting Membranes", *J. Electrochem. Soc.* 145, 2684-2699, 1998

Eikerling, M., Kornyshev, A. A., "Proton Transfer in a Single Pore of a Polymer Electrolyte Membrane", *J. Electroanal. Chem.* 502, 1-14 2001

Erkan, S., MSc. Thesis in Chemical Engineering, Middle East Technical University, Ankara, Turkey., 2005

Eapen M.J., Reddy K.S.N., Shiralkar V.P., 'Hydrothermal crystallization of zeolite beta using tetraethylammonium bromide', *Zeolites*, 14, 295-302, 1994

Erdener, H., MSc. Thesis in Chemical Engineering, Middle East Technical University, Ankara, Turkey., 2007

Fuel Cell Handbook, 5th ed., EG & G Services Parsons, Inc., Science Applications, Morgantown, West Virginia, 2000

Gasteiger, H.A., and Mathias, M.F., "Fundamental Research and Development Challenges in Polymer Electrolyte Fuel Cell Technology". Paper presented at the Workshop on High Temperature PEM Fuel Cells, Pennsylvania State University, 2003.

Genova-Dimitrova, P.; Baradie, B.; Foscallo, D.; Poinignon, C.; Sanchez, J.Y. *J. Membr. Sci.*, 185, 59, 2001.

Giordano, N., Staiti, P., Hocevar, S., Arico, A. S., *Electrochimica Acta* 41, 397, 1997.

Guan, R., Zou, H., Lu, D., Gong, C., Liu, Y., "Polyethersulfone sulfonated by chlorosulfonic acid and its membrane characteristics",

European Polymer Journal, 41, 1554–1560, 2005

Gür N., MSc. Thesis in Chemical Engineering, Middle East Technical University, Ankara, Turkey., 2005

Hajipour, A. R.; Mirjalili, B. F.; Zarei, A.; Khazdooz, L.; Ruoho, A. E. Tetrahedron Lett., 45, 6607, 2004.

He, R.; Li, Q.; Xiao, G. and Bjerrum, N.J. submitted to J. Membr. Sci. 2002.

Hickner, M.; Kim, Y.S.; Wang, F.; Zawodzinski, T.A.; McGrath, J.E. Proc. 33rd Int. SAMPE Techn. Conference 2001, 33, 1519, 2001.

Hogarth, M., Glipa, X., Johnson Matthey Technology Centre, ETSU F/02/00189/REP DTI/Pub URN 01/893

Holmberg B.A., Hwang S-J., Davis M. E., Yan Y., ‘Synthesis and Proton Conductivity of Sulfonic acid functionalized Zeolite BEA Nanocrystals’, Microporous and Mesoporous Materials, Volume 80, 347-356 (2005)

Huang, R. Y. M., Shao, P., Burns, C. M., Feng, X., “Sulfonation of Poly(Ether Ether Ketone)(PEEK): Kinetic Study and Characterization”, Journal of Applied Polymer Science, Vol. 82, 2651–2660, 2001.

Kaliaguine, S., Mikhailenko, S. D., Wang, K. P., Xing, P., Robertson, G., Guiver, M., “Properties of SPEEK based PEMs for Fuel Cell Application”, Catalysis Today, vol. 82, pp. 213-222, 2003.

Kerres. J., Cui, W., Reichele, S., “New Sulfonated Engineering Polymers via the Metalation Route. I. Sulfonated Poly(ethersulfone) PSU Udel® via Metalation-Sulfination-Oxidation Journal of Polymer Science: Part A: Polymer Chemistry, Vol. 34, 2421-2438, 1996.

Kim, I.C., Choi, J.G., Tak, T.M., “Sulfonated Polyethersulfone by Heterogeneous Method and its Membrane Performances”, Journal of Applied Polymer Science, 74, 2046-2055, 1999

Kobayashi, T., Rikukawa, M., Sanui, K., Ogata, N., “Proton-conducting polymers derived from poly(ether-etherketone) and poly(4-phenoxybenzoyl-1,4-phenylene)”, *Solid State Ionics*, 106, 219– 225, 1998

Kucera, F., Jancar, J., “Homogeneous and Heterogeneous Sulfonation of Polymers: A Review”, *Polymer and Engineering Science*, vol. 38, No. 5, 1998.

Lambert, J., B., Mazzola, E., P., "Nuclear Magnetic Resonance Spectroscopy: An Introduction to Principles, Applications, and Experimental Methods", Prentice Hall, 1st edition, 2003

Lee, C. H., Park, H. B., Lee, Y. M., Lee, R. D., "Importance of Proton Conductivity Measurement in Polymer Electrolyte Membrane for Fuel Cell Application", *Ind. Eng. Chem. Res.*, 44, 7617-7626, 2005

Li, L., Zhang, J., Wang, Y., "Sulfonated poly(ether ether ketone) membranes for direct methanol fuel cell", *Journal of Membrane Science*, 226, 159–167, 2003

Libby, B., "Improving Selectivity in Methanol Fuel Cell Membranes: A study of a Polymer-Zeolite Composite Membrane", Dissertation, Graduate School of the University of Minnesota, May 2001.

Liu, F., Yi, B., Xing, D., Yu, J., Hou, Z., Fu, Y., "Development of novel self-humidifying composite membranes for fuel cells", *Journal of Power Sources*, 124, 81–89, 2003

Ma, C., Zhang, L., Mukerjee, S., Ofer, D., Nair, B., *Journal of Membrane Science*, 219, 123–136, 2003.

Ma, S., Kuse, A., Siroma, Z., Yasuda, K., "Measuring Conductivity of Proton Conductive Membranes in the Direction of Thickness", ESPEC Technical Report, 2006.

Malhotra, S., Datta, R., "Membrane-Supported Nonvolatile Acidic Electrolytes Allow Higher Temperature Operation of Proton-Exchange Membrane Fuel Cells", *J. Electrochem. Soc.*, 144, 2, L23-L26, 1997

Michel Guisnet, Philippe Ayrault, Christophe Coutanceau, Maria Fernanda Alvarez and Jerzy Datka, "Acid Properties of Dealuminated Beta Zeolites Studied by IR Spectroscopy", *Journal of Chemical Society, Faraday Trans.*, Volume 93, 1661-1665, (1997)

Mikhailenko, D., Robertson, G. P., Guiver, M. D., Kaliaguine, S., *J. Chem. Soc. Faraday Trans* 94:1613-1618, 1998

Mikhailenko, S.D.; Zaidi, S.M.J. and Kaliaguine, S. *Catal. Today*, 67, 225, 2001.

Nicoloso, N., Löbert, A. A., Weppner, W., Rabenau, A., *Solid State Ionics*, Volumes 40-41, Part 1, 320-323, 1990

Nolte, R.; Ledjeff, K.; Bauer, M.; Mu"lhaupt, R. Partially Sulfonated Poly(arylene ether sulfone)-A versatile proton conducting membrane material for modern energy conversion technologies. *J. Membr. Sci.*, , 83, 211, 1993.

Nunes, S.P., Ruffmann, B., Rikowski, E., Vetter, S., Richau, K., J. *Membr. Sci.*, 203, 215, 2002.

Park, S. M., Yoo, J. S., "Electrochemical Impedance Spectroscopy for Better Electrochemical Measurements", November 1 , 2 0 0 3, American Chemical Society, Analytical Chemistry, 455 A-461 A, 2003
Poinsignon, C.; Le Gorrec, B.; Vitter, G.; Montella, C.; Diard, J.P. *Mater. Res. Soc. Symp. Proc.*, 575, 273, 2000.

Ramirez-Salgado, J., "Study of basic biopolymer as proton membrane for fuel cell systems", *Electrochimica acta*, 52, no11, pp. 3766-3778, 2007

Rikukawa M., S. K. 'Proton-conducting polymer electrolyte membranes based on hydrocarbon polymers', *Progress in Polymer Science*, 25, 1463-1502, (2000)

Rogers, R., E., "Composite Membranes for Fuel Cell Applications", MSc. Thesis in Chemical Engineering, North Eastern University, Boston, Massachusetts, USA, 2004

Rozière, J.; Jones, D.J.; Tchicaya-Bouckary, L.; Bauer, B., World Patent WO 0205370, 2000.

Salamone, J. C., *Polymeric Materials Encyclopedia*, vol. 7, CRC Press Inc., 1996

Savadogo O. "Emerging membranes for electrochemical systems: (I) solid polymer electrolyte membrane for fuel cell systems", *Journal of New Materials for Electrochemical Systems I*, 47, (1998)

Sengül, E., MSc. Thesis in Chemical Engineering, Middle East Technical University, Ankara, Turkey., 2007.

Slade, S., Campbell, S. A., Ralph, T. R., and Walsh, F. C., "Ionic Conductivity of an Extruded Nafion 1100 EW Series of Membranes", *Journal of The Electrochemical Society*, 149, 12, A1556-A1564, 2002

Sone et al (1996): "Proton Conductivity of Nafion 117 as Measured by a Four-Electrode AC Impedance Method", Springer, 1997

Srinivasan, S., Editors, PV 97-13, pp. 15-24, The Electrochemical Society Proceedings Series, Pennington, NJ, 1997

Srinivasan, S., "Fuel cells: from fundamentals to applications", New York, Springer, p. 203, 2006

Staiti, P.; Minutoli, M.; Hocevar, S. J. Power Sources 2000, 90, 231, 2000.

Staiti, P., Minutoli, M. J., Power Sources, 94, 9, 2001.

Thampan, T., Malhotra, S., Tang, H., Datta, R., "Modeling of Conductive Transport in Proton-Exchange Membranes for Fuel Cells", Journal of The Electrochemical Society, 147, 9, 3242-3250, 2000

Thampan, T. M., Jalani, N. H., Choi, P., Datta, R., "Systematic Approach to Design Higher Temperature Composite PEMs, Journal of The Electrochemical Society, 152, 2, A316-A325, 2005

Tricoli, V., "Proton and methanol transport in poly (perfluorosulfonate) membranes containing Cs⁺ and H⁺ cations", Journal of Electrochemical Society, 145, 3798–801, 1998

Wainright, J.S., Litt, M.H., and Savinell, R.F., "High-Temperature Membranes. in *Handbook of Fuel Cells: Fundamentals, Technology, and Applications*, Vol. 3, W.Vielstich, A. Lamm, and H.A. Gasteiger, Editors, Wiley, 2003.

Watanabe, M., Uchida, H., and Emori, M., "Polymer Electrolyte Membranes Incorporated with Nanometer- Size Particles of Pt and/or Metal-Oxides-Experimental Analysis of the Self Humidification and Suppression of Gas Crossover in Fuel Cells", Journal of Physical Chemistry B, 102, 3129-3137, 1998.

Yang, C., "Lecture notes: Fuel Cell Fundamentals, Introduction to Fuel Cell Science and Engineering",
[http://www.its.ucdavis.edu/education/classes/pathwaysclass/5-FuelCells\(Yang\).pdf](http://www.its.ucdavis.edu/education/classes/pathwaysclass/5-FuelCells(Yang).pdf), 2004

Yurdakul, A. Ö., MSc. Thesis in Chemical Engineering, Middle East Technical University, Ankara, Turkey., 2007

Zalbowitz, M., Thomas, S., Fuel Cells-Green Power, Los Alamos

National Laboratory, 1999

Zaidi, S.M.J., Mikhailenko, S.D., Robertson, G.P., Guiver, M.D., Kaliaguine, S., "Proton conducting composite membranes from polyether ether ketone and heteropolyacids for fuel cell applications", *Journal of Membrane Science*, 173 17–34, 2000.

Zawodzinski, T. A., Derouin, C., Radzinski, S., Sherman, R. J., Smith, V. T., Springer, T. E., and Gottesfeld, S., *ibid.*, 140, 1041 (1993).

APPENDICES

APPENDIX A

Measurement of Impedance: Preliminary Results (HP-Agilent 4294A-40 Hz to 110 MHz)

Sample Data and Calculation: $\sigma=l/(R*S)$

SPEEK (DS=70): Thickness=40 μm , $l=1.5$ cm, $w=1$ cm, $S=0.004*1$ cm², $R=8300$ Ω @ 21 kHz, $\theta=1.5$

$$\sigma=l/(R*S)=1.5/(8300*0.004)=0.045 \text{ Scm}^{-1}$$

Nafion 112: Thickness=58 μm , hydrogen peroxide treated for organic removal and acid treated at 80 C.

$$\sigma=0.11 \text{ S/cm}$$

Table A1. Frequency, impedance and phase data for Nafion 112

f	Z	θ
40 Hz	4.37	-26.5
100 Hz	3.66	-14.7
500 Hz	3.22	-7.67
1 kHz	3.06	-6.14
10 kHz	2.77	-2.46
100 kHz	2.69	-1.34
1 MHz	2.65	-5.83

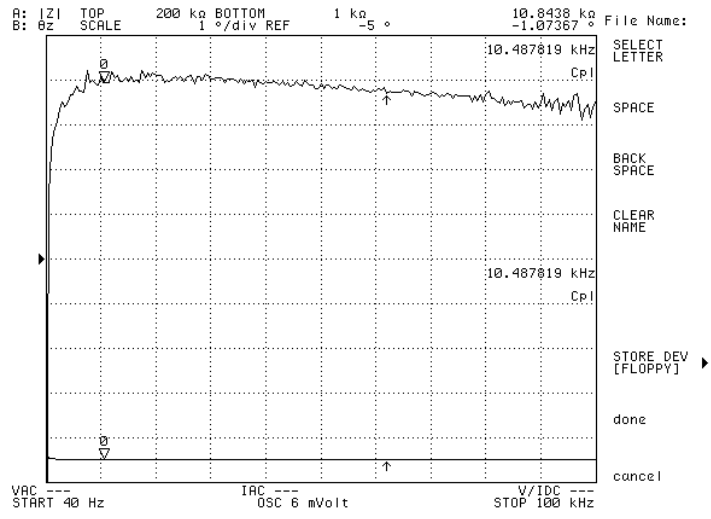


Figure A2. Output screen of Agilent 4294

APPENDIX B

Calibration Data for GC for Methanol Permeability Measurements

Table B1: Methanol Concentration with respect to Methanol Peak Area for Calibration

Conc. (M)	Peak Area
0	0
0.05	57714
0.1	123212
0.2	238212
0.4	485195
1	1212305

0.5 μ L injection at 140 $^{\circ}$ C

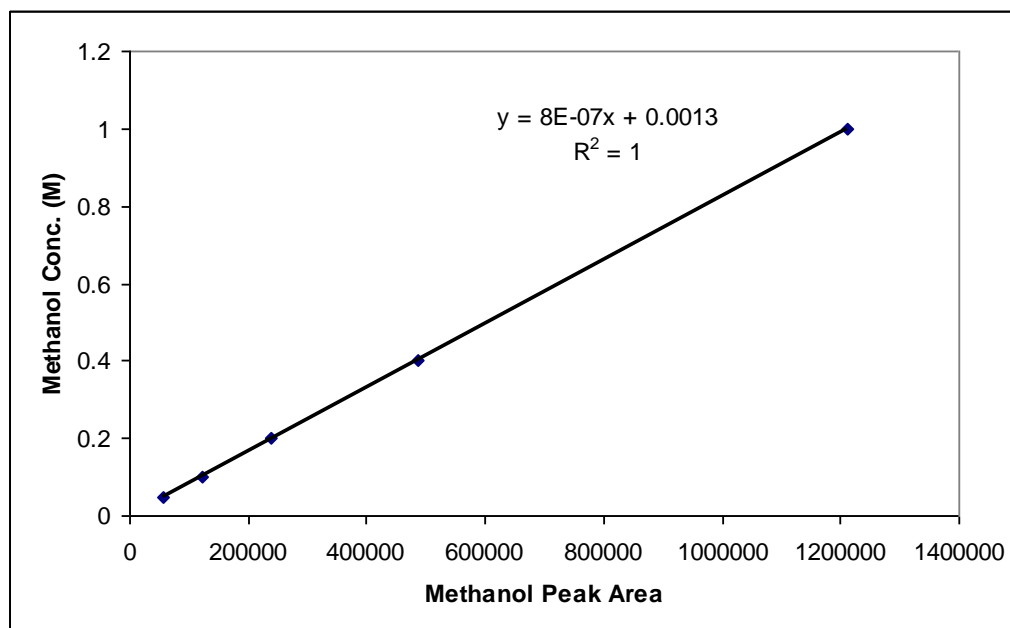


Figure B1. Calibration Curve of GC for Methanol Permeability Measurements

APPENDIX C

A Typical Single Cell Test Procedure

MEA PREPARATION

Method: MEA preparation by GDL spraying + hotpress GDL on membrane

GDL type: SGL Carbon group GDL 3 0 BC

Catalyst type: ETEK 20 % Pt on Vulcan XC-72

Active MEA area: 5 cm²

Catalyst loading: 0.4 mg/cm² (anode) 0.4 mg/cm² (cathode)

METHOD DESCRIPTION

Ink preparation

Nafion solution (5 wt %) content = 8.6 g/1gr cat., $V_{H_2O}/V_{n-Prop}=1/2$ $V_{H_2O}=6$ ml/0.1 gr cat

Membrane treatment:

1 M H₂SO₄ for 2 hours

Technique:

1. Prepare blank GDL samples
2. Load them by spraying catalyst ink until desired catalyst loading is achieved
3. Hotpress catalyst loaded GDLs on membrane at T=150 °C P=250 for 3 min

Performance testing:

$T_{cell}=70$ °C $T_{humid}= 80$ °C for both anode and cathode $T_{cgasline}=80$ °C for both anode and cathode . $V_{gas} = 0.1$ slm for both H₂ and O₂. $V= 0.6$ V
CD=160 mA/cm² (T=70 °C).

CURRICULUM VITAE

Name Surname : Ramiz Gültekin Akay
Date of Birth : December 08, 1975
Nationality : Turkish
e-mail : gultekin@metu.edu.tr, gultek1@hotmail.com

Education

Degree	Institution	Year of Graduation
PhD	Chemical Engineering, Middle East Technical University (METU), Ankara	2008
MS	Chemical Engineering, Middle East Technical University (METU), Ankara	2001
BS	Chemical Engineering, Middle East Technical University (METU), Ankara	1998
High School	Atatürk Anadolu High School, Ankara	1993

Research Experience

- Research Assistant, Chemical Engineering, Middle East Technical University (METU), Ankara 2002- Present
- Visiting Scholar, Civil & Environmental Engineering, Ottawa University, Ontario, Canada, February-June 2001

FOREIGN LANGUAGES

Advanced English, German (pre-intermediate)

PUBLICATIONS-PRESENTATIONS

- 1) D. O. Üner, I. Önal, G. Akay, F. Şahin, E. Engin, E. Okandan 'Egzoz gazlarından kaynaklanan HC Emisyonlarının Analizi ve Değerlendirilmesi' Yanma ve Hava Kirliliği Kontrolü 5. Ulusal Sempozyumu, 19-21 Haziran 2000, Elazığ, Türkiye.
- 2) D. Ö. Üner, G. Akay, B. Erişmiş, 'Motorlu Kara Taşıtlarında Yapılan Egzoz emisyon Ölçümlerinin İstatistiksel Olarak Değerlendirilmesi' Yanma ve Hava Kirliliği Kontrolü 5. Ulusal Sempozyumu, 19-21 Haziran 2000, Elazığ, Türkiye.
- 3) D. Üner, G. Akay, E.Engin, F. Şahin, E. Okandan, 'Benzinli Motorların Egzoz Gazlarından Kaynaklanan HC emisyonlarının Analizi ve Değerlendirilmesi' 4. Ulusal Kimya Mühendisliği Kongresi, 4-7 Eylül 2000, İstanbul, Türkiye.
- 4) D. Karman, Ö. Oğuz, G. Akay, "Measurement Of Air Toxics in The Cabins Of Commuter Vehicles Under Summer And Winter Conditions in Ottawa, Canada", 11th CRC On-road Vehicle Emissions Workshop, San Diego, California, March 26-28, 2001.
- 5) R. G. Akay and D. Uner, "Status-quo of motor vehicle emissions and inspection maintenance programs in Turkey", 2002 Automotive and Transportation Technology Congress & Exhibition, 9-11 July, in Paris, France
- 6) Gür, N. Akay G, Baç, N, "Synthesis Of Zeolite Beta For Composite Membranes", 30 Temmuz-02 Ağustos 2006, International Symposium on Zeolites and Microporous Crystals (ZMPC2006), Yonago-Tottori, Japonya

- 7) Akay G, Gür,N., Ba, N., “Pem Yakıt Pilleri İin Kompozit Membran Geliřtirilmesi”, 7. Ulusal Kimya Mühendislięi Kongresi (UKMK7), 5-8 Eylül 2006, Anadolu Üniversitesi, Eskiřehir
- 8) N. Bac, G. Akay, S. Mukerjee, "Composite Membranes Based on Post-Sulfonated Non-Fluorinated Aromatic Polymers", AIChE, The 2006 Annual Meeting, San Francisco, California, 2006.
- 9) řengül E., Erdener H., Akay G., Eroęlu İ., Ba N.,, “Effects of sulfonated-polyether-ether-ketone (SPEEK) and composite membranes on the proton exchange membrane fuel cell (pemfc) performance”, World Hydrogen Technologies Convention, Italy 2007.